Department of Medical Science

PhD in Medical physiopathology

35th cycle

IL-3Rα: a new tool to reprogram tumor microenvironment

Presented by	**Malvina Koni**
Tutor	**Prof. Maria Felice Brizzi**
Coordinator	**Prof. Franco Veglio**
SSD	**Internal Medicine (MED/09)**

2019-2022

Index

Introduction

Breast cancer

Breast cancer (BC) is the most diagnosed malignancy worldwide and the leading cause of death related cancer [1]. BC accounts more than 12% of all new annual cancer cases and represents a widespread pathology in less-developed countries [2].The 90% of breast malignancies are defined as sporadic i.e. developed in the absence of a genetic or familial substrate, while 10% are due to a genetic predisposition. In this subgroup of patients, the most frequent germline mutations are in the breast cancer gene 1 and 2 (BRCA1/BRCA2), which together confer a 70% lifetime risk of developing cancer (72% for BRCA1 and 69% for BRCA2) [3]. Patients carrying this type of mutation are at a higher risk of developing other malignancies such as ovarian, pancreatic, and prostate carcinoma [4]. Other germline mutations that are associated with an increased risk of developing BC are the tumor protein 53 (TP53) (Li-Fraumeni syndrome) and phosphatase and tensin homolog (PTEN) (Cowden syndrome) mutation, E-Cadherin (CDH1), serine/threonine kinase 11 (STK11), partner and localiser of BRCA2 (PALB2) [5–8]. In addition to genetic and familial predisposition, additional risk factors for developing BC have been identified. Risk factors can be further divided into modifiable and non-modifiable.

Not modifiable risk factors include: age, family history of breast neoplasia, ethnicity, breast tissue density, personal history of benign breast disease, personal history of irradiation, reproductive history [9,10].

Numerous modifiable risk factors are involved in the development of BC. Among modifiable risk factors the following are included: body mass index, hormonal factors, alcohol consumption, and cigarette smoking [9].

Beyond factors positively influencing the likelihood of developing breast cancer, several protective factors such as breastfeeding, physical activity, and low-fat dietary intake in post-menopausal women are included [11–14].

Risk reduction can be also achieved by chemoprevention (performed with aromatase inhibitors in post-menopausal women or with tamoxifen in pre- and post-menopausal

women) or by prophylactic mastectomy. These medical-surgical strategies are only applicable in well-selected subjects [15–17].

Classification of breast carcinoma

Histological classification

Breast carcinoma can be initially classified as carcinoma in situ (ductal carcinoma in situ - DCIS) or as invasive breast carcinoma when the neoplastic cells go beyond the basal lamina. According to the latest World Health Organisation (WHO) classification of 2019, invasive BC can be divided into 44 different types [18]

The most frequent subtype is no special type (NST), previously defined as ductal carcinoma, which individually accounts for 40% to 80% invasive breast carcinomas [19]. Consequently, NST breast carcinoma represents a 'basket category' into which heterogeneous neoplasms fall. In the latest WHO classification several histotypes previously considered as separate entities (i.e. oncolytic, lipid-rich, glycogen-rich, clear cell, sebaceous and medullary carcinoma) have been reclassified as morphological variants of NST carcinoma [20]. Other types of BC include: invasive lobular carcinoma, mixed ductular-tubular carcinomas, tubular and cribriform carcinoma, mucinous carcinoma, papillary carcinoma, and apocrine carcinoma.

Several entities are also described by the WHO (e.g. inflammatory breast carcinoma, male breast carcinoma). From practical and clinical research, the main mode of subdivision involves the distinction between NST, lobular and sometimes mixed carcinoma [20].

Molecular classification

Since 2000s, a molecular classification has been introduced, independent of the histological subtype, while related to the gene expression pattern of the neoplasm.

The classification originally comprised 4 molecular subtypes: 1) luminal (based on gene expression of estrogen receptor (ER), ER regulatory genes and genes normally expressed by luminal epithelial cells) 2) human epidermal growth factor receptor (Her-2) positive (based

on Her-2 overexpression/amplification); 3) basal (based on expression of ER genes, progesterone receptor (PgR), negativity for Her-2 and expression of genes normally expressed in breast myoepithelial cells) and 4) normal-like, which mimics the gene expression of healthy breast tissue.

Numerous studies have subsequently identified the possibility of reproducibly predicting the molecular subtype by assessing the expression of only 3 genes (ER, PgR and HER-2) and have shown that the molecular profile of these genes is also conserved on microarray analysis [21,22].

These studies pose the way for the foundations of current molecular classification representing the mainstay of breast carcinoma medical treatment.

The current molecular subtypes include luminal A, luminal B, Her-2/neu positive and basal-like (i.e. triple-negative breast cancer (TNBC)) and their main clinical-pathological features are reported in Table 1.

Table 1. Clinical-pathological features of breast cancer molecular subtypes.

	Luminal A	Luminal B	Her-2/neu	Basal-like/TNBC
Diagnostic criteria	Expression of ER and/or PgR on at least 1 in 100 cells. Her-2/neu not amplified. Ki-67 < 20%	Expression of ER and/or PgR on at least 1 cell per 100. Amplification of Her-2/neu and/or Ki-67 ≥ 20 %.	Negative for ER and PgR, amplification of Her-2/neu	Negative for ER and PgR. Her-2/neu not amplified
Frequency	50% of invasive breast carcinomas	20% of invasive breast carcinomas	15 % of invasive breast carcinomas	15 % of invasive breast carcinomas
Most represented histotypes	Tubular, cribriform, lobular, low-grade NST	NST, micropapillary	High-grade NST	High-grade NST, medullary, metaplastic
Response to therapy and prognosis	Good response to hormone therapy. Variable response to	Response to hormone therapy inferior to luminal A.	Response to anti-Her-2 target therapy (e.g. Trastuzumab).	Non-responsive to hormone and target therapy. Sensitive to platinum-based

	chemotherapy. Good prognosis	Response to chemotherapy greater than luminal A. Intermediate prognosis, less than luminal A	Response to anthracycline-based regimens. Worse prognosis compared to other subtypes	regimens. Generally has a worse prognosis than the other subtypes

NST: No Special Type, ER: estrogen receptor, PgR: progesterone receptor.

Triple-negative breast cancer (TNBC)

As previously described, TNBC refers to a particularly aggressive molecular subtype of breast carcinoma lacking the expression of ER, PgR, and Her-2/neu amplification [23].

According to the American society of clinical oncology/college of American pathologists (ASCO/CAP), this entity is defined by the expression at the immunohistochemistry (IHC) of ER and PgR in less than 1 in 100 cells and the expression at the IHC of Her-2/neu classified as 0 or 1+ [24].

TNBC accounts for about 15% of invasive BC, tends to affect younger women than the other subtypes, and is more frequent in African-American women [25].

Moreover, TNBC appears to affect, disproportionately compared to other molecular types, individuals carrying PALB2. TNBC patients' prognosis is closely related to insensitivity to hormone therapy and the absence of targeted therapies. Prognosis is 8-16% lower than in hormone-sensitive neoplasms [25].

TNBC classification

Following the studies of Perou et al. [26] who introduced the molecular classification of BC, several systems were developed providing the fundamentals of current TNBC molecular classification [27,28]. It is increasingly evident, that TNBC represents a group of molecularly heterogeneous neoplasms that share the same immune phenotype rather than a single entity, and a similar approach has been applied to TNBC sub-classification. Lehman et al. [29] were the first to propose a classification into 6 molecular subtypes based on gene

expression and activation of different molecular pathways: basal-like 1 (BL1) and basal-like 2 (BL2), immunomodulatory (IM), mesenchymal (M), mesenchymal stem-like (MSL) and luminal androgen receptor (LAR). Subtype BL1 has predominant expression of genes involved in the cell cycle and DNA repair while BL2 of growth factors. The IM subtype expresses the genes responsible for immune cell function, the M and MSL subtypes express genes responsible for epithelial to mesenchymal transition (EMT), and the LAR subtype is characterised by the activation of the androgen receptor (AR) signalling. The same team has shown that gene expression of IM and MSL subtypes is due to the lymphocyte infiltrate and mesenchymal stromal cells rather than tumour cells, respectively, and consequently refined the classification into four subtypes: BL1, BL2, M and LAR [30]. Finally, a further classification derives from the studies of Burstein et al. [31] who proposed the following subtypes: basal-like immune suppressed (BLIS), basal-like immune activated (BLIA), M and LAR. The subtypes introduced with respect to Lehrman's classification are BLIS and BLIA. Both share TP53 mutation (>90%) and DNA repair defects (e.g.* mutation of BRCA1/2) while are characterized by the high prevalence of stromal tumor infiltrating lymphocytes (TILs) in the BLIA subtype and the depletion of TILs in the BLIA subtype. BLIS and BLIA tumours have respectively the worst and best prognosis among all TNBC molecular subtypes [31].

Table 2 shows the main molecular features of the subtypes according to the classification proposed by Burstein et al.

Table 2. Main characteristics of the molecular subtypes of triple-negative breast cancer.

Molecular subtype	Gene expression and recurrent mutations and microenvironment
BLIS	Common TP53 mutation (>90%) Common homologous repair defects (>80%) Poor lymphocytic infiltrate
BLIA	Common TP53 mutation (>90%) Common homologous repair defects (>80%) Abundant lymphocytic infiltrate
M	Relatively frequent (50%) homologous repair defects Frequent PI3K pathway activation Very poor lymphocytic infiltration

LAR	Rare homologous repair defects (5%)
	Activation of the AR pathway
	Poor lymphocytic infiltrate

Angiogenesis and vascular mimicry

Angiogenesis is the process by which new blood vessels are generated and is orchestrated by many soluble factors that stimulate (pro-angiogenetic) or inhibit (anti-angiogenetic) neo-vessel formation [32]. In normal tissues, the balance between pro- and anti-angiogenetic factors controls physiological angiogenesis. This depends on various exogenous and endogenous stimuli, mainly related to the concentration of O_2 at the tissue level. Pro-angiogenic factors include growth factors (e.g.: vascular-endothelial growth factor (VEGF), platelet-derived growth factor (PDGF), tumor necrosis factor α (TNF-α), angiogenin, cytokines (interleukin 1 (IL-1), IL-6, IL-8)), as well as numerous anti-angiogenic factors (e.g.: IL-10, IL-12, angiostatin, plasminogen activator inhibitor-1 (PAI-1), interferon-α (INF-α)). Within solid neoplasms, the balance between angiogenesis-inducing and angiogenesis-inhibiting factors is abnormal and imbalanced, thereby favouring pro-angiogenic factor action and the genesis of newly formed vessels in an aberrant process known as tumour angiogenesis [33].

Angiogenesis is a key step in tumour progression and recognised as one of the main hallmarks of cancer [34].

Weinder et al. [35] first correlated the microvascular density with lymph node and distant metastases in BC. Other studies, investigating the prognostic significance of angiogenesis in BC, have also demonstrated a poorer survival in patients with tmours connoted by the presence of high microvascular density [36]. In TNBC, micro-vascular density appears even more represented than in other non-TNBC BC subtypes (p<0.001), as shown by Mohammed et al. [37] in a study including 830 breast carcinomas. In the same study, the 20-year survival of TNBCs with vascular invasion was almost halved compared to cases without vascular invasion. VEGF is one of the main regulators of angiogenesis and therefore, its increase reflects neo-vascular formation. The more active tumour angiogenesis in TNBC was further

supported by the presence of VEGF in the TME. Based on these observations it has been stated that tumour vasculature is even more relevant to therapeutically target TNBC. For instance, Lopatina et al. [38] have recently shown that blocking the signal mediated by interleukin-3 receptor α (IL-3Rα), expressed on tumour endothelial cells (TECs), interferes with the formation of neo-vessels and metastasis formation in mouse models of BC. Unfortunately, trials investigating the therapeutic role of anti-angiogenic drugs alone in metastatic TNBC failed to provide a clear survival benefit [39–41].

Vascular mimicry (VM) is a process by which tumour cells differentiate and arrange themselves to form neo-vessels. This was first described in 1999 by the observation that vascular structures containing erythrocytes were negative for the expression of endothelial markers (factor VII, CD31) while positive for Shiff's periodic acid reaction (PAS) in uveal melanoma [42]. Subsequent experiments on cell lines of different human neoplasms identify the main signalling pathways involved in VM. Indeed, it has been shown that hypoxia in the tumour microenvironment (TME) stabilises the level of hypoxia inducible factor-1α (HIF-1α) and induces EMT resulting in vascular-endothelial cadherin (VE-cadherin), ephrin type-A receptor 2 (EPHA2) and CD44 expression [43].

As represented in Figure 1, VE-cadherin-mediated activation of EPHA2 can activate signals through phosphatidylinositol 3-kinase (PI3K), extracellular signal-regulated protein kinase 1/2 (ERK1/2), the expression of metalloproteinases MMP14, MMP2 and laminin, and induce cell migration [44,45]. In fact, inhibition of these molecules interferes with VM [46,47].

In addition to the above mentioned molecules, orchestrating VM, BC has additional molecular peculiarities. In a study of 200 human breast carcinoma samples, Gu et al. [48] demonstrated an association of VM with the expression of osteopontin. Cell lines capable of forming tubular structures *in vitro* expressed more osteopontin, and this was inversely correlated to the expression of the microRNA hsa-mir-299-5p [49]. In addition, miR-204, was also found inversely correlated with VM in BC [50]. VM is not an isolated process but is closely related to the stemness of neoplastic cells (the presence of CD133+ cells) and EMT through the activation of several transcription factors such as zinc finger E-box binding homeobox (ZEB), twist-related protein (TWIST), and suppressor of mothers against

decapentaplegic (SMAD). VM was also found in the other molecular subtypes. However, given its higher prevalence in TNBC and the lack of targeted therapies in this group of malignancies, it has been considered a potential therapeutic target.
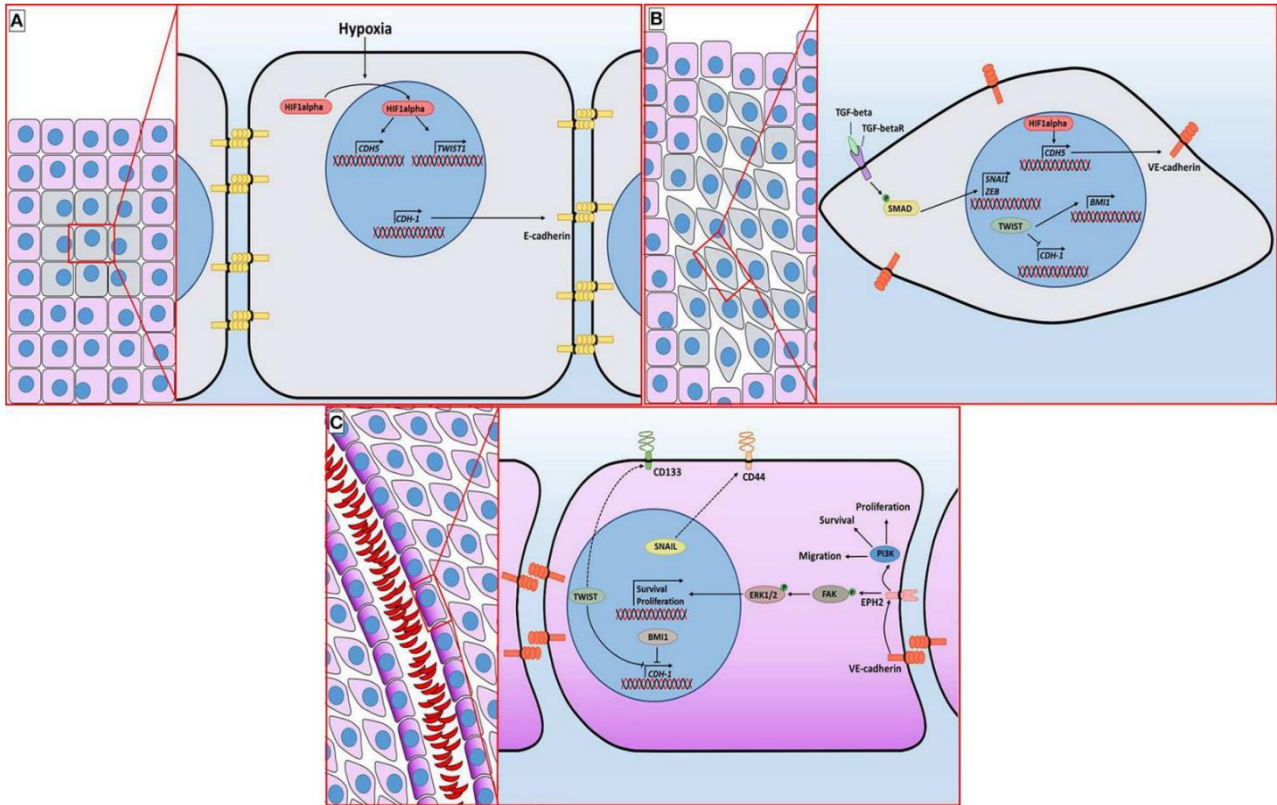

Figure 1. Molecular pathways involved in vascular mimicry. Source: Andonegui Elguera et al., 2020

The interleukin-3/interleukin-3 receptor α axis

Interleukin-3 (IL-3), also referred to as multilineage-colony stimulating factor (Multi-CSF), is a cytokine with a molecular weight of 20-26 kDa predominantly produced by CD4+ T lymphocytes, monocyte and stromal cells initially identified as a growth factor for immature bone marrow cells [51,52]. The gene coding for IL-3 is located on chromosome 5q31 [53]. IL-3 plays an important role in haemopoiesis: it has been shown to induce the proliferation of haematopoietic stem cells, neutrophils, megakaryocytes, macrophages, lymphoid and erythroid cells [54].

To exert its action on target cells, IL-3 binds to its receptor resulting in the activation of downstream signalling pathways. The interleukin-3 receptor is a heterodimeric receptor consisting of two subunits: an α subunit (IL-3Rα, also known as CD123) and a β subunit

shared with the interleukin-5 receptor (IL-5R) and the granulocyte-macrophage colony-stimulating factor receptor (GM-CSF), called the β subunit (βc) (Figure 2).

Generally, in the absence of stimulation, the receptor is not in its dimer form but, in the presence of IL-3, undergoes ligand-induced hetero-dimerization. IL-3Rα, specifically, contains an extracellular domain, a transmembrane domain, and a cytoplasmic domain. Several molecular studies have shown that IL-3Rα is required for the activation and phosphorylation of signal transducer and activator of transcription 5 (STAT-5) [55,56]. In addition to its well-documented role in haemopoiesis, Evans et al. [57] demonstrated that activation of IL-3Rα in murine pluripotent cells can induce not only proliferation but also differentiation, suggesting that within haemopoiesis, IL-3Rα activation is involved in cell fate determination. The role of the IL-3/IL-3R axis in conditions other than haemopoiesis has been also investigated over the years. A great deal of evidence has shown that IL-3 is involved in several pathological processes. IL-3Rα expression is frequent (45-95%) in acute myeloid leukaemia and its expression has been associated with a worse prognosis [58,59]. IL-3Rα seems to be involved in the pathogenesis of some lymphoid neoplasms, 90% of Hodgkin's lymphomas express CD123 [60].

IL-3 also contributes to the remodelling of the pathological vasculature, particularly tumour vasculature. Dentelli et al. [61] have shown that TECs produce IL-3 which, in an autocrine manner, promotes their migration through the induction of membrane-bound c-kit ligand (mbKitL). It was also shown that the inhibition of the IL-3/IL-3Rα axis switched off β-catenin signalling in tumour endothelial cells by interfering with the formation of tumour neo-vessels [62]. Despite its action as hemopoietic growth factor, its pro-inflammatory action, and role in neoplastic angiogenesis, CD123 expression has been poorly investigated in solid neoplasms.
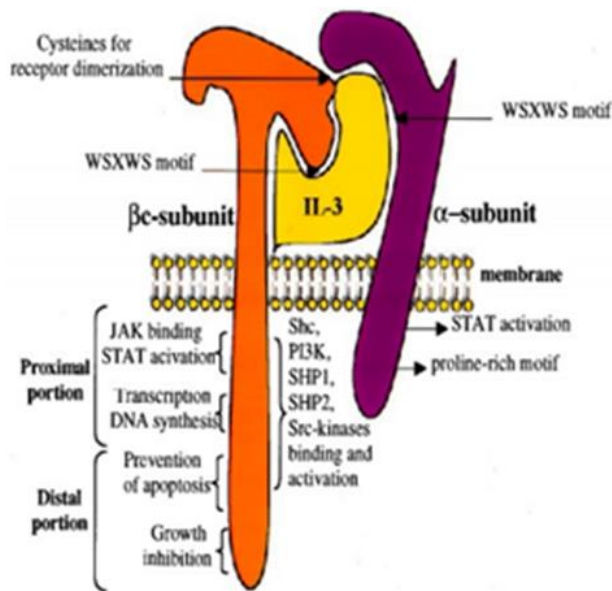
Figure2. Representation of the interleukin-3 receptor with its two subunits.

Aim of the study

TNBC is a specific molecular subtype that lacks immunohistochemical expression of ER, PgR, and Her2/neu expression and/or amplification. Unlike other molecular subtypes, TNBC does not benefit from the use of hormonal therapies or targeted anti-Her2/neu therapies. For these reasons, TNBC tends to be characterized by a lower therapeutic response and a worse prognosis.

In recent years, the concept that, despite its extreme heterogeneity, TNBC shares the lack of expression of the aforementioned markers has been increasingly consolidated. Therefore, the identification of immunohistochemical and molecular markers capable to distinguishing specific tumor entities could both improve patient prognostic stratification and provide new therapeutic targets for a neoplasm currently lacking targeted therapies. The IL-3/IL-3Rα axis was initially studied for its hematopoietic function but, over the years, it has been considered for its pro-inflammatory and angiogenic activities.

Despite the biological relevance covered by the IL-3/IL-3Rα axis, its expression, and its role in solid tumors, and in particular in TNBC, has never been investigated.

Therefore, the aim of the work was to retrospectively evaluate the expression of IL-3Rα on human TNBC samples and to study its role as prognostic marker and possible TNBC therapeutic target. The results of this study are reported in the attached published paper.

Results:

- **Interleukin-3-Receptor-α in Triple-Negative Breast Cancer (TNBC): An Additional Novel Biomarker of TNBC Aggressiveness and a Therapeutic Target.**

  <u>**Koni M**</u>, Castellano I, Venturelli E, Sarcinella A, Lopatina T, Grange C, Cedrino M, Femminò S, Cossu-Rocca P, Orrù S, D'Ascenzo F, Cotellessa I, Tampieri C, Debernardi C, Cugliari G, Matullo G, Camussi G, De Miglio MR, Brizzi MF.

  Cancers (Basel). 2022 Aug 13;14(16):3918. doi: 10.3390/cancers14163918.

  https://www.mdpi.com/2072-6694/14/16/3918

Article

Interleukin-3-Receptor-α in Triple-Negative Breast Cancer (TNBC): An Additional Novel Biomarker of TNBC Aggressiveness and a Therapeutic Target

Malvina Koni [1], Isabella Castellano [1], Emilio Venturelli [1], Alessandro Sarcinella [1], Tatiana Lopatina [1], Cristina Grange [1], Massimo Cedrino [1], Saveria Femminò [1], Paolo Cossu-Rocca [2,3], Sandra Orrù [3], Fabrizio D'Ascenzo [1], Ilaria Cotellessa [1], Cristian Tampieri [1], Carla Debernardi [1], Giovanni Cugliari [1], Giuseppe Matullo [1], Giovanni Camussi [1], Maria Rosaria De Miglio [4,*] and Maria Felice Brizzi [1,*]

[1] Department of Medical Sciences, University of Turin, 10126 Turin, Italy
[2] Anatomic Pathology Unit, Department of Diagnostic Services, "Giovanni Paolo II" Hospital, ASL Gallura, 07026 Olbia, Italy
[3] Department of Pathology, "A. Businco" Oncologic Hospital, ARNAS Brotzu, 09121 Cagliari, Italy
[4] Department of Medical, Surgical and Experimental Sciences, University of Sassari, 07100 Sassari, Italy
[*] Correspondence: demiglio@uniss.it (M.R.D.M.); mariafelice.brizzi@unito.it (M.F.B.);
Tel.: +39-079-228-016 (M.R.D.M.); +39-011-670-6653 (M.F.B.)

Simple Summary: Molecular and histological profiling is crucial for biomarker and therapeutic target discovery, for example, in TNBC. We demonstrated that IL-3Rα expression led to the identification of a subgroup of TNBC patients displaying a poor overall survival. Moreover, we refined TNBC molecular annotation and drew a model including IL-3Rα, PD-L1, and genes related to EMT, which finely discriminates cancer aggressiveness. Finally, we first demonstrated that IL-3Rα is instrumental in granting tumour adaptation and progression by reprogramming TNBC cells to form large dysfunctional vessels and reshaping PD-L1 expression in primary tumours and metastases. Therefore, the IL-3/IL-3Rα axis may be proposed as a marker of TNBC aggressiveness, as a novel TNBC therapeutic challenge.

Abstract: Tumour molecular annotation is mandatory for biomarker discovery and personalised approaches, particularly in triple-negative breast cancer (TNBC) lacking effective treatment options. In this study, the interleukin-3 receptor α (IL-3Rα) was investigated as a prognostic biomarker and therapeutic target in TNBC. IL-3Rα expression and patients' clinical and pathological features were retrospectively analysed in 421 TNBC patients. IL-3Rα was expressed in 69% human TNBC samples, and its expression was associated with nodal metastases ($p = 0.026$) and poor overall survival (hazard ratio = 1.50; 95% CI = 1.01–2.2; $p = 0.04$). The bioinformatics analysis on the Breast Invasive Carcinoma dataset of The Cancer Genome Atlas (TCGA) proved that IL-3Rα was highly expressed in TNBC compared with luminal breast cancers ($p = 0.017$, $p$adj = 0.026). Functional studies demonstrated that IL-3Rα activation induced epithelial-to-endothelial and epithelial-to-mesenchymal transition, promoted large blood lacunae and lung metastasis formation, and increased programmed-cell death ligand-1 (PD-L1) in primary tumours and metastases. Based on the TCGA data, IL-3Rα, PD-L1, and EMT coding genes were proposed to discriminate against TNBC aggressiveness (AUC = 0.86 95% CI = 0.82–0.89). Overall, this study identified IL-3Rα as an additional novel biomarker of TNBC aggressiveness and provided the rationale to further investigate its relevance as a therapeutic target.

Keywords: interleukin-3/interleukin-3 receptor α; triple-negative breast cancer; vascular mimicry; programmed cell death-ligand 1

1. Introduction

Triple-negative breast cancer (TNBC) is a subtype of breast cancer characterised by the lack of oestrogen, progesterone, and human epidermal growth factor receptor-2 (HER2) [1].

TNBC mostly arises in young women and accounts for approximately 10–15% of all breast cancers [2]. TNBC is generally a highly aggressive metastatic carcinoma, displaying a high mortality rate and recurrence [3]. Moreover, TNBC patients identified by the WNT/β-catenin network classifier have a greater risk of metastases [4]. The complexity of the disease also stems from the lack of accepted predictors of response to therapy. More importantly, as TNBC lacks oestrogen, progesterone, and HER2 receptors, it is unresponsive to currently available targeted approaches [5]. Thus, new prognostic molecular markers and therapeutic target(s) are required. Currently, many clinical trials targeting specific receptors in tumour and stromal cells are ongoing, and targeted therapies based on immunohistochemical studies are under investigation [6,7].

The human IL-3R is a heterodimeric receptor consisting of an IL-3 specific binding subunit, the α chain (IL-3Rα) [8], and a common β chain (βc) [9] shared with the granulocyte–macrophage colony-stimulating factor (GM-CSF) and interleukin-5 (IL-5) receptor [10,11]. Hemopoietic stem cell commitment as well as monocyte [12], eosinophil [13], basophil [14,15], and neutrophil [16] functional activation requires IL-3R. IL-3 binding to its receptor (IL-3R) triggers a variety of cellular signals upholding the homeostasis of the haemopoietic tissue [17,18]. However, vascular cells also express IL-3R, the activation of which increases the expression of adhesion molecules as well as the inflammatory and immune responses [19–21]. We have recently shown that the interleukin-3 binding subunit (IL-3Rα) is expressed in human TNBC samples by endothelial and inflammatory cells [22]. IL-3 was originally described as a haematopoietic factor [17]; however, IL-3, mainly released by tumour-infiltrating lymphocytes (TILs) [23], acts as a proinflammatory and proangiogenic cytokine [24]. Moreover, it has been shown that, in response to IL-3, tumour-derived endothelial cells (TECs) release extracellular vesicles (EVs) able to promote vessel growth [25], epithelial-to-mesenchymal transition (EMT), TNBC metastatic spread [22], and tumour immune evasion by upregulating the programmed cell death-ligand 1 (PD-L1) in myeloid cells [26]. All these data sustain the contribution of IL-3 signalling in the tumour microenvironment (TME). The TME consists of different cell types that provide the ground for tumour development and progression either directly through different mechanisms or by means of the release of soluble factors. Moreover, each of these events most likely contributes to the dynamic changes triggering both tumour immune editing and tumour plasticity [27]. Tumour cell plasticity refers to the dynamic changes that affect cancer cells and explains the reversible mesenchymal transition, the acquisition of stemness traits, and the epithelial-to-endothelial transition [28]. The acquisition of an endothelial phenotype by tumour cells and their ability to form blood vessel lacunae is a process denoted as vascular mimicry (VM), generally referred to as a hallmark of TNBC aggressiveness [29–31]. VM represents an alternative mechanism of tumour adaptation to the demands of oxygen and nutrients required for their outgrowth [32] and spreading [33]. Indeed, in TNBC, VM correlates with different prognostic features including haematogenous and lymph node metastases, and the rate of survival [34].

Therefore, the pleiotropic actions of the IL-3/IL-3Rα axis provide the rationale to explore IL-3Rα as a prognostic additional biomarker, and a potential therapeutic target in TNBC aggressiveness and, thus, a forthcoming therapeutic challenge.

2. Materials and Methods

2.1. Sample Recruitment

To evaluate the clinical significance of the IL-3Rα expression, we selected patients diagnosed with TNBC who underwent surgical treatment and with available follow-up data ($n = 421$). According to the guidelines and clinical indications, some patients were also treated with neo-adjuvant chemotherapy, adjuvant chemotherapy, radiation therapy, or a combination of these treatment modalities. The data of 163 primary TNBC patients who underwent surgery from 2001 to 2019 were collected from the Pathology Unit of Città della Salute e della Scienza Hospital in Turin, while those of 258 patients undergoing surgeries from 2000 to 2015 were recovered from the Department of Histopathology of Oncologic

Hospital in Cagliari, Italy. The specimens were processed as previously described [22] in the two different Pathology Units. Three experienced pathologists independently evaluated all tumour cases. Histologic subtyping referred to the 2019 WHO classification [35]. The TNBC database includes the personal and medical data collected from the medical records of each TNBC patient. The study was conducted in accordance with the guidelines and regulations defined by the Research Ethics Committee for Human Biospecimen Utilisation (Department of Medical Sciences—ChBU) of the University of Turin and from the Research Ethics Committee of Sardinia Region (#224/CE/12). Written consent was not required considering the retrospective nature of the study and no impact on patients' care. Tumour samples were analysed using IHC to assess the expression of IL-3Rα (anti-IL-3Rα clone S-12 antibody Santa Cruz Biotechnology, Dallas, TX, USA, sc-455). To classify each individual tumour sample as IL-3Rα-positive or -negative, the results of IHC were compared via light microscopy using acute myeloid leukaemia cells (M07 cell line) as a positive control, which displays a high receptor expression. Based on this control, we categorised tumours as IL-3Rα-negative or -positive (cut-off 1-3 plus).

2.2. Immunohistological Analysis

Tissue microarrays including representative formalin-fixed, paraffin-embedded (FFPE) blocks of TNBC specimens were used to cut 3 µm thick tissue sections for haematoxylin-and-eosin stains (H&E). The TIL evaluation was reported as the percentage of cells in the stromal tissue inside the invasive tumour, avoiding areas with crushed artefacts, necrosis, and inflammation around biopsy sites or hyalinisation [36]. Immunohistochemistry for the expression of IL-3Rα was performed as previously described [22].

2.3. Cell Lines

The following TNBC cell lines were used: MDA-MB-231, MDA-MB-453, MDA-MB-436, MDA-MB-157, BT-549, HCC-1395, and Hs-578T. The pathological features of each cell line are reported in Supplementary Table S1; the MCF10A cell line, a non-neoplastic breast cancer cell subtype, was cultured as indicated by the manufacturer and served as a negative control. All cell lines were provided by the ATCC (Manassas, VA, USA) and cultured as indicated by the manufacturers. The M07 leukaemic cells were established in the lab [37]. Supplementary Information reports the details.

2.4. Western Blot Analysis

Cells were lysed using a RIPA buffer and processed as previously described [22]. The following antibodies were used: anti-Vimentin (Abcam #ab8978), anti-N-Cadherin (Abcam #ab18203), anti-GAPDH (Abcam # ab8245), anti-β-Actin (Abcam #ab8227), anti-CD31 (Abcam #ab28364), and anti-IL-3Rα/CD123 (R&D Systems #MAB301-100). Secondary antibodies conjugated with peroxidase were purchased from Cell Signalling Technologies (Danvers, MA, USA). Supplementary Information reports the details.

2.5. FACS Analysis

For the FACS analysis of IL-3Rα/CD123 surface marker, MDA-MB-231, MDA-MB-453, MDA-MB-436, MDA-MB-157, BT-549, Hs-578T, HCC-1395, MCF10A, and M07 cells were harvested and stained with human anti-CD123 antibody for 30 min. Flow cytometric analysis was performed using a Cytoflex flow cytometer (Beckman Coulter, Brea, CA, USA). Supplementary Information reports the details.

2.6. Real-Time PCR Analysis

Real-time polymerase chain reaction (PCR) was performed to detect SLUG, ZEB 1, and TWIST transcript in Hs-578T, HCC-1395, MDA-MB-231, and MDA-MB-436 cell lines untreated or treated with IL-3 (5 ng/mL of recombinant human IL-3) (BD Biosciences, San Jose, CA, USA) for 24 h. The Primer sequences and additional details are reported in Supplementary Information.

16

2.7. Tube-like Structure Formation Assay

Cells were non-enzymatically detached and seeded onto a thick layer of growth factor reduced Matrigel (BD Biosciences, San Jose, CA, USA) in a 24-well plate (Corning, Corning, NY, USA). Supplementary Information reports the details.

2.8. In Vivo Model

Animal studies were performed in accordance with the Italian National Institute of Health Guide for the Care and Use of Laboratory Animals. All procedures were approved by the Ethics Committee of the University of Turin and the Italian Health Ministry (protocol No. 833/2020-PR). The Committee approved the research before the study began. Mice were housed according to the guidelines of the Federation of European Laboratory Animal Science Association. Blinded investigators (at least 2) assessed the outcome. Tumours were obtained by injecting MDA-MB-231 or MDA-MB-436 cells (2×10^6 cells) in 100 µL of growth factor reduced Matrigel into the mammary fat pad of NSG mice purchased from Charles River Laboratories (Calco, Italy) (8 weeks/female) (3 mice/group: control vs. rhIL-3-treated mice (20 ng/mL)). From T0, corresponding to tumour cell injection, the animals were locally treated with saline or rhIL-3 (20 ng/mL) every 2 days for 4 weeks. Once a week, the size of the tumours was blindly evaluated using a digital calliper: Maximum and minimum diameters were measured, and the volume was calculated using the following ellipsoid formula: (4/3π (d/2)^2*D/2). Mice were euthanised using a CO_2 chamber 4 weeks later. Primary tumours were collected and fixed as previously described [22], for further analyses. Immunohistochemistry was performed using an automated slide-processing platform (Ventana BenchMark AutoStainer, Ventana Medical Systems, Tucson, AZ, USA), with Universal DAB Detection Kit detection systems. Briefly, 5 µm paraffin-embedded tumour sections were stained with CD31 and PAS to quantify CD31+ vessels and VM (expressed as CD31−/PAS+ vessels). Ten sections/tumour were examined using ImageJ 1.50g software (Wayne Rasband, National Institutes of Health, Bethesda, MD, USA), and the results are expressed as the number of CD31+/PAS+/fields ± SEM. PD-L1 expression was evaluated using an anti-human PD-L1 rabbit polyclonal antibody (Abcam #ab233482) diluted in a ratio of 1:100. Secondary HRP-labelled anti-rabbit antibody (Goat Anti-Rabbit IgG (H + L)-HRP Conjugate, Bio-Rad, Hercules, CA, USA) was used at 1:1000 dilution for 1 h at room temperature. Sections were counterstained with haematoxylin, dehydrated, and mounted. The quantification of the PD-L1 expression was performed using Fiji software (ImageJ). Lung metastases were counted according to human PD-L1 expression. The results are expressed as the mean ± SEM of PD-L1-positive area (related units) per sample ($n = 3$/each condition).

2.9. Bioinformatics Analysis

Using The Cancer Genome Atlas (TCGA), limited to the BRCA data, the datasets were downloaded from the TCGA website (https//tcga-data.nci.nih.gov, accessed on 14 November 2021) for gene expression analyses [38–40]. Supplementary Information reports the details.

2.10. Sample Size Calculation

For animal studies, according to our previous data, the minimum sample size that would permit us to detect a 40% difference between the experimental groups with 90% power was $n = 3$ mice/group. For patient validation, based on the data provided by Urru et al. [41], a simulation study of the number of events per variable in logistic regression analysis [42] revealed that 250 patients are needed to test the independent predictive power of the IL-3Rα expression.

2.11. Statistical Analysis

Data are representative of at least 3 independent in vitro experiments, performed in triplicate. Comparison between 2 groups was performed using Student's *t*-test, while

comparisons between 3 or more groups were performed using a one-way ANOVA test, and the significance level ($p < 0.05$, $p < 0.01$, $p < 0.001$) was evaluated using the Newman–Keuls multicomparison post hoc test. The correlation and distribution of IL-3Rα and baseline clinical–pathological parameters were assessed using the χ^2 test and Fisher's exact test. Baseline parameters such as age at diagnosis (we arbitrarily set the cut-off at 55 years old since we failed to detect differences in the median of age); histotype (ductal, lobular, or others); pT = primary tumour; pN = lymph nodal invasion; M = metastasis (TNM classification); G = grade (G1, G2, G3); Ki67 (%), and the percentage of TILs = tumour-infiltrating lymphocytes in every single tumour specimen were considered. The overall survival (OS) analysis was performed using the Kaplan–Meier estimates. We used Cox regression and the Wilcoxon–Breslow–Gehan test to assess the hazard ratio and expected-versus-observed events in the two groups of patients. Cox multivariate adjustment was performed including the IL-3Rα expression and pT. The association between the relative gene expression values was performed through Spearman's correlation analysis. Logistic regressions were performed to evaluate the synergistic effect of several genes in discriminating the tumour subtype based on its aggressiveness. The receiver operative characteristic (ROC) curve considering the area under the curve (AUC) was used to judge the discrimination potential of the models. Statistical analyses were performed using R v4.1.2, R Core Team (2017); R: a language and environment for statistical computing; R Foundation for Statistical Computing, Vienna, Austria. URL (https://www.R-project.org/, accessed on 1 November 2021); Software and Bioconductor (https://www.r-project.org/, accessed on 1 November 2021). Figure results were plotted using the Ggplot2 R package (https://CRAN.R-project.org/package=ggplot2, accessed on 25 January 2022) and STATA (https://www.stata.com, accessed on 20 April 2021), Copyright 1985–2019 StataCorp LLC, serial number: 401709301228; licensed to Università degli Studi di Torino). Statistical significance was set at $p < 0.05$.

3. Results

3.1. IL-3Rα Is Expressed and Associated with Poor Prognosis in Human TNBC

We performed a retrospective study to evaluate the expression of IL-3Rα in TNBC samples obtained from two different centres in Italy ($n = 421$). Notably, IL-3Rα expression was found in 291 out of 421 human TNBC samples, and at baseline, IL-3Rα-positive patients displayed a significantly high nodal invasion (N2) ($p = 0.026$) (Table 1). The representative images of positive and negative IL-3Rα samples are shown in Figure 1A,B. In our cohort, we detected 133 events, 99 in IL-3Rα-positive and 34 in IL-3Rα-negative patients. The hazard ratio for IL-3Rα-positive samples corresponded to 1.50 (CI = 95% 1.01–2.2; $p = 0.04$) and was near to significance after multivariate adjustment (hazard ratio = 2.01:0.89–4.89, $p = 0.089$). Additionally, using the Wilcoxon–Breslow–Gehan test, we found that the expected events were significantly lower (IL-3Rα-positive: 88 vs. 99) and higher (IL-3Rα-negative: 45 vs. 34) than the observed ($p = 0.0245$) (Figure 2).

Table 1. Clinical and pathological features of TNBC patients. Histologic classification refers to the WHO classification. IL-3Rα = IL-3 receptor α, NST = no special type, N/A = not available, pT = primary tumour, pN = lymph nodal invasion, M = metastasis, G = grade, TILs = tumour-infiltrating lymphocytes. * The *p*-value refers to differences between IL-3Rα expression (positive and negative) using Fisher's exact test (in bold the significant data).

	Total	IL-3Rα-Positive	IL-3Rα-Negative	*p*-Value
	n = 421	*n* = 291 (69%)	*n* = 130 (31%)	
Age, *n* (%)				
<55 y	191 (45%)	128 (44%)	63 (48%)	0.394
≥55 y	230 (55%)	163 (56%)	67 (52%)	

Table 1. *Cont.*

	Total	IL-3Rα-Positive	IL-3Rα-Negative	*p*-Value
	n = 421	*n* = 291 (69%)	*n* = 130 (31%)	
Histologic subtype, *n* (%)				
NST	295 (70%)	201 (69%)	94 (72%)	
Lobular	20 (5%)	18 (6%)	2 (2%)	0.169
Others	96 (23%)	64 (22%)	32 (24%)	
N/A	10 (2%)	8 (3%)	2 (2%)	
Primary Tumour, *n* (%)				
pT1	162 (38%)	117 (40%)	45 (35%)	
pT2	194 (46%)	130 (45%)	64 (49%)	
pT3	31 (8%)	22 (8%)	9 (7%)	0.794
pT4	24 (6%)	15 (5%)	9 (7%)	
N/A	10 (2%)	7 (2%)	3 (2%)	
Lymph node involvement, *n* (%)				
pN0	230 (55%)	157 (54%)	73 (56%)	
pN1	94 (22%)	61 (21%)	33 (25%)	
pN2	**40 (10%)**	**36 (12%)**	**4 (3%)**	**0.026** *
pN3	31 (7%)	21 (7%)	10 (8%)	
N/A	26 (6%)	16 (6%)	10 (8%)	
Metastasis, *n* (%)				
M0	409 (97%)	283 (97%)	126 (97%)	
M1	5 (1%)	3 (1%)	2 (2%)	0.899
N/A	7 (2%)	5 (2%)	2 (2%)	
Grade, *n* (%)				
G1	4 (1%)	3 (1%)	1 (1%)	
G2	56 (13%)	45 (15%)	11 (8%)	0.115
G3	354 (84%)	240 (82%)	114 (88%)	
N/A	7 (2%)	3 (1%)	4 (3%)	
Ki67, *n* (%)				
<15%	21 (5%)	13 (4%)	8 (6%)	0.463
≥15%	400 (95%)	278 (96%)	122 (94%)	
TILs, *n* (%)				
Present	164 (40%)	106 (37%)	58 (46%)	
Absent	121 (30%)	90 (32%)	31 (25%)	0.204
N/A	124 (30%)	87 (31%)	37 (29%)	

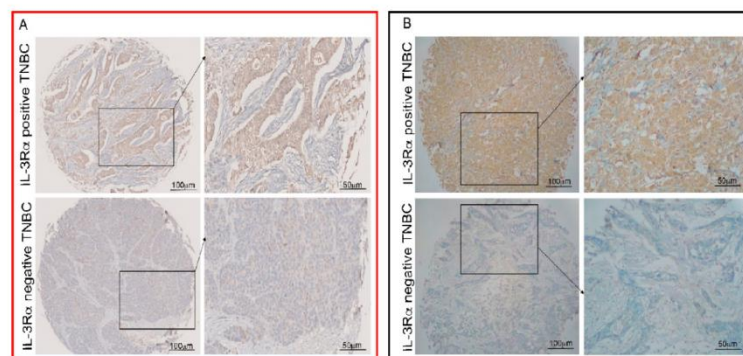**Figure 1.** Human TNBC cells express IL-3Rα. Representative tissue microarrays from human TNBC samples were stained with anti-IL-3Rα antibodies. IL-3Rα-positive and -negative TNBC samples are shown. Original magnification 10× and 20×, scale bar: 100 μm and 50 μm, respectively. Panel (**A**) (red square) refers to Turin samples and panel (**B**) (black square) to Sassari samples.
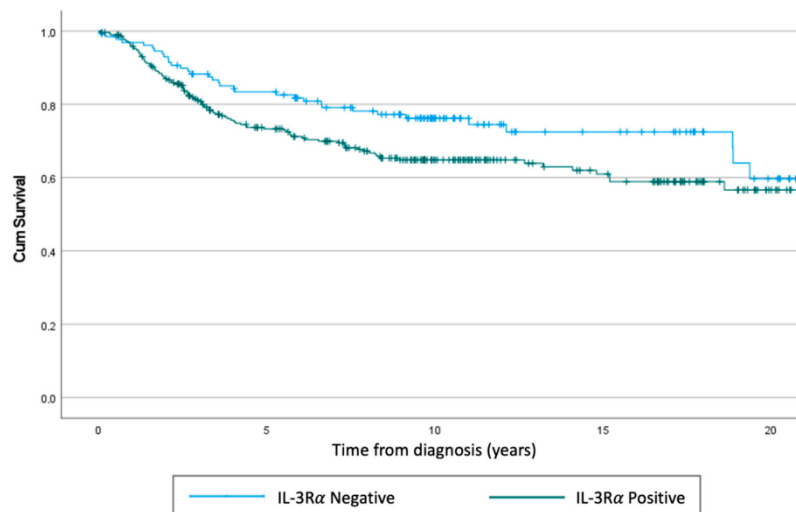
Figure 2. Kaplan–Meier of overall survival. Using the Cox regression test, we obtained a $p = 0.04$, while using the Wilcoxon–Breslow–Gehan test, the p corresponded to $p = 0.0245$.

3.2. IL-3Rα Activation Impacts EMT and Reprograms TNBC Cells towards an Endothelial-like-Phenotype

To gain insights into the biological relevance of IL-3Rα in TNBC, its expression was first investigated by selecting a panel of TNBC cell lines displaying different phenotypic features (Table S1). As in human samples, IL-3Rα was expressed in TNBC cell lines (Figure 3A,B).

Based on our retrospective study, we selected four different TNBC cell lines (two originated from pleural effusion and two from primary tumours) to evaluate whether the activation of the IL-3/IL-3Rα axis impacts TNBC aggressiveness. For this purpose, IL-3 was used to activate IL-3Rα and to investigate cell proliferation and the expression of EMT markers in TNBC. IL-3 was unable to promote TNBC proliferation in all the analysed cell lines. Therefore, Vimentin and N-Cadherin were selected as EMT markers (Figure 4A–D). IL-3 upregulated N-Cadherin in MDA-MB-231 and MDA-MB-436 and Vimentin in Hs-578T and HCC-1395 cells, while downregulated N-Cadherin in HCC-1395 cells (Figure 4D). β-catenin expression was not affected by IL-3. The SLUG, TWIST, and ZEB1 mRNA expression levels were analysed and are reported in Figure 4E–H. Possibly due to the high basal expression of these genes in TNBC cell lines, IL-3 significantly upregulated their expression only in HCC-1395 cells (Figure 4H).

Epithelial-to-endothelial transition and the formation of tumour-cell-derived vessel-like structures (vascular mimicry (VM)) are common hallmarks of TNBC aggressiveness [32,34]. Thereby, the ability of IL-3 to reprogram TNBC cells towards an endothelial-like phenotype was investigated in vitro using a three-dimensional tube-formation assay. As shown in Figure 5A,B, IL-3 induced morphological changes in cancer cells, translating in their ability to form tube-like structures.

3.3. IL-3 Boosts VM and PD-L1 Expression in Primary Tumours and Lung Metastases

The impact of the IL-3/IL-3Rα axis in TNBC biology was also investigated in vivo by injecting MDA-MB-231 and MDA-MB-436 cells in NSG mice. These cell lines were selected for their parallel EMT marker modulation, phenotype, and growth in mice [43]. The protocol is shown in Figure 6A. We failed to detect significant differences in primary tumour size between the untreated and IL-3-treated animals (Figure S1). Therefore, based on the in vitro results, the tumour-associated vasculature was examined. As shown in Figure 6B–D and Figure 6F–H, tumours from animals treated with IL-3 displayed a significant increase

in PAS-positive/CD31-negative vessels, corresponding to the vascular network built by tumour cells and denoted as VM. Conversely, vessels, mainly formed by endothelial cells, were found in control mice. Moreover, a significant increase in vessel size was detected in the animals treated with IL-3 (Figure 6E,I).
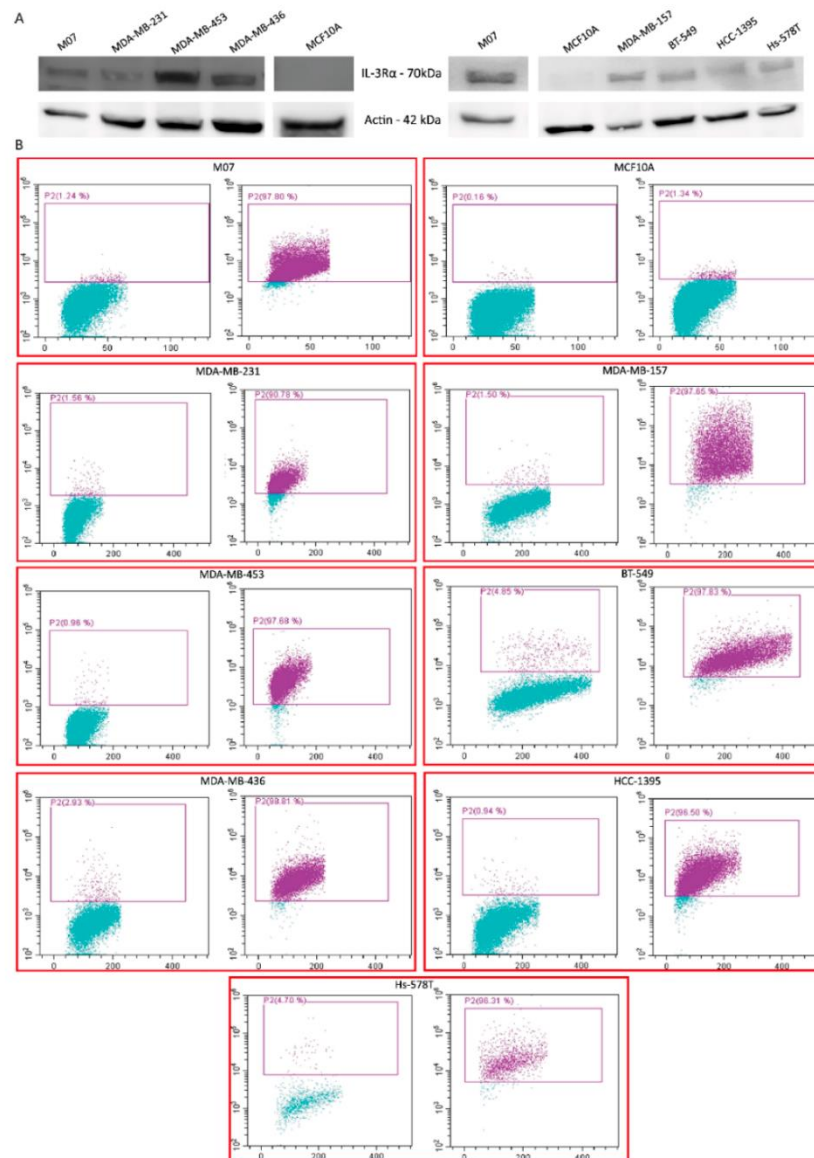
Figure 3. IL-3Rα expression in different TNBC cell lines: (**A**) representative Western blot of IL-3Rα expression in the indicated TNBC cell lines. Actin served as housekeeping gene. The uncropped blots are shown in Figure S2; (**B**) FACS dot plots of IL-3Rα expression (purple dots) and appropriate IgG controls (left panel in each cell line) of the indicated TNBC cell lines. M07 and MCF10A cells served as positive and negative controls, respectively.
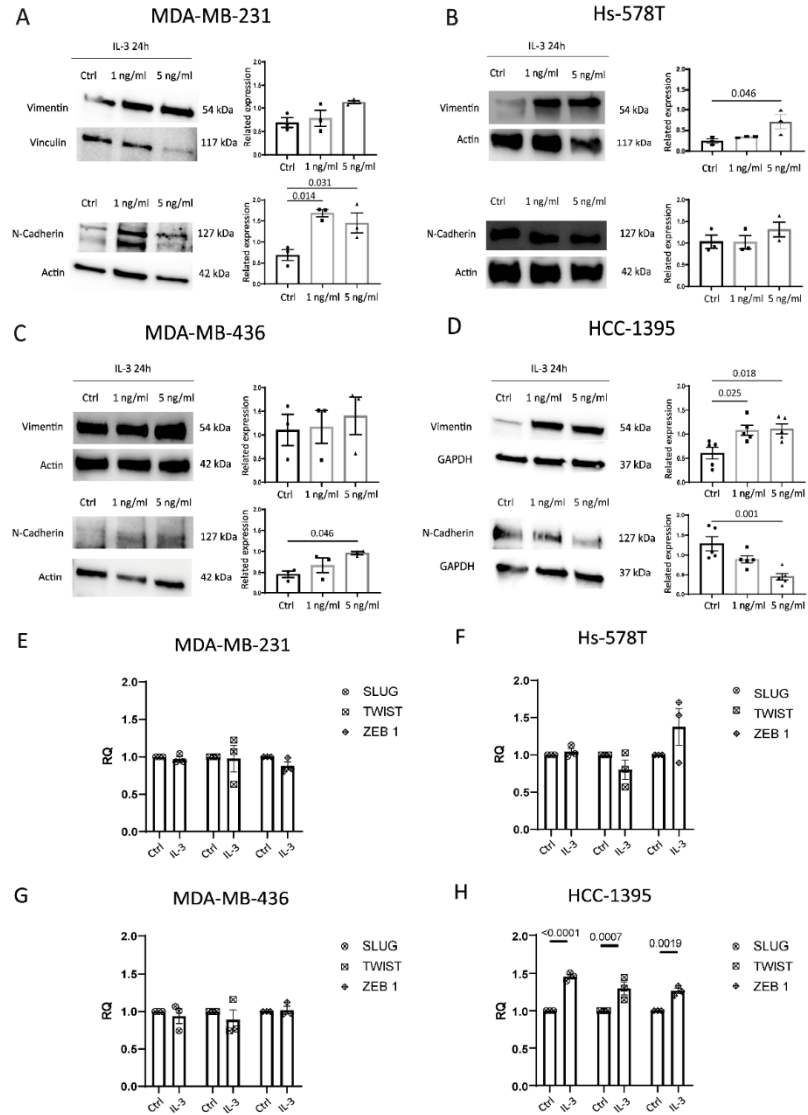
Figure 4. IL-3Rα activation impacts EMT: (**A**–**D**) representative Western blot and quantification of Vimentin and N-Cadherin expression levels in MDA-MB-231, Hs-578T, MDA-MB-436, and HCC-1395 cells untreated (Ctrl, circles on diagrams) or treated with IL-3 (1 ng/mL, squares on diagrams or 5 ng/mL, triangles on diagrams). Data are expressed as the mean ± SEM normalised to housekeeping genes (Vinculin, Actin, and GAPDH). (**E**–**H**) SLUG, TWIST1, and ZEB 1 mRNA expression levels in MDA-MB-231, Hs-578T, MDA-MB-436, and HCC-1395 cells untreated (Ctrl) or treated with IL-3 (1 ng/mL or 5 ng/mL). Data are expressed as the mean ± SEM normalised to housekeeping genes. The uncropped blots are shown in Figure S3.

We have recently shown that the EVs released by TEC upon IL-3Rα blockade modulate PD-L1 expression in myeloid cells [26]. Since cancer cells also express PD-L1, and its expression contributes to TNBC aggressiveness, PD-L1 was also evaluated in our in vivo model. IL-3 was able to significantly increase PD-L1 expression in primary tumours (Figure 7A,B),

as well as the number of lung lesions and the magnitude of the scattered PD-L1-positive tumour cells in the lung (Figure 7C–H). Overall, these data provide evidence that the IL-3/IL-3Rα signalling is a crucial remodelling pathway contributing to TNBC aggressiveness.
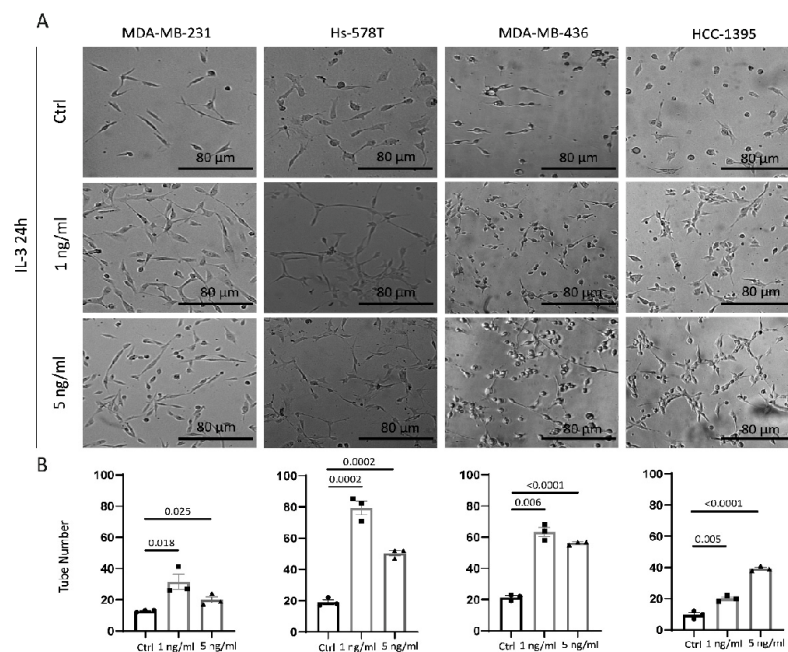
Figure 5. IL-3Rα activation reprograms TNBC cells towards an endothelial-like phenotype: (**A**) phase images of cells plated on growth factor reduced Matrigel in serum-free medium or supplemented with 1 ng/mL or 5 ng/mL of IL-3; (**B**) quantification of the vessel number was performed over at least three independent replicates for each cell line. MDA-MB-231, Hs-578T, MDA-MB-436, and HCC-1395 cells untreated (Ctrl, circles on diagrams) or treated with IL-3 (1 ng/mL, squares on diagrams or 5 ng/mL, triangles on diagrams) are shown. The results are expressed as mean ± SEM. Original magnification 20×, scale bar: 80 µm. Comparisons were performed using one-way ANOVA followed by Tukey's multiple-comparison test.

3.4. Bioinformatics Analysis on TCGA Data Recognises IL-3Rα as a Marker of TNBC Aggressiveness

The association between the expression of IL-3Rα and breast cancer aggressiveness was also evaluated by interrogating The Cancer Genome Atlas (TCGA) data. The results of the differential expression analysis, based on a limited number of TNBC data, indicated that IL-3Rα was highly expressed in TNBCs compared with luminal breast cancers ($p = 0.017$, $p$adj = 0.026, (Figure 8A). The TCGA data analysis also identified EMT and VM coding genes as differentially expressed in the two breast tumour groups. Moreover, IL-3Rα positively correlated with VIM (rho = 0.52, $p < 2.2 \times 10^{-16}$), ZEB2 (rho = 0.47, $p < 2.2 \times 10^{-16}$), SPRY2 (rho = 0.42, $p < 2.2 \times 10^{-16}$), MMP2 (rho = 0.37, $p < 2.2 \times 10^{-16}$), and CD274 (PD-L1) (rho = 0.38, $p < 2.2 \times 10^{-16}$) (Figure 8B). Univariate and multivariate logistic regression analyses were performed by selecting those genes with the best individual p-value (SNAI1, NFKB2, ZEB1, SMAD3, VIM, CD274, CTNNB1, MMP2, SPRY2, SNAI2, and IL-3Rα) as candidate predictors for breast cancer aggressiveness (Figure 8B). Finally, by considering the genes recapitulating IL-3 biological functions, we proposed a model, including IL-3Rα, SNAI1, ZEB1, VIM, CTNNB1, MMP2, SPRY2, and CD274, that remarkably discriminates cancer aggressiveness (AUC = 0.86 95% CI = 0.82–0.89) (Figure 8C).
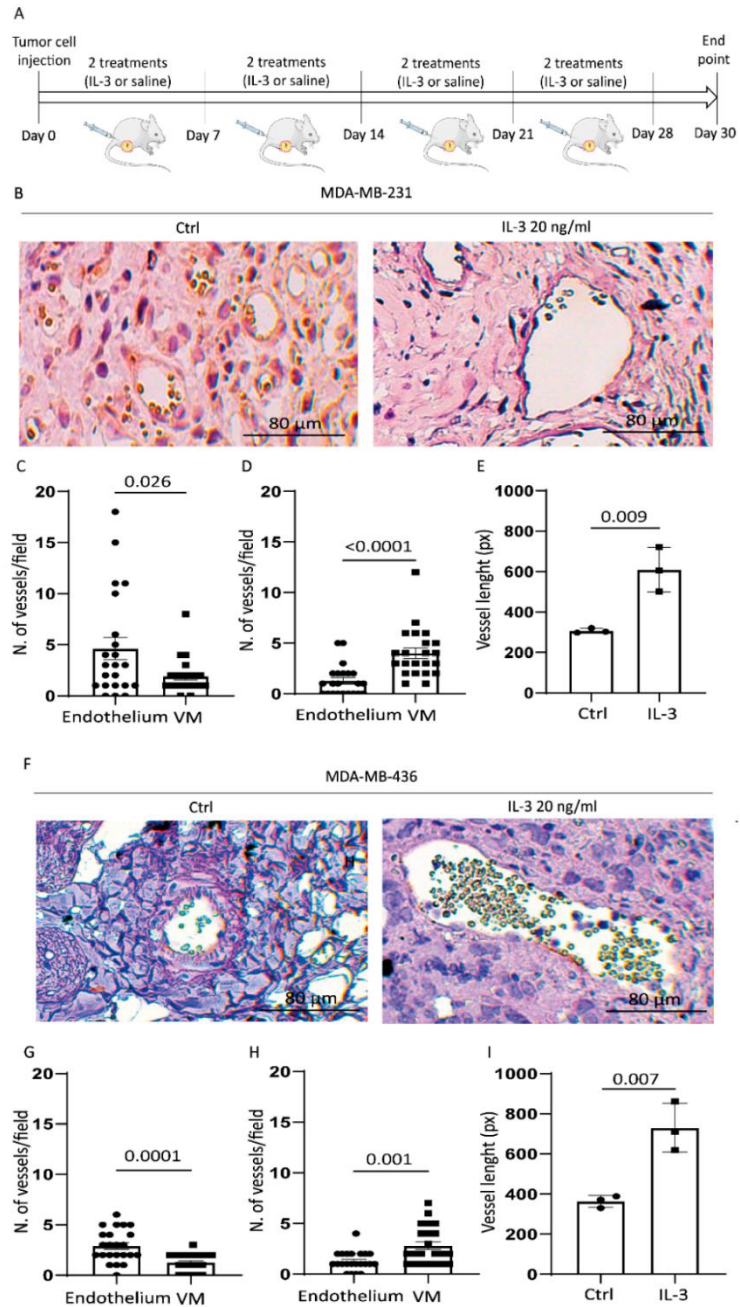
Figure 6. IL-3Rα activation promotes VM and increases the vessel size in vivo: (**A**) NSG mice were injected with tumour cells (as indicated) and treated from day 0 with saline or IL-3 (20 ng/mL) twice a week for 4 weeks. The figure was partly generated using Servier Medical Art templates, which are licensed under a Creative Commons Attribution 3.0 Unported License; https://smart.servier.com, (accessed on 5 August 2022). Tumours were recovered at day 30; (**B**) representative images of MDA-MB-

23- derived tumours untreated (Ctrl) or treated with IL-3 (20 ng/mL) stained with anti-CD31 antibody (brown colour) and PAS (violet colour); (**C,D**) relative quantification of VM/endothelium expressed as the number of CD31+/PAS+ per field ± SEM ((**C**) corresponds to control, while (**D**) refers to IL-3 treatment); (**E**) quantification of the vessel size in MDA-MB-231-derived tumours. The results are expressed as mean ± SEM; (**F**) representative images of MDA-MB-436-derived tumours untreated (Ctrl) or treated with IL-3 (20 ng/mL) stained with anti-CD31 antibody and PAS; (**G,H**) relative quantification of VM/endothelium expressed as the number of CD31+/PAS+ per field ± SEM ((**G**) corresponds to control, while (**H**) refers to IL-3 treatment); (**I**) Quantification of the vessel size in MDA-MB-436 derived tumours. Circles on diagrams represent the quantity of CD31+ structures per field, squares represent the quantity of PAS+ structures per field. The results are the mean ± SEM. Original magnification 20×, scale bar: 80 μm. Comparisons were performed using Student's *t*-test.
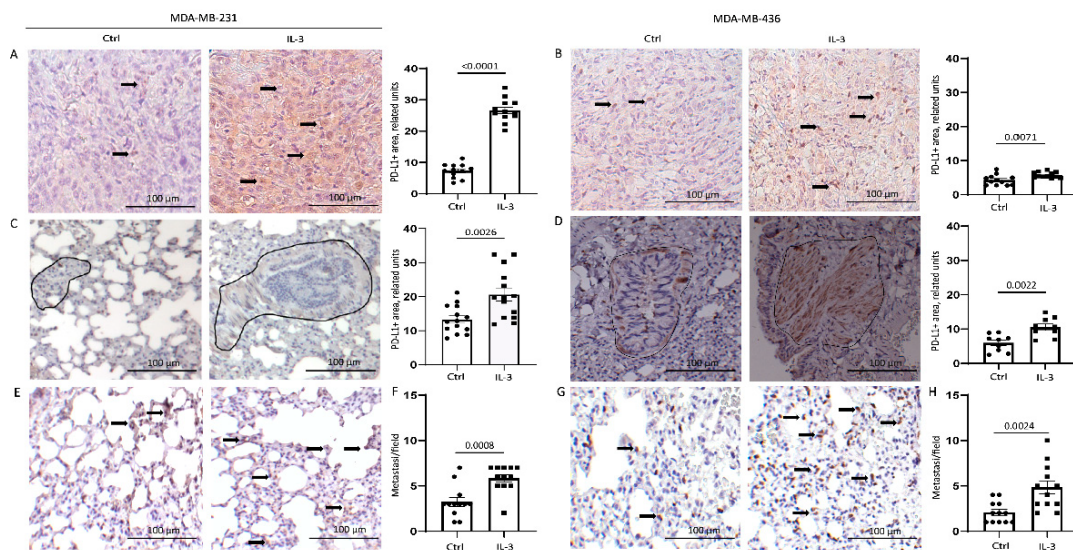
Figure 7. IL-3Rα activation boosts PD-L1 expression in primary tumours and lung metastases: (**A,B**) representative images and quantification of PD-L1 expression in primary tumours derived from mice injected with MDA-MB-231 (**A**) and MDA-MB-436 (**B**) cells untreated or treated with IL-3; (**C,D**) representative images and quantification of PD-L1 expression in the lung tissues of mice injected with MDA-MB-231 (**C**) and MDA-MB-436 (**D**) cells left untreated or treated with IL-3. Diagram data are presented as PD-L1+ area/lung ± SEM; (**E,G**) representative images of scattered PD-L1+ cells in the lung tissues of mice injected with MDA-MB-231 (**E**) and MDA-MB-436 (**G**) cells untreated or treated with IL-3; (**F,H**) diagrams reporting the number of lung metastases counted according to PD-L1 expression in mice injected with MDA-MB-231 (**F**) or MDA-MB-436 (**H**) cells untreated or treated with IL-3. Diagram data are expressed as PD-L1+ metastasis/field ± SEM. Circles on diagrams represent PD-L1 quantification in control mice tissues, squares represent the quantity of PD-L1+ structures in the mice treated with IL-3. Original magnification 20× scale bar: 100 μm. Comparisons were performed using Student's *t*-test.

B		Correlation Test (Spearman)		Univariate Model		Multivariate Model
GENE	RHO	p-value	AUC	p-value	p-value
IL-3Ra	[reference]		0.52	0.045*	0.017*
SNAI1	0.34	$<2.2\times10^{-16}$ ***	0.73	1.01×10^{-9} ***	0.00015 ***
NFKB2	0.29	$<2.2\times10^{-16}$ ***	0.66	9.98×10^{-9} ***	0.085
ZEB1	0.33	$<2.2\times10^{-16}$ ***	0.30	8.72×10^{-8} ***	0.00027 ***
SMAD3	0.06	0.0242 *	0.35	1.06×10^{-5} ***	0.081
VIM	0.52	$<2.2\times10^{-16}$ ***	0.67	1.73×10^{-5} ***	0.0001 ***
CTNNB1	−0.10	0.0005 ***	0.56	0.00078 ***	0.00149 **
MMP2	0.37	$<2.2\times10^{-16}$ ***	0.41	0.00276 **	0.0045 **
SPRY2	0.42	$<2.2\times10^{-16}$ ***	0.64	0.00459 **	0.0752
SNAI2	0.32	$<2.2\times10^{-16}$ ***	0.53	0.0107 *	0.2853
SMAD2	−0.15	3.44×10^{-7} ***	0.51	0.191	[excluded]
TWISTNB	−0.13	6.56×10^{-5} ***	0.57	0.442	[excluded]
ZEB2	0.47	$<2.2\times10^{-16}$ ***	0.50	0.54	[excluded]
BRCA1	−0.39	$<2.2\times10^{-16}$ ***	0.46	0.612	[excluded]
NFKB1	0.12	3.93×10^{-5} ***	0.48	0.958	[excluded]

Figure 8. Bioinformatics analysis of TCGA dataset: (**A**) volcano plots of DEGs in TNBC and luminal breast cancers. Log2FC is displayed on the y-axis and the −log10 of *p*-value on the x-axis. Dots represent upregulated and downregulated genes; the blue points are those whose *p*-values were statistically significant ($p < 0.05$); (**B**) correlation of gene expression between IL-3Rα and genes involved in EMT and CD274 (PD-L1) (correlation test). The closer the RHO corresponds to 1, the more the correlation. Results of the univariate model show the discriminating power of single genes (AUC). The *p*-value of the multivariate model showed that all selected genes were relevant for the efficiency of the model. * *p*-value ≤ 0.05; ** *p*-value ≤ 0.01; *** *p*-value ≤ 0.001; (**C**) ROC curve representing the multivariate logistic model. This model, composed of IL-3Rα, SNAI1, ZEB1, VIM, CTNNB1, MMP2, SPRY2, and CD274 (PD-L1), showed the effectiveness in discriminating breast cancer aggressiveness. (AUC = 0.86 95% CI = 0.82–0.89).

4. Discussion

In the present study, we identified IL-3Rα as an additional TNBC prognostic biomarker and provided the proof of concept that TNBC aggressiveness also stems from the IL-3/IL-3Rα signalling pathway.

TNBC is a deep heterogeneous breast cancer lacking canonical breast cancer markers such as the oestrogen, progesterone, and HER2 receptors [1], and thus targeted treatments [5]. Herein, we demonstrated that 291 out of the 421 TNBC specimens examined (69%) were positive for IL-3Rα. The TCGA data analysis, grouping 1080 luminal breast cancer samples and 125 TNBC samples, confirmed this observation.

IL-3 is a proinflammatory and proangiogenic cytokine mainly released by activated T lymphocytes and mast cells in the TME [44] and acts as an autocrine factor for human breast and kidney tumour-derived endothelial cells [24]. The biological relevance of IL-3 and its receptor has been extensively investigated in the haemopoietic and vascular compartments [45], while their role in TNBC is yet unknown. We herein demonstrated that the expression of IL-3Rα in human TNBC samples correlates with the presence of metastatic nodes and with a poor overall survival rate. The data from TCGA established that several genes closely linked to EMT, and angiogenesis positively correlate with the IL-3Rα expression in TNBC. The angiogenic process is instrumental for tumour development and metastatic spread [46]. However, cancer dissemination also relies on the ability of cancer cells to build their own vascular network embedded into the endothelial layer, in a process known as VM [47]. Notably, EMT regulators and EMT-related transcription factors are generally regarded as hallmarks of VM and TNBC progression [48]. Consistent with the TCGA molecular annotation, our data proved that the IL-3/IL-3Rα axis drives changes in EMT markers and acts as a booster of VM in vivo, translating into tumour cell homing and outgrowth in the lung.

Tumour cells sense cues released by TME components and promptly adapt to any favouring challenge [49]. These reciprocal interactions within the TME translate into tumour cell reprogramming and shift towards specific "phenotypic identity", outgrowth, and dissemination [50]. Among these reprogramming plans, the dynamic and reversible EMT to mesenchymal–epithelial transition and the epithelial-to-endothelial switch appear relevant [50]. We herein reported that the activation of IL-3Rα drives endothelial-like features, enhances the formation of large blood lacunae, which replace and fulfil endothelial cell functions, and boosts TNBC metastatic spread. VM is highly prevalent and more frequently identified in TNBC compared with luminal or HER2+ breast cancers and is generally associated with tumour progression [51,52]. Therefore, the close relationship between VM, EMT, and the expression of a functional IL-3Rα provides additional insight into the role of IL-3/IL-3Rα in the complex molecular programme guiding TNBC metastatic spread and aggressiveness. Moreover, since resistance to antiangiogenic treatments also relies on the occurrence of VM [53], the activation of the IL-3/IL-3Rα-mediated signalling may represent one of the rescue pathways granting tumour cell survival in this clinical scenario. In addition, consistent with "omics technologies" [54], our results provide evidence of the heterogeneity of IL-3Rα response in different TNBCs (the ability to induce the expression of EMT marker was tumour-specific), as well as on the ability of IL-3Rα to activate common pathways (the induction of the epithelial-to-endothelial switch was detected in all the cell lines tested).

The TME in TNBCs is unique and dynamically contributes to tumour immune evasion via discrete mechanisms including the aberrant expression of immune checkpoint proteins, such as PD-L1 and the programmed cell death-ligand 1 receptor [55]. PD-L1 is highly expressed in several cancer types [56] and much more in TNBCs compared with other breast cancer subtypes [57]. Genetic and epigenetic mechanisms, as well as inflammatory stimuli, control PD-L1 expression in cancers [58,59]. We demonstrated that IL-3Rα activation increases PD-L1 expression in primary tumours and in metastatic lung lesions, sustaining a role in the control of anti-tumour immune response. Soluble factors released in the TME also dictate the clinical benefits of checkpoint inhibitors [54]. As an example, the vascular

endothelial growth factor (VEGF) was found instrumental for TME immunosuppression by inducing vascular defects and rearranging the anti-tumour immune response [60]. Therefore, our observations that, in tumour-bearing mice, the IL-3Rα-mediated signal blunted the "physiological" angiogenesis, boosted the VM, and increased the PD-L1 expression indicate that, as VEGF, IL-3 can "highjack" the TME, thereby contributing to tumour evasion.

5. Conclusions

A molecular classification based on both transcriptomics and genomics is mandatory to identify novel targets and develop innovative therapeutic options [61]. Our study, besides refining the TNBC molecular annotation, proposed a model recapitulating cancer aggressiveness. Moreover, since tumour molecular profiling supported the IL-3Rα expression in human samples and its potential role in driving tumour aggressiveness in vivo, we proved that its activation drives tumour progression; thus, investigating IL-3Rα as a potential therapeutic target presents a valuable challenge.

References

1. Yao, H.; He, G.; Yan, S.; Chen, C.; Song, L.; Rosol, T.J.; Deng, X. Triple-Negative Breast Cancer: Is There a Treatment on the Horizon? *Oncotarget* **2017**, *8*, 1913–1924. [CrossRef] [PubMed]
2. da Silva, J.L.; Cardoso Nunes, N.C.; Izetti, P.; de Mesquita, G.G.; de Melo, A.C. Triple Negative Breast Cancer: A Thorough Review of Biomarkers. *Crit. Rev. Oncol. Hematol.* **2020**, *145*, 102855. [CrossRef] [PubMed]
3. Dent, R.; Trudeau, M.; Pritchard, K.I.; Hanna, W.M.; Kahn, H.K.; Sawka, C.A.; Lickley, L.A.; Rawlinson, E.; Sun, P.; Narod, S.A. Triple-Negative Breast Cancer: Clinical Features and Patterns of Recurrence. *Clin. Cancer Res. Off. J. Am. Assoc. Cancer Res.* **2007**, *13*, 4429–4434. [CrossRef]
4. Fatima, I.; El-Ayachi, I.; Playa, H.C.; Alva-Ornelas, J.A.; Khalid, A.B.; Kuenzinger, W.L.; Wend, P.; Pence, J.C.; Brakefield, L.; Krutilina, R.I.; et al. Simultaneous Multi-Organ Metastases from Chemo-Resistant Triple-Negative Breast Cancer Are Prevented by Interfering with WNT-Signaling. *Cancers* **2019**, *11*, 2039. [CrossRef] [PubMed]
5. Won, K.-A.; Spruck, C. Triple-negative Breast Cancer Therapy: Current and Future Perspectives (Review). *Int. J. Oncol.* **2020**, *57*, 1245–1261. [CrossRef] [PubMed]

6. He, L.; Wick, N.; Germans, S.K.; Peng, Y. The Role of Breast Cancer Stem Cells in Chemoresistance and Metastasis in Triple-Negative Breast Cancer. *Cancers* **2021**, *13*, 6209. [CrossRef]

7. Xie, Y.-H.; Chen, Y.-X.; Fang, J.-Y. Comprehensive Review of Targeted Therapy for Colorectal Cancer. *Signal Transduct. Target. Ther.* **2020**, *5*, 22. [CrossRef]

8. Kitamura, T.; Sato, N.; Arai, K.-i.; Miyajima, A. Expression Cloning of the Human IL-3 Receptor CDNA Reveals a Shared Beta Subunit for the Human IL-3 and GM-CSF Receptors. *Cell* **1991**, *66*, 1165–1174. [CrossRef]

9. Hayashida, K.; Kitamura, T.; Gorman, D.M.; Arait, K.-I.; Yokotat, T.; Miyajima, A. Molecular Cloning of a Second Subunit of the Receptor for Human Granulocyte-Macrophage Colony-Stimulating Factor (GM-CSF): Reconstitution of a High-Affinity GM-CSF Receptor (Cytokine Receptor/Hemopoietic Growth Factor/Hemopoiesis Gene Family). *Proc. Natl. Acad. Sci. USA* **1990**, *87*, 9655–9659. [CrossRef]

10. Lopez, A.F.; Elliott, M.J.; Woodcock, J.; Vadas, M.A. GM-CSF, IL-3 and IL-5: Cross-Competition on Human Haemopoietic Cells. *Immunol. Today* **1992**, *13*, 495–500. [CrossRef]

11. Nicola, N.A.; Metcalf, D. Subunit Promiscuity among Hemopoietic Growth Factor Receptors. *Cell* **1991**, *67*, 1–224. [CrossRef]

12. Elliott, M.; Vadas, M.; Eglinton, J.; Park, L.; To, L.; Cleland, L.; Clark, S.; Lopez, A. Recombinant Human Interleukin-3 and Granulocyte-Macrophage Colony- Stimulating Factor Show Common Biological Effects and Binding Characteristics on Human Monocytes. *Blood* **1989**, *74*, 2349–2359. [CrossRef]

13. Lopez, A.F.; To, L.B.; Yang, Y.C.; Gamble, J.R.; Shannon, M.F.; Burns, G.F.; Dyson, P.G.; Juttner, C.A.; Clark, S.; Vadas, M.A. Stimulation of Proliferation, Differentiation, and Function of Human Cells by Primate Interleukin 3. *Proc. Natl. Acad. Sci. USA* **1987**, *84*, 2761–2765. [CrossRef] [PubMed]

14. Haak-Frendscho, M.; Arai, N.; Arai, K.I.; Baeza, M.L.; Finn, A.; Kaplan, A.P. Human Recombinant Granulocyte-Macrophage Colony-Stimulating Factor and Interleukin 3 Cause Basophil Histamine Release. *J. Clin. Investig.* **1988**, *82*, 17–20. [CrossRef] [PubMed]

15. Lopez, A.F.; Eglinton, J.M.; Lyons, A.B.; Tapley, P.M.; To, L.B.; Park, L.S.; Clark, S.C.; Vadas, M.A. Human Interleukin-3 Inhibits the Binding of Granulocyte-Macrophage Colony-Stimulating Factor and Interleukin-5 to Basophils and Strongly Enhances Their Functional Activity. *J. Cell Physiol.* **1990**, *145*, 69–77. [CrossRef] [PubMed]

16. Smith, W.B.; Guida, L.; Sun, Q.; Korpelainen, E.I.; van den Heuvel, C.; Gillis, D.; Hawrylowicz, C.M.; Vadas, M.A.; Lopez, A.F. Neutrophils Activated by Granulocyte-Macrophage Colony-Stimulating Factor Express Receptors for Interleukin-3 Which Mediate Class II Expression. *Blood* **1995**, *86*, 3938–3944. [CrossRef] [PubMed]

17. Clark, S.C.; Kamen, R. The Human Hematopoietic Colony-Stimulating Factors. *Science* **1987**, *236*, 1229–1237. [CrossRef]

18. Metcalf, D. The Molecular Control of Cell Division, Differentiation Commitment and Maturation in Haemopoietic Cells. *Nature* **1989**, *339*, 27–30. [CrossRef]

19. Moldenhauer, L.M.; Cockshell, M.P.; Frost, L.; Parham, K.A.; Tvorogov, D.; Tan, L.Y.; Ebert, L.M.; Tooley, K.; Worthley, S.; Lopez, A.F.; et al. Interleukin-3 Greatly Expands Non-Adherent Endothelial Forming Cells with pro-Angiogenic Properties. *Stem Cell Res.* **2015**, *14*, 380–395. [CrossRef]

20. Korpelainen, E.I.; Gamble, J.R.; Smith, W.B.; Dottore, M.; Vadas, M.A.; Lopez, A.F. Interferon-γ Upregulates Interleukin-3 (IL-3) Receptor Expression in Human Endothelial Cells and Synergizes with IL-3 in Stimulating Major Histocompatibility Complex Class II Expression and Cytokine Production. *Blood* **1995**, *86*, 176–182. [CrossRef]

21. Korpelainen, E.I.; Gamble, J.R.; Smith, W.B.; Goodall, G.J.; Qiyu, S.; Woodcock, J.M.; Dorrore, M.; Vadas, M.A.; Lopez, A.F.; Miller, J.F.A.P. The Receptor for Interleukin 3 Is Selectively Induced in Human Endothelial Cells by Tumor Necrosis Factor a and Potentiates Interleukin 8 Secretion and Neutrophil Transmigration (Lnlammation/Leukocytes/Cytokines/Allerg). *Proc. Natl. Acad. Sci. USA* **1993**, *90*, 11137–11141. [CrossRef] [PubMed]

22. Lopatina, T.; Grange, C.; Cavallari, C.; Navarro-Tableros, V.; Lombardo, G.; Rosso, A.; Cedrino, M.; Pomatto, M.A.C.; Koni, M.; Veneziano, F.; et al. Targeting IL-3Rα on Tumor-Derived Endothelial Cells Blunts Metastatic Spread of Triple-Negative Breast Cancer via Extracellular Vesicle Reprogramming. *Oncogenesis* **2020**, *9*, 90. [CrossRef] [PubMed]

23. Peoples, G.E.; Goedegebuure, P.S.; Valerie, J.; Andrews, R.; Schoof, D.D.; Eberlein, T.J. HLA-A2 Presents Shared Tumor-Associated Antigens Derived from Endogenous Proteins in Ovarian Cancer'. *J. Immunol.* **1993**, *151*, 5481–5491. [PubMed]

24. Dentelli, P.; Rosso, A.; Olgasi, C.; Camussi, G.; Brizzi, M.F. IL-3 Is a Novel Target to Interfere with Tumor Vasculature. *Oncogene* **2011**, *30*, 4930–4940. [CrossRef]

25. Lombardo, G.; Gili, M.; Grange, C.; Cavallari, C.; Dentelli, P.; Togliatto, G.; Taverna, D.; Camussi, G.; Brizzi, M.F. IL-3R-Alpha Blockade Inhibits Tumor Endothelial Cell-Derived Extracellular Vesicle (EV)-Mediated Vessel Formation by Targeting the β-Catenin Pathway. *Oncogene* **2018**, *37*, 1175–1191. [CrossRef]

26. Lopatina, T.; Koni, M.; Grange, C.; Cedrino, M.; Femminò, S.; Lombardo, G.; Favaro, E.; Brizzi, M.F. IL-3 Signalling in the Tumour Microenvironment Shapes the Immune Response via Tumour Endothelial Cell-Derived Extracellular Vesicles. *Pharmacol. Res.* **2022**, *179*, 106206. [CrossRef]

27. Bhatia, S.; Monkman, J.; Blick, T.; Pinto, C.; Waltham, M.; Nagaraj, S.H.; Thompson, E.W. Interrogation of Phenotypic Plasticity between Epithelial and Mesenchymal States in Breast Cancer. *J. Clin. Med.* **2019**, *8*, 893. [CrossRef] [PubMed]

28. Zheng, X.; Yu, C.; Xu, M. Linking Tumor Microenvironment to Plasticity of Cancer Stem Cells: Mechanisms and Application in Cancer Therapy. *Front. Oncol.* **2021**, *11*, 2552. [CrossRef]

29. Plantamura, I.; Casalini, P.; Dugnani, E.; Sasso, M.; D'Ippolito, E.; Tortoreto, M.; Cacciatore, M.; Guarnotta, C.; Ghirelli, C.; Barajon, I.; et al. PDGFRβ and FGFR2 Mediate Endothelial Cell Differentiation Capability of Triple Negative Breast Carcinoma Cells. *Mol. Oncol.* **2014**, *8*, 968–981. [CrossRef]

30. Wagenblast, E.; Soto, M.; Gutiérrez-Ángel, S.; Hartl, C.A.; Gable, A.L.; Maceli, A.R.; Erard, N.; Williams, A.M.; Kim, S.Y.; Dickopf, S.; et al. A Model of Breast Cancer Heterogeneity Reveals Vascular Mimicry as a Driver of Metastasis. *Nature* **2015**, *520*, 358–362. [CrossRef]

31. Liu, T.J.; Sun, B.C.; Zhao, X.L.; Zhao, X.M.; Sun, T.; Gu, Q.; Yao, Z.; Dong, X.Y.; Zhao, N.; Liu, N. CD133+ Cells with Cancer Stem Cell Characteristics Associates with Vasculogenic Mimicry in Triple-Negative Breast Cancer. *Oncogene* **2013**, *32*, 544–553. [CrossRef] [PubMed]

32. Hernández de la Cruz, O.N.; López-González, J.S.; García-Vázquez, R.; Salinas-Vera, Y.M.; Muñiz-Lino, M.A.; Aguilar-Cazares, D.; López-Camarillo, C.; Carlos-Reyes, Á. Regulation Networks Driving Vasculogenic Mimicry in Solid Tumors. *Front. Oncol.* **2019**, *9*, 1419. [CrossRef] [PubMed]

33. Hendrix, M.J.C.; Seftor, E.A.; Hess, A.R.; Seftor, R.E.B. Vasculogenic Mimicry and Tumour-Cell Plasticity: Lessons from Melanoma. *Nat. Rev. Cancer* **2003**, *3*, 411–421. [CrossRef] [PubMed]

34. Liu, Q.; Qiao, L.; Liang, N.; Xie, J.; Zhang, J.; Deng, G.; Luo, H.; Zhang, J. The Relationship between Vasculogenic Mimicry and Epithelial-Mesenchymal Transitions. *J. Cell Mol. Med.* **2016**, *20*, 1761–1769. [CrossRef] [PubMed]

35. Tan, P.H.; Ellis, I.; Allison, K.; Brogi, E.; Fox, S.B.; Lakhani, S.; Lazar, A.J.; Morris, E.A.; Sahin, A.; Salgado, R.; et al. The 2019 World Health Organization Classification of Tumours of the Breast. *Histopathology* **2020**, *77*, 181–185. [CrossRef] [PubMed]

36. Dieci, M.V.; Radosevic-Robin, N.; Fineberg, S.; van den Eynden, G.; Ternes, N.; Penault-Llorca, F.; Pruneri, G.; D'Alfonso, T.M.; Demaria, S.; Castaneda, C.; et al. Update on Tumor-Infiltrating Lymphocytes (TILs) in Breast Cancer, Including Recommendations to Assess TILs in Residual Disease after Neoadjuvant Therapy and in Carcinoma in Situ: A Report of the International Immuno-Oncology Biomarker Working Group on Breast Cancer. *Semin. Cancer Biol.* **2018**, *52*, 16–25. [CrossRef]

37. Avanzi, G.C.; Brizzi, M.F.; Giannotti, J.; Ciarletta, A.; Yang, Y.C.; Pegoraro, L.; Clark, S.C. M-07e Human Leukemic Factor-Dependent Cell Line Provides a Rapid and Sensitive Bioassay for the Human Cytokines GM-CSF and IL-3. *J. Cell Physiol.* **1990**, *145*, 458–464. [CrossRef]

38. Weinstein, J.N.; Collisson, E.A.; Mills, G.B.; Shaw, K.R.M.; Ozenberger, B.A.; Ellrott, K.; Shmulevich, I.; Sander, C.; Stuart, J.M. The Cancer Genome Atlas Pan-Cancer Analysis Project. *Nat. Genet.* **2013**, *45*, 1113–1120. [CrossRef] [PubMed]

39. Spratt, D.E.; Chan, T.; Waldron, L.; Speers, C.; Feng, F.Y.; Ogunwobi, O.O.; Osborne, J.R. Racial/Ethnic Disparities in Genomic Sequencing. *JAMA Oncol.* **2016**, *2*, 1070–1074. [CrossRef] [PubMed]

40. Blum, A.; Wang, P.; Zenklusen, J.C. SnapShot: TCGA-Analyzed Tumors. *Cell* **2018**, *173*, 530. [CrossRef]

41. Urru, S.A.M.; Gallus, S.; Bosetti, C.; Moi, T.; Medda, R.; Sollai, E.; Murgia, A.; Sanges, F.; Pira, G.; Manca, A.; et al. Clinical and Pathological Factors Influencing Survival in a Large Cohort of Triple-Negative Breast Cancer Patients. *BMC Cancer* **2018**, *18*, 56. [CrossRef] [PubMed]

42. Peduzzi, P.; Concato, J.; Kemper, E.; Holford, T.R.; Feinstein, A.R. A Simulation Study of the Number of Events per Variable in Logistic Regression Analysis. *J. Clin. Epidemiol.* **1996**, *49*, 1373–1379. [CrossRef]

43. Iorns, E.; Drews-Elger, K.; Ward, T.M.; Dean, S.; Clarke, J.; Berry, D.; El Ashry, D.; Lippman, M. A New Mouse Model for the Study of Human Breast Cancer Metastasis. *PLoS ONE* **2012**, *7*, e47995. [CrossRef] [PubMed]

44. Dougan, M.; Dranoff, G.; Dougan, S.K. GM-CSF, IL-3, and IL-5 Family of Cytokines: Regulators of Inflammation. *Immunity* **2019**, *50*, 796–811. [CrossRef] [PubMed]

45. Park, L.S.; Waldron, P.E.; Friend, D.; Sassenfeld, H.M.; Price, V.; Anderson, D.; Cosman, D.; Andrews, R.G.; Bernstein, I.D.; Urdal, D.L. Interleukin-3, GM-CSF, and G-CSF Receptor Expression on Cell Lines and Primary Leukemia Cells: Receptor Heterogeneity and Relationship to Growth Factor Responsiveness. *Blood* **1989**, *74*, 56–65. [CrossRef] [PubMed]

46. Lugano, R.; Ramachandran, M.; Dimberg, A. Tumor Angiogenesis: Causes, Consequences, Challenges and Opportunities. *Cell Mol. Life Sci.* **2020**, *77*, 1745–1770. [CrossRef]

47. Belotti, D.; Pinessi, D.; Taraboletti, G. Alternative Vascularization Mechanisms in Tumor Resistance to Therapy. *Cancers* **2021**, *13*, 1912. [CrossRef] [PubMed]

48. Wu, Q.; Wang, J.; Liu, Y.; Gong, X. Epithelial Cell Adhesion Molecule and Epithelial-Mesenchymal Transition Are Associated with Vasculogenic Mimicry, Poor Prognosis, and Metastasis of Triple Negative Breast Cancer. *Int. J. Clin. Exp. Pathol.* **2019**, *12*, 1678–1689. [PubMed]

49. Sistigu, A.; Musella, M.; Galassi, C.; Vitale, I.; De Maria, R. Tuning Cancer Fate: Tumor Microenvironment's Role in Cancer Stem Cell Quiescence and Reawakening. *Front. Immunol.* **2020**, *11*, 2166. [CrossRef]

50. Kröger, C.; Afeyan, A.; Mraz, J.; Eaton, E.N.; Reinhardt, F.; Khodor, Y.L.; Thiru, P.; Bierie, B.; Ye, X.; Burge, C.B.; et al. Acquisition of a Hybrid E/M State Is Essential for Tumorigenicity of Basal Breast Cancer Cells. *Proc. Natl. Acad. Sci. USA* **2019**, *116*, 7353–7362. [CrossRef] [PubMed]

51. Liu, T.; Sun, B.; Zhao, X.; Gu, Q.; Dong, X.; Yao, Z.; Zhao, N.; Chi, J.; Liu, N.; Sun, R.; et al. HER2/Neu Expression Correlates with Vasculogenic Mimicry in Invasive Breast Carcinoma. *J. Cell Mol. Med.* **2013**, *17*, 116–122. [CrossRef] [PubMed]

52. Zhang, D.; Sun, B.; Zhao, X.; Ma, Y.; Ji, R.; Gu, Q.; Dong, X.; Li, J.; Liu, F.; Jia, X.; et al. Twist1 Expression Induced by Sunitinib Accelerates Tumor Cell Vasculogenic Mimicry by Increasing the Population of CD133+ Cells in Triple-Negative Breast Cancer. *Mol. Cancer* **2014**, *13*, 207. [CrossRef] [PubMed]

53. Ribatti, D.; Solimando, A.G.; Pezzella, F. The Anti-VEGF(R) Drug Discovery Legacy: Improving Attrition Rates by Breaking the Vicious Cycle of Angiogenesis in Cancer. *Cancers* **2021**, *13*, 3433. [CrossRef] [PubMed]
54. Marra, A.; Trapani, D.; Viale, G.; Criscitiello, C.; Curigliano, G. Practical Classification of Triple-Negative Breast Cancer: Intratumoral Heterogeneity, Mechanisms of Drug Resistance, and Novel Therapies. *NPJ Breast Cancer* **2020**, *6*, 54. [CrossRef] [PubMed]
55. Bou Zerdan, M.; Ghorayeb, T.; Saliba, F.; Allam, S.; Bou Zerdan, M.; Yaghi, M.; Bilani, N.; Jaafar, R.; Nahleh, Z. Triple Negative Breast Cancer: Updates on Classification and Treatment in 2021. *Cancers* **2022**, *14*, 1253. [CrossRef]
56. Han, Y.; Liu, D.; Li, L. PD-1/PD-L1 Pathway: Current Researches in Cancer. *Am. J. Cancer Res.* **2020**, *10*, 727–742.
57. Schmid, P.; Adams, S.; Rugo, H.S.; Schneeweiss, A.; Barrios, C.H.; Iwata, H.; Diéras, V.; Hegg, R.; Im, S.-A.; Shaw Wright, G.; et al. Atezolizumab and Nab-Paclitaxel in Advanced Triple-Negative Breast Cancer. *N. Engl. J. Med.* **2018**, *379*, 2108–2121. [CrossRef]
58. Shi, Y. Regulatory Mechanisms of PD-L1 Expression in Cancer Cells. *Cancer Immunol. Immunother.* **2018**, *67*, 1481–1489. [CrossRef]
59. Chen, B.; Hu, J.; Hu, X.; Chen, H.; Bao, R.; Zhou, Y.; Ye, Y.; Zhan, M.; Cai, W.; Li, H.; et al. DENR Controls JAK2 Translation to Induce PD-L1 Expression for Tumor Immune Evasion. *Nat. Commun.* **2022**, *13*, 2059. [CrossRef]
60. Khan, K.A.; Kerbel, R.S. Improving Immunotherapy Outcomes with Anti-Angiogenic Treatments and Vice Versa. *Nat. Rev. Clin. Oncol.* **2018**, *15*, 310–324. [CrossRef]
61. Yin, L.; Duan, J.-J.; Bian, X.-W.; Yu, S.-C. Triple-Negative Breast Cancer Molecular Subtyping and Treatment Progress. *Breast Cancer Res.* **2020**, *22*, 61. [CrossRef] [PubMed]

31

Overall, we have demonstrated for the first time that IL-3Rα is highly expressed in human TNBC tumor cells. In our study, 291 out of 421 tumors, corresponding to 69%, expressed IL-3Rα at the immunohistochemical evaluation. The use of two cohorts from two different centres allowed us to confirm the percentage of its positivity, suggesting that the expression of IL-3Rα on TNBC is highly reproducible and frequent in this neoplasm. The expression of IL-3Rα was then confirmed in cell lines derived from human TNBCs, confirming that the receptor is widely expressed in tumor derived from both primary and metastatic lesions. To corroborate its relevance as a biomarker, we demonstrated that IL-3Rα was not expressed on non-neoplastic breast cells (MCF-10A). The association with a higher lymph node invasion and a significantly lower survival together with the high reproducibility of the immunohistochemical expression of IL-3Rα, suggest that the receptor can be used as a biomarker for the characterization of a more aggressive and poorer prognosis subset of TNBC. We also demonstrated that IL-3, when administered *in vitro* to TNBC cell lines confers a more aggressive phenotype by including EMT, VM, and impairing the anti-tumor immune response. We demonstrated that, when stimulated with IL-3, TNBC cells, undergo profound phenotypic changes forming tubular structures assuming endothelial-like characteristics. IL-3 has been also shown to regulate EMT- and VM-related transcription factors.

The deep association of IL-3Rα expression with other genes involved in EMT and MV was further confirmed by gene expression analysis on a large number of TCGA-derived BC. IL-3Rα expression positively correlates with the expression of pivotal VM genes, suggesting that stimulation of the IL-3/IL-3Rα axis is instrumental in the activation of mechanisms that confer tumor aggressiveness. From the analysis of the TCGA data also emerged that a set of genes related to EMT and VM, together with the expression of IL-3Rα accurately discriminate this molecular subtype.

Finally, we evaluated the role of IL-3Rα in an *in vivo* model using NGS mice. *In vivo* experiments demonstrated that IL-3 administration increases the metastatic potential and the formation of large vascular lacunae lined with tumor cells. We also demonstrated that

the activation of the IL-3/IL-3Rα axis *in vivo* favours VM and dissemination of tumor cells. Moreover, IL-3 showed the ability to remodel tumor immunogenicity by increasing the expression programmed cell death ligand 1 (PD-L1). PD-L1 is differentially expressed by neoplastic cells and contributes to the inhibition of the anti-tumor immune response, thereby facilitating tumor cell evasion. IL-3 *in vivo* administration, significantly increased the expression of PD-L1 on both primary tumor and metastases, thus promoting an immunosuppressed environment.

In conclusion, this study identified IL-3Rα as a potential new biomarker of aggressiveness in TNBC, thus, supporting the possibility that the IL-3/IL-3Rα axis may represent a new therapeutic frontier in TNBC.

During the three years of my PhD, I also contributed to other studies investigating the pro-tumor effects of the extracellular vesicles and to the preparation of a review focused on Wnt signalling pathway.

Extracellular Vesicles

Extracellular vesicles (EVs) were first identified in 1967 as membrane particles, termed 'platelet dust', released from activated platelets and considered as cellular components lacking any function [63]. Since then, many studies have been performed to understand the composition of EVs and their biological function. EVs are heterogeneous small membrane-bound carriers secreted in physiological and pathological conditions. EVs are composed by a lipid bilayer which encloses several cytoplasmic proteins, lipids, as well as nucleic acids, recapitulating the "cargo" of their cell of origin.

Almost any cell release EVs and they have an important role in intercellular communication modifying the behaviour of target cells at close or distant sites. EVs are shed by almost any cell including primary cells, stem cells and cancer cells [64,65], and can be identified in many biological fluids, including blood and urine [66,67].

According to the International Society of Extracellular Vesicles (ISEV), EVs can be classified as small EVs (less than 100 nm in diameter) and medium–large EVs (more than 100 nm in diameter) [68].

Since EVs are important in cell-to-cell communication, they have gained increasing interest in the past decades, and several studies have provided methodologies of isolation and characterization from several cell types and their presence was also demonstrated in body fluids [69].

Once released, EVs can act on target cells through different mechanisms. Transmembrane proteins on EVs membrane can interact with receptors expressed on target cells [70]. These receptor–ligand interactions can then activate signalling cascades affecting target cell activities. EVs can also fuse with their recipient cells to release their cargo, either by direct fusion with the cell membrane or by endocytosis [71]. The cargo and EVs function depend

on their producing cells, and it has been shown that cellular stress also affects EVs content, suggesting that intercellular communication through EVs is dynamic [11].

As above stated, EVs may differ in both protein and genetic cargo depending on their parental cell and most of the researches have focused on cancer. It has been shown that tumor-derived EVs (TEVs) carrying pro-tumorigenic proteins, such as transcription factors, miRNAs, and growth factors, strictly control tumor growth and metastasis [72,73]. Therefore, inhibiting TEVs functional effects would most likely yield some significant advantages in the treatment of neoplasms.

TEVs: trafficking, sorting, and function in TME

The TME is highly complex and dynamic affecting cancer dissemination and progression. The milieu comprises stromal cells, endothelial cells, immune cells, and various resident cells [74].

Several studies have extensively demonstrated that TEVs are active components of the TME, providing autocrine, paracrine, and other signals supporting EMT and leading to tumor growth, metastasis, immune evasion [75–77] The ratio of TEVs/normal cell–derived EVs is various, but generally, TEVs represent a majority of total EVs in patients with advanced malignancies. In the TME, TEVs participate to the intercellular crosstalk and transfer messages from the parent tumor cells to recipient cells. It has been shown that TEVs impact in non-tumorigenic cells within the TME [78]. Indeed, Paggetti et al. [79] demonstrated that TEVs released by chronic lymphocytic leukemic cells induced the transition of stromal cells into cancer-associated fibroblasts. On the same line, a recent study demonstrated that TEVs shed from non-small cell lung cancer cells drive invasion and permeability of normal epithelial cells [80].

In the TME, TEVs can also "seed the soil" for metastasis. Cancer metastasis is a complex process where cancers spread from a primary tumor to different organs [81]. The priming of the secondary site occurs before cancer cell colonization. This process employs soluble factors such as cytokines, growth factors, proteins, metabolites as well as TEVs. TEVs also

play significant and flexible roles in cell-to-cell communication at long-distance. This property makes them ideal candidates for cancer cells to find and prime healthy tissue in distant organs to form metastatic niches.

A study has tracked GFP-labelled TEVs released by BC demonstrating that they can be up taken by other cancer cells and by normal lung tissue in orthotopic nude-mouse model, providing strong evidence that TEVs also work as long-distance messengers [82]. Another study by Costa-Silva at al. [83], demonstrated the TEVs priming activity. TEVs from pancreatic ductal adenocarcinomas induced the production of transforming growth factor-β (TGF-β) and fibronectin by hepatic stellate cells. TEVs cargo was found enriched in macrophage migration inhibitory factor involved in liver pre-metastatic niche formation. Moreover, macrophage migration inhibitory factor was found higher in TEVs of patients who developed liver metastasis.

Recently, Maji et al. have shown that TEVs originated from metastatic BC carry high levels of annexin II. Annexin II-TEVs triggered the nuclear factor kappaB (NF-kB), p38, mitogen-activated protein kinase (MAPK), and STAT3 pathways in macrophages. These pathways lead to the secretion of inflammatory cytokines, IL6 and TNF-α, and supported the establishment of the pre-metastatic niche both in brain and lung [84].

EV-mediated mechanisms of metastatic regulation also involve the recruitment of mesenchymal stem cells. Mesenchymal stem cells derived from bone marrow were found crucial to initiating metastatic process. Lindoso et. al [85] have shown that mesenchymal stem cells are susceptible to renal cancer stem cell-EVs. Indeed, it has been shown that TEVs can boost the expression of genes associated with cell migration (C-X-C chemokine receptor type 4 (CXCR4) and CXCR7), matrix remodelling (collagen type IV alpha 3 chain (COL4A3)), angiogenesis and tumor growth.

The role of TEV cargo in tumor angiogenesis

Tumor cell proliferation and metastasis highly depend on new blood vessel formation. Angiogenesis consists of sequential steps: i) degradation of basal membrane and the

subsequent extracellular matrix surrounding the blood vessels; ii) endothelial cells activation, migration and proliferation; iii) the formation of capillary tubes developing into novel basal membrane [86]. The literature suggests that angiogenesis is caused by hypoxia. The sprouting process is regulated by the balance between proangiogenic and anti-angiogenic factors, dominated by the overproduction of VEGF triggered by tissue hypoxia [87]. VEGF mediates angiogenesis and results as a key in the "angiogenic switch".

As tumor expands and grow excessively in size, cancer cells are exposed to an imbalanced oxygen supply due to diffusion from normal functional vessels. To overcome hypoxic microenvironment, malignant cells increase the TEVs release with a subsequent enhancement of EV-mediated angiogenesis. In a recent study, it was demonstrated that BC patients released TEVs into circulation that stimulate cellular changes involved in angiogenesis. More specifically, EV fractions deprived of platelet EVs increased migration, invasion and formation of new tubules when compared to the same fraction of EVs released by healthy subjects [88]. Another study demonstrated that TEVs carry VEGF on their surface promoted tumor angiogenesis. Moreover, the enrichment of VEGF in TEVs was also associated with tumor progression in patients with anti-cancer therapy [89].

HIF is a highly conserved transcription factor that controls the expression of genes regulating angiogenesis, metabolism, and cell cycle. Accordingly, hypoxia promotes vessel growth by upregulating multiple pro-angiogenic pathways that mediate key aspects of the vascular network. Interestingly, recent studies show that hypoxia influences additional aspects of angiogenesis, including vessel patterning, maturation, and function. Through extensive research, Seo et al. [90] demonstrated that E74-like ETS transcription factor 3 (ELF3) is over-expressed in epithelial ovarian cancer under hypoxia. ELF3 transcriptionally upregulated insulin-like growth factor-1 (IGF1). IGF1 promoted the stability of HIF-1α thereby increasing its protein level and enhancing VEGF expression and tumor angiogenesis.

TEVs influence endothelial cells to stimulate vascular permeability and angiogenesis. Studies suggested that these TEVs contribute to angiogenesis. Dentelli et al. [61] showed that BC tissue released IL-3, which influences TECs in the TME. IL-3-treated cancer cells also

secreted TEVs, serving as a paracrine mechanism for neighbour cells. When tumor TECs were treated with a blocking IL-3Rα antibody, TEVs miR-214-3p content was upregulated, while miR-24-3p downregulated. These two miRNAs regulated neovessel structures through the Wnt/β-catenin pathway. Moreover, TEVs derived from TECs pre-treated with anti-IL-3Rα antibody induce regression of tumor neovessels *in vivo* [62].

A hypoxic TME, due to a fast and uncontrollable growth of cancer influences tumor cells to secrete not only several chemical mediators but also EVs, which contribute to neovasculature.

TEVs: multi-faced tools for tumor immune escape

To guarantee and support its development, tumors adopt many strategies to affect the surrounding microenvironment. One of the most powerful strategies through which cancer protects its growth involves the immune evasion [91].

The mechanisms underlying immune escape has attracted particular attention in the scientific community in the last years. Recent data highlighted the contribute of TEVs in cancer immune evasion acting on T cells exhaustion, regulatory T cells (Treg) and myeloid-derived suppressor cells (MDSCs) expansion.

In a study published by Shen et al. [92], it has been shown that prostatic cancer TEVs negatively regulate T cell functions. They treated CD8+ T cells with prostatic cancer TEVs and demonstrated that TEVs induced apoptosis in CD8+ T cells by activating endoplasmic reticulum stress via the p38 MAPK signalling pathway. Furthermore, TEVs induced Treg amplification through the upregulation of forkhead box O (FOXO) transcription factor and nuclear translocation in FOXP3+ Treg cells. Another study showed that TEVs induced the expansion of human Treg. More specifically, TEVs-associated IL-10 and TGF-β1 mediate Treg induction and expression of FasL, IL-10, TGF-β1, cytotoxic T-lymphocyte antigen 4 (CTLA4), granzyme B, and perforin [93].

T cells exhaustion exhibits dysfunctional function and decreased viability and proliferation. There is a consensus that exhausted T cells display some common marker, including:

programmed cell death protein-1(PD-1), lymphocyte activation gene 3 (LAG3), CTLA4 and T cell immunoglobulin mucin 3 (TIM3) along with a reduced proliferative capacity when stimulated [94].

In a study by Wang et colleagues [95] the relationship between CTLA4 and LAG3 in TILs from patients with esophageal squamous cell carcinoma was investigated. They found a positive correlation between LAG3 and CTLA4 expression. The double positive cells (LAG3+ and CTLA4+) were significantly associated with worse recurrence-free survival and overall survival.

A recent study demonstrated how B cell lymphoma derived TEVs were able to activate CD19 CAR-T cells and induce the release of multiple inflammatory cytokines including: IL-2, IL-4, interferon gamma (IFN-γ), IL-10, IL-6, and TNF-α. A persistent contact of CD19 CAR-T cells to TEVs resulted in exhausted cells. CD19 CAR-T exhausted cells upregulated PD-1 and CTLA4 expression, decreased their expansion, overstated effector cell differentiation, and impaired the anti-tumor activities [96].

Tumor cells can generate an immunosuppressive TME by increasing the expression of the inhibitory ligand PD-L1. PD-L1 prevents T cells response by binding to PD-1 expressed by T lymphocytes, avoiding cancer cell death. PD-L1 expression was found higher in advanced tumor stage and associated with poor prognosis [97]. A study demonstrated that glioblastoma TEVs carried PD-L1 on the surface. PD-L1 by binding to PD-1 blocked T cell activation and proliferation in response to T cell receptor stimulation. The use of an anti-PD-1 receptor blocking antibody reversed TEV-mediated inhibition of T cell activation [98]. During tumor development and expansion cancer cells can promote the expansion of MDSCs, a heterogeneous group of immature cells that derive from the myeloid lineage and are able to enhance immunosuppression within the TME.

Moreover, TEVs had the power to transform normal myeloid cells into MDSCs, impairing the anti-tumor immune response. Melanoma cells released TEVs able to upregulate PD-L1 expression on bone marrow immature myeloid cells as well as on immortalized myeloid suppressor cells, leading to the loss of T cell expansion. The mechanism under PD-L1 expression and the immunosuppressive potential of TEVs was found dependent on the

expression of toll-like receptors (TLR) as well as on the heat-shock protein 86 (HSP86) carried by TEVs [99].

The ability of TEVs to promote MDSCs expansion has been attributed to their functional cargo. Recently, a study provided evidence of glioma TEVs in MDSCs expansion. Authors collected TEVs from normoxic and hypoxic glioblastomas. Hypoxia-TEVs allowed a significant immunosuppressive function of MDSCs compared both *in vitro* and *in vivo*. MicroRNA sequencing revealed that miR-10a and miR-21 enriched in glioma TEVs promoted the expansion and function of MDSCs in hypoxia condition. This was mediated by RAR Related Orphan Receptor A (RORA), a miR-10a target, and Phosphatase and tensin homolog (PTEN), a miR-21 target gene [100].

Results:

- **Targeting IL-3Rα on tumor-derived endothelial cells blunts metastatic spread of triple-negative breast cancer via extracellular vesicle reprogramming**
  Lopatina T, Grange C, Cavallari C, Navarro-Tableros V, Lombardo G, Rosso A, Cedrino M, Pomatto MAC, **Koni M**, Veneziano F, Castellano I, Camussi G, Brizzi MF. Oncogenesis. 2020 Oct 10;9(10):90. doi: 10.1038/s41389-020-00274-y
  https://www.nature.com/articles/s41389-020-00274-y

- **IL-3 signalling in the tumour microenvironment shapes the immune response via tumour endothelial cell-derived extracellular vesicles**
  Lopatina T*, **Koni M***, Grange C, Cedrino M, Femminò S, Lombardo G, Favaro E, Brizzi MF. Pharmacol Res. 2022 May;179:106206. doi: 10.1016/j.phrs.2022.106206.
  * Contributed equally
  https://www.sciencedirect.com/science/article/pii/S1043661822001517?via%3Dihub

- **The Wnt Signalling Pathway: A Tailored Target in Cancer**
  Koni M, Pinnarò V, Brizzi MF. Int J Mol Sci. 2020 Oct 18;21(20):7697. doi: 10.3390/ijms21207697
  https://www.mdpi.com/1422-0067/21/20/7697

ARTICLE

Targeting IL-3Rα on tumor-derived endothelial cells blunts metastatic spread of triple-negative breast cancer via extracellular vesicle reprogramming

Tatiana Lopatina[1], Cristina Grange[1], Claudia Cavallari[2], Victor Navarro-Tableros[2], Giusy Lombardo[1], Arturo Rosso[1], Massimo Cedrino[2], Margherita Alba Carlotta Pomatto[1], Malvina Koni[1], Francesca Veneziano[1], Isabella Castellano[1], Giovanni Camussi[1] and Maria Felice Brizzi [1]

Abstract
The lack of approved targeted therapies highlights the need for new treatments for triple-negative breast cancer (TNBC) patients. Interleukin-3 (IL-3) acts as an autocrine factor for tumor–endothelial cells (TEC), and exerts pro-angiogenic paracrine action via extracellular vesicles (EVs). IL-3Rα blockade on TEC changes TEC-EV (anti-IL-3R-EV) microRNA (miR) content and promotes the regression of established vessels. As TEC is the doorway for "drug" entry into tumors, we aimed to assess whether IL-3R blockade on TEC impacts tumor progression via its unique EV cargo. First, the expression of IL-3Rα was evaluated in 27 human TNBC samples. It was noticed that, besides TEC and inflammatory cells, tumor cells from 55.5% of the human TNBC samples expressed IL-3Rα. Using human TNBC cell lines for in vitro studies, we found that, unlike native TEC-EVs (nEVs), anti-IL-3R-EVs increase apoptosis and reduced cell viability and migration. In vivo, anti-IL-3R-EV treatment induced vessel regression in established tumors formed of MDA-MB-231 cells, decreased Vimentin, β-catenin, and TWIST1 expression, almost abolished liver and lung metastases from primary tumors, and reduced lung metastasis generated via the intravenous injection of MDA-MB-231 cells. nEVs depleted of miR-24-3p (antago-miR-24-3p-EVs) were effective as anti-IL-3R-EVs in downregulating TWIST1 and reducing metastatic lesions in vivo. Consistent with network analyses of miR-24-3p gene targeting, anti-IL-3R-EVs and antago-miR-24-3p-EVs upregulate SPRY2 in MDA-MB-231 cells. Finally, SPRY2 silencing prevented anti-IL-3R-EV and antago-miR-24-3p-EV-mediated apoptotic cues.
Overall, these data provide the first evidence that IL-3Rα is highly expressed in TNBC cells, TEC, and inflammatory cells, and that IL-3Rα blockade on TEC impacts tumor progression.

Introduction

Interleukin-3 (IL-3), a cytokine mainly produced by activated T and mast cells, is involved in the regulation of hemopoietic pluripotent and progenitor cell expansion[1]. Moreover, the role of IL-3 in controlling the proliferation/survival of various target cells, including normal and tumor-derived endothelial cells (TEC), has also been reported[2,3]. IL-3 binding to its receptor promotes numerous biological effects by regulating the expression of proteins, transcriptional factors[4,5], and regulatory noncoding RNA, such as microRNAs (miRs)[6,7].

IL-3 has seen most study in hematologic malignancies[8,9]. However, the observation that tumor-infiltrating lymphocytes (TILs)[10] and TEC are able to produce IL-3[11], sustains the possibility that IL-3 can also control the tumor microenvironment (TME). IL-3 acts as an autocrine pro-survival factor, particularly in TEC[11]. It is widely accepted that the autocrine mechanism of growth, increased AKT signaling pathway activation[12,13], and the expression of pro-tumorigenic and angiogenic

Correspondence: Maria Felice Brizzi (mariafelice.brizzi@unito.it)
[1]Department of Medical Sciences, University of Turin, Turin, Italy
[2]2i3T Scarl University of Turin, Turin, Italy
These authors contributed equally: Tatiana Lopatina, Cristina Grange

receptors and proteins reflects the unique TEC phenotype, which is distinct from that of normal endothelial cells[14–17]. Moreover, TEC, besides providing oxygen and nutrient supply, regulates tumor cell viability and the epithelial–mesenchymal transition (EMT) in the TME[18]. EMT is a highly regulated process that occurs during developmental processes and contributes to chemoresistance and metastasis[19]. A number of different transcriptional factors, including the zinc finger enhancer (E)-box-binding homeobox (ZEB), SNAIL, and TWIST1, strictly control EMT[20]. Moreover, there is considerable evidence for the interplay between these transcriptional factors and miRs coordinating the entire EMT process[20]. Cancer aggressiveness has also been associated with the ability of cancer cells to build their own vascular network without recruiting endothelial cells, a process denoted as vasculogenic mimicry (VM)[21,22].

Triple-negative breast cancer (TNBC) is the most aggressive and prevalent subtype of breast cancer in women worldwide. Chemotherapy is still the main therapeutic approach at the early stage, as no approved targeted therapy for TNBC is currently available[23]. Tumor initiation, metastasis, relapse, and therapeutic resistance are triggered by dynamic changes in tumors that mainly depend on the conditions to which tumors are usually exposed, and on cell-to-cell communication in the TME, which occurs via soluble mediators and extracellular vesicles (EVs)[24]. EVs regulate cell-to-cell communication both locally in the TME and at distant sites[25]. EVs are complex multifunctional structures containing receptors, growth factors, other proteins, and different types of RNA[26]. It has been shown that EV molecular composition and functions depend on numerous cues, including those emanated inside TME by different cell types[27,28]. For example, tumor-derived EVs carrying pro-tumorigenic proteins, such as transcription factors, miRs, and growth factors, strictly control tumor growth and metastasis[29,30]. Moreover, EVs released by TECs (TEC-EVs) acquire unique miR-EV cargo, granting them their paracrine pro-angiogenic properties[31].

Antibody-based anticancer therapy is currently seen as one of the most successful strategies for the treatment of both hematologic and solid tumors[32]. Monoclonal antibodies (mAbs) can directly act on tumor cells, induce cell killing by immune-mediated mechanisms, and specifically interfere with tumor vasculature and stromal cells. IL-3Rα is highly expressed in hematological malignant cells[33,34], and its expression translates into blast proliferation, increased cellularity, and poor prognosis[35]. Therefore, the anti-IL-3Rα antibody has been proposed, and a Phase I clinical trial in patients with acute myeloid leukemia has demonstrated its safety[36].

We have recently provided evidence that blocking IL-3Rα (anti-CD123mAb) on TEC leads to the release of EVs

(anti-IL-3R-EVs) that display antiangiogenic properties[31]. In particular, we have shown that the IL-3Rα blockade changes EV miR composition, translating into the inhibition of the Wnt/β-catenin pathway. The loss of miR-24-3p was found to be crucial in mediating anti-IL-3R-EV vessel regression in vivo. Since TEC is the gateway to tumors, we sought to determine whether IL-3Rα blockade on TEC could challenge tumors and hamper progression via their reprogrammed EVs.

Results
Human TNBC expresses the IL-3Rα in TME
Mesenchymal and mesenchymal stem-like subtypes of TNBC tumors have recently been associated with high angiogenetic signatures[37]. Since IL-3 is released in TME[10] and acts as an autocrine growth factor for breast and renal TEC[11], the expression of its binding subunit, IL-3Rα, was analyzed in 27 TNBC human samples. Supplementary Table S1 reports human TNBC features. As shown in Fig. 1, immunohistochemical analysis demonstrated that IL-3Rα is expressed by inflammatory cells and TEC. Interestingly, tumor cells also expressed IL-3Rα in 15 out of 27 (55.5%) samples. To confirm these data, IL-3Rα was also evaluated in the TNBC cell lines, MDA-MB-231 and MDA-MB-453, and in the nonneoplastic breast cancer cell line, MCF10A. As shown in Supplementary Fig. S1, TNBC cell lines, but not MCF10A, express IL-3Rα.

Since TEC in TNBC expresses IL-3Rα and TEC targeted by the anti-IL-3Rα antibody release paracrine signals that induce vessel regression[31], we hypothesize that IL-3Rα blockade on TEC, via EVs, would be effective in driving dynamic changes in tumors/TME interfering with cancer progression.

Anti-IL-3R-EVs, unlike naive EVs (nEVs), reduce cell number and migration and increase apoptosis of TNBC cell lines
Naive EVs derived from TEC (nEVs) and anti-IL-3R-EVs were isolated from TEC and analyzed by TEM (Supplementary Fig. S2A) and NanoSight (data not shown). No differences in nEV and anti-IL-3R-EV size were detected. Fluorescence-activated cell sorting (FACS) analysis, using the MACSPlex exosome kit, revealed a similar pattern of surface marker expression. They expressed exosomal markers (CD9, CD63, and CD81) (Supplementary Fig. S2C) and integrins (CD49e/Integrin α-5 and CD29/Integrin β-1). The CD63 exosomal marker was also demonstrated by western blot (Supplementary Fig. S2B). Therefore, their effects were first evaluated on MDA-MB-231 and MDA-MB-453 cell lines in vitro. We demonstrated that, while nEVs were effective in increasing cell number, anti-IL-3R-EVs significantly reduced their number compared to untreated and nEV-treated cells (Fig. 2a, Supplementary Fig. S3A). Apoptosis and

Fig. 1 IL-3Rα immunoreactivity on human TNBC samples.
Representative tissue microarrays obtained from human TNBC samples stained with anti-IL-3Rα antibody (n = 27). **a** Positive and negative expression of anti-IL-3Rα in neoplastic cells (ductal and lobular TNBC samples as indicated). Original magnification 40×, scale bar: 200 μm. **b** Focal and moderate IL-3Rα immunoreactivity of stromal inflammatory and endothelial cells indicated by arrows. Original magnification, 100× and 150×, scale bar: 100 μm and 75 μm, respectively.

cell migration were also evaluated. Unlike nEV-, anti-IL-3R-EV treatment increased the number of apoptotic cells, and significantly reduced cell migration (Fig. 2b, c, Supplementary Fig. S3B, C). These results were also supported by the expression of E- and N-cadherin (Fig. 2d) and by the in vitro sphere-formation assay of nEVs and anti-IL-3R-EV-treated MDA-MB-231 cells (Fig. 2e). nEVs and anti-IL-3R-EVs were ineffective in inducing proliferation of MCF10A cells (Supplementary Fig. S3D). Overall, these results suggested that nEVs boost tumor

cell growth/migration, while anti-IL-3R-EVs induce inhibition of cell growth and migration, and drive apoptosis. To evaluate whether this effect specifically relied on the abnormal TEC phenotype, EVs released by normal endothelial cells (EC) exposed to IL-3 (EV IL-3) were evaluated in tumor cells. Naive EC-derived EVs (EV ctr) served as controls. As shown in Fig. 2f–h, EV IL-3 failed to increase tumor cell number, its migration, or apoptotic rate. This indicates that the pro-tumorigenic action of nEVs mainly relies on TEC unique phenotype.

Anti-IL-3R-EVs impair tumor angiogenesis and the formation of lung and liver metastasis of established tumors

To investigate the effects of nEVs and anti-IL-3R-EVs in vivo, MDA-MB-231 cells were used for mammary fat pad injection into SCID mice. After 3 weeks when palpable tumors were detected, vehicle, nEVs, or anti-IL-3R-EVs were locally injected twice a week and the tumors followed for an additional 21 days (Fig. 3a). Mice were sacrificed at day 45, and primary tumors, the liver and lung, were analyzed by histology. As shown by the analysis of tumor vascular density, tumors from animals treated with anti-IL-3R-EVs displayed significantly reduced CD31-positive vessels (Fig. 3b, c, Supplementary Fig. S4). Moreover, a slight, but not significant reduction of PAS-positive/CD31-negative vessels, corresponding to the vascular network built by tumor cells (VM), was observed upon anti-IL-3R-EV treatment (Supplementary Fig. S5). Accordingly, increased apoptosis was found in the tumors of animals treated with anti-IL-3R-EVs (Fig. 3d). Of note, when compared to control animals, we found an increased apoptotic rate in tumors from animals treated with nEVs. Although we do not have direct pieces of evidence, we can speculate that hypoxia or depletion of survival factors may suppress apoptotic cues in control tumors[38].

Since the inhibition of the canonical Wnt/β-catenin pathway was reported as a relevant mechanism of anti-IL-3R-EV action[31], β-catenin expression was evaluated. As shown in Fig. 3e, treatment with anti-IL-3R-EVs was associated with significant downregulation in β-catenin. Moreover, as with β-catenin, the downregulation of Vimentin was detected in tumors from animals treated with anti-IL-3R-EVs (Fig. 3f). It has been shown that the Wnt/β-catenin network correlates with high metastatic TNBC behavior[39,40]. Therefore, metastases generated from primary tumors were evaluated. Liver macroscopic evaluation, shown in Fig. 4a, demonstrated the presence of huge metastatic nodules in tumors from mice treated with saline and nEVs, but not with anti-IL-3R-EVs. To confirm these data, immunofluorescence analysis was performed on the liver and lung, using an anti-human HLA I antibody to identify human cells in the mouse
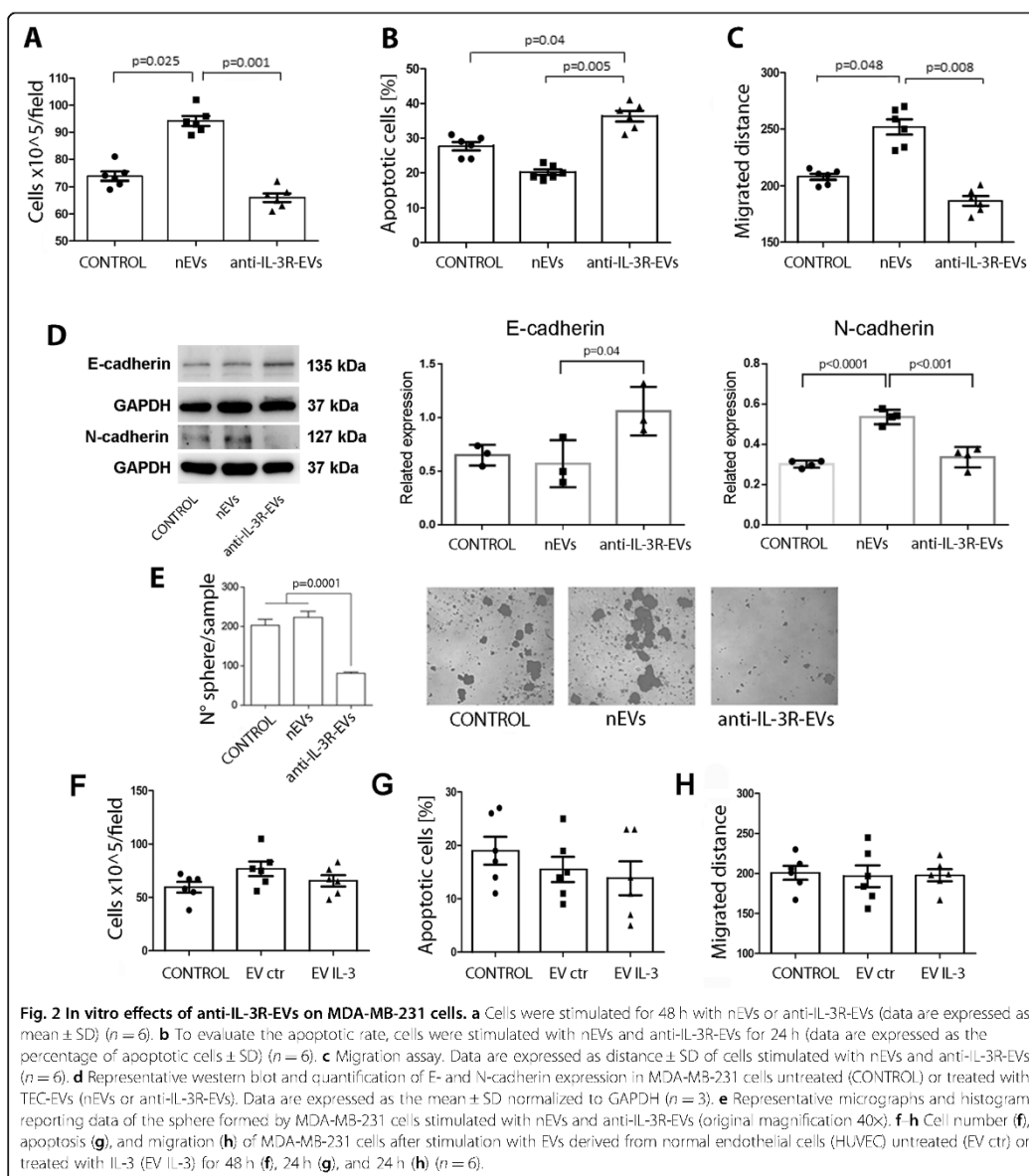
Fig. 2 In vitro effects of anti-IL-3R-EVs on MDA-MB-231 cells. a Cells were stimulated for 48 h with nEVs or anti-IL-3R-EVs (data are expressed as mean ± SD) (*n* = 6). **b** To evaluate the apoptotic rate, cells were stimulated with nEVs and anti-IL-3R-EVs for 24 h (data are expressed as the percentage of apoptotic cells ± SD) (*n* = 6). **c** Migration assay. Data are expressed as distance ± SD of cells stimulated with nEVs and anti-IL-3R-EVs (*n* = 6). **d** Representative western blot and quantification of E- and N-cadherin expression in MDA-MB-231 cells untreated (CONTROL) or treated with TEC-EVs (nEVs or anti-IL-3R-EVs). Data are expressed as the mean ± SD normalized to GAPDH (*n* = 3). **e** Representative micrographs and histogram reporting data of the sphere formed by MDA-MB-231 cells stimulated with nEVs and anti-IL-3R-EVs (original magnification 40×). **f**–**h** Cell number (**f**), apoptosis (**g**), and migration (**h**) of MDA-MB-231 cells after stimulation with EVs derived from normal endothelial cells (HUVEC) untreated (EV ctr) or treated with IL-3 (EV IL-3) for 48 h (**f**), 24 h (**g**), and 24 h (**h**) (*n* = 6).

tissues. Interestingly, mice treated with anti-IL-3R-EVs displayed a significantly reduced number of HLA I+ cells in the liver and lung compared to saline- and nEV-treated animals (Fig. 4b–d). In several pathological contexts, including cancer, phenotypic processes that drive migratory and invasive properties rely on the expression of specific transcriptional factors[20], and TWIST1 has been recognized as one of the main regulators[41]. Accordingly, anti-IL-3R-EV treatment led to the downregulation of TWIST1, both in vitro (Supplementary Fig. S6A, B) and in tumor tissues (Fig. 4e). We failed to detect changes in the expression of SNAI1 and SNAI2 (data not shown).

Fig. 3 (See legend on next page.)
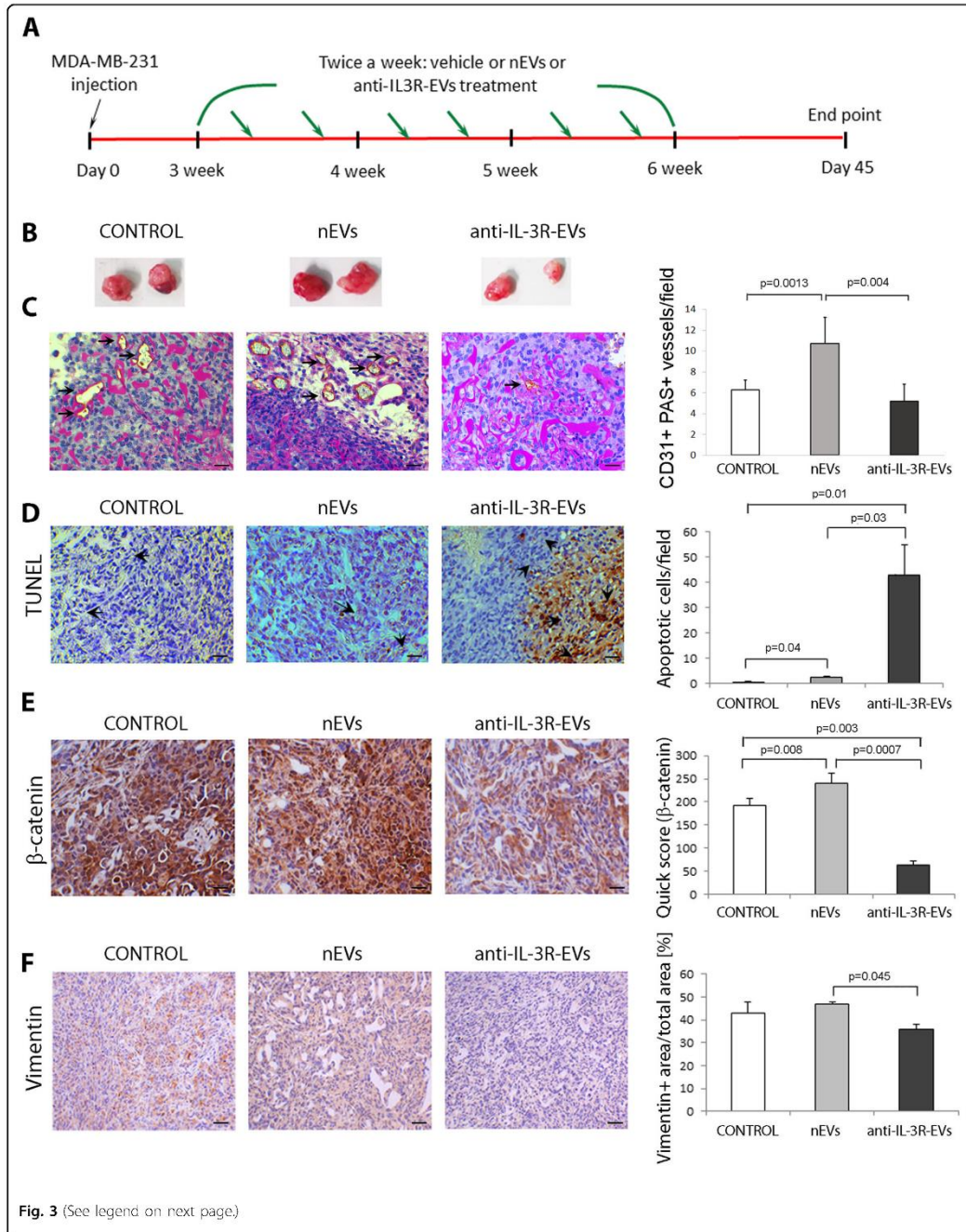
(see figure on previous page)
Fig. 3 Effects of nEV and anti-IL-3R-EV treatment on MDA-MB-231-derived in vivo tumors. a Schematic representation of the experimental design to test TEC-EVs (nEVs and anti-IL-3R-EVs) on MDA-MB-231-derived tumors. **b** Representative images of tumors untreated (CONTROL) or treated with TEC-EVs (nEVs and anti-IL-3R-EVs) (*n* = 4). **c** Representative images of tumors untreated (CONTROL) or treated with TEC-EVs (nEVs and anti-IL-3R-EVs) stained with anti-CD31 antibody and PAS. Vessels within MDA-MB-231 tumors were expressed as the number of CD31+/PAS+ per field ± SD (*n* = 4). Original magnification 400×, scale bar: 25 μm. **d** Representative micrographs showing apoptosis within tumors stained using the Tunel assay. Quantification of tumor apoptosis expressed as the number of apoptotic cells/field (*n* = 4). Original magnification 400×, scale bar: 25 μm. **e** Representative immunohistochemical images of β-catenin-positive staining of MDA-MB-231-derived tumors of animals that had been left untreated (CONTROL) or treated with TEC-EVs (nEVs and anti-IL-3R-EVs). Quantification of β-catenin positivity was calculated using the Quick score ± SD (*n* = 4). Original magnification 400×, scale bar: 25 μm. **f** Representative immunohistochemical images of Vimentin-positive staining on MDA-MB-231-derived tumors from animals that had been left untreated (CONTROL) or treated with TEC-EVs (nEVs and anti-IL-3R-EVs). Quantification of Vimentin-positive area expressed as the percentage of Vimentin + area/total area ± SD (*n* = 4). Original magnification 200×, scale bar: 50 μm.

TEC-EVs depleted of miR-24-3p (antago-miR-24-3p-EVs) impair proliferation and migration of MDA-MB-231 cells

and, as anti-IL-3-EVs, interfere with lung metastasis generated by intravenous injection of MDA-MB-231 cells

We have previously shown that the regression of TEC-derived vessels observed in mice subjected to anti-IL-3R-EVs can be recapitulated by EVs recovered from TEC transfected with antago-miR-24-3p[31]. A comparison of MIRNOMIC analyses of anti-IL-3R-EVs and antago-miR-24-3p-EVs demonstrated that antago-miR-24-3p-EVs carried a rearranged miR cargo that was still therapeutically effective and able to recapitulate the in vivo anti-IL-3R-EV effects[31]. We therefore sought to evaluate whether the same cargo could be effective in mediating anti-IL-3R-EV antitumor effects. To this end, MDA-MB-231 cells were first investigated for miR-24-3p expression upon treatment with either nEVs or anti-IL-3R-EVs. We found that anti-IL-3R-EVs were able to decrease miR-24-3p content, compared to nEVs (Supplementary Fig. S6A). Similar results were detected when antago-miR-24-3p-EVs, obtained by transfecting TEC with antago-miR-24-3p (Supplementary Fig. S7), were used (Supplementary Fig. S6A). Although no difference in miR-24-3p content was detected when control and nEV-treated cells were compared, an increased miR-24-3p/TWIST1 level was found in cells transfected with scramble EVs (Supplementary Fig. S6A). Cell transfection may explain such a difference.

One of our previous studies has demonstrated that two proteins of the β-catenin disruption complex were targeted by miR-24-3p in TEC[31]. These data and the in vivo results led us to evaluate β-catenin expression in TNBC cell lines treated with nEVs, anti-IL-3R-EVs, and antago-miR-24-3p-EVs. Unlike in tumor samples recovered from mice subjected to anti-IL-3R-EVs, we failed to demonstrate changes in β-catenin in vitro (data not shown). However, antago-miR-24-3p-EVs, like anti-IL-3R-EVs, were able to significantly reduce TWIST1 expression, tumor cell number, and migration, and increase the apoptotic rate in vitro (Supplementary Fig. S6C–E).

Possibly, due to a rapid mRNA translation, a high level of TWIST1 protein was detected, even in control cells. The basal level of TWIST1 detected in MDA-MB-231 cells may explain the high SD noticed in our experimental conditions.

Hence, since nEVs were able to promote the metastases generated from primary tumors, we first sought to determine whether circulating nEVs can also contribute to lung metastasis formation of intravenously injected MDA-MB-231 cells. The effect of nEVs was compared to that of anti-IL-3R-EVs. To address this issue, either nEVs or anti-IL-3R-EVs were injected intravenously for 5 consecutive days. On day 5, MDA-MB-231 cells were injected intravenously, and the animals were followed for 5 weeks (Fig. 5a). As shown in Fig. 5b, lung metastasis formation increased in mice treated with nEVs. Interestingly, this effect was significantly reduced by anti-IL-3R-EV treatment. We therefore investigated whether antago-miR-24-3p-EVs could recapitulate anti-IL-3R-EV-mediated protection against lung metastasis formation. As shown in Fig. 5c, antago-miR-24-3p-EVs were as effective as anti-IL-3R-EVs in reducing lung metastasis formation. Saline and scramble miR served as controls. To evaluate whether vascularization could contribute to these results, the whole lung vessel area was evaluated in mice primed with nEVs, anti-IL-3R-EVs, or antago-miR-24-3p-EVs. Indeed, a significantly reduced number of the lung vessels was found in the mice primed with anti-IL-3R-EVs or antago-miR-24-3p-EVs (Fig. 5d), indicating that circulating TEC-EVs may provide the soil for cancer cell homing possibly due to their pro-angiogenic properties.

SPRY2 undergoes upregulation in response to anti-IL-3R-EV and antago-miR-24-3p-EV challenge

To gain further insight into anti-IL-3R-EV and antago-miR-24-3p-EV mechanisms of action, an integrated miR-24-3p interaction network was performed. The network that was predicted by ingenuity pathway analysis (IPA) for miR-24-3p target genes identified several genes (Fig. 6a). Some genes with a direct relationship with miR-24-3p,

Fig. 4 Effect of nEVs and anti-IL-3R-EVs on metastases generated from primary tumors. a Representative images of liver derived from primary tumors of mice that had been left untreated (CONTROL) or treated with TEC-EVs (nEVs and anti-IL-3R-EVs) (*n* = 4). b Representative images of negative (murine liver) and positive (primary tumors) immunofluorescence using an anti-HLA I antibody. Original magnification 100×, scale bar: 100 μm. c Representative immunofluorescence images of liver derived from mice (primary MDA-MB-231 tumors) that had been left untreated (CONTROL) or treated with TEC-EVs (nEVs and anti-IL-3R-EVs) and stained with an anti-HLA I antibody. Data are expressed as the percentage of HLA I + cells/total area ± SD (*n* = 4). Original magnification 200×, scale bar: 50 μm. d Representative immunofluorescence images of lung derived from mice (primary MDA-MB-231 tumors) that had been left untreated (CONTROL) or treated with TEC-EVs (nEVs and anti-IL-3R-EVs) and stained with an anti-HLA I antibody. Data are expressed as the percentage of HLA I+ cells/total cells/field ± SD (*n* = 4). Original magnification 400×, scale bar: 25 μm. e Representative immunohistochemical images of TWIST1-positive staining of MDA-MB-231-derived primary tumors from animals that had been left untreated (CONTROL) or treated with TEC-EVs (nEVs and anti-IL-3R-EVs). Quantification of TWIST1 corresponds to the percentage of TWIST1 + area/total area ± SD (*n* = 4). Original magnification 200×, scale bar: 50 μm.

Fig. 5 Anti-IL-3R-EV and antago-miR-24-3p-EV priming reduces lung metastasis formation. a Schematic representation of the experimental design to test the effect on metastasis formation of nEVs, anti-IL-3R-EV, and antago-miR-24-3p pretreatment before intravenous injection of tumor cells. **b** Representative hematoxylin and eosin images and quantification of lung metastasis derived from mice that had been left untreated (CONTROL) or treated with TEC-EVs (nEVs and anti-IL-3R-EVs) ($n = 4$). Original magnification 100×, scale bar: 100 μm. The number of metastases was expressed as the number of metastases/lung ± SD ($n = 4$). **c** Representative hematoxylin and eosin images and quantification of lung metastases derived from mice that had been left untreated (CONTROL) or treated with scrambled EVs and antago-miR-24-3p-EVs ($n = 4$). Original magnification 100×, scale bar: 100 μm. The number of metastases was expressed as the number of metastases/lung ± SD ($n = 4$). **d** Evaluation of vessel density in lungs derived from mice that had been left untreated (CONTROL) or treated with nEVs and anti-IL-3R-EVs and with scramble EVs and antago-miR-24-3p-EVs. Data are expressed as number of vessels per field ± SD ($n = 4$).

such as HNF1A, HNF1B, SPRY2, TAZ, YAP, C-MYC, NET1, PARP1, and NDST1, were therefore evaluated in MDA-MB-231 cells treated with anti-IL-3R-EVs and antago-miR-24-3p-EVs. As shown in Fig. 6b and Supplementary Fig. S8, only SPRY2 was significantly upregulated upon anti-IL-3R-EV and antago-miR-24-3p-EV

Fig. 6 miR-24-3p gene network identified using Ingenuity Pathway Analysis (IPA). a IPA predicted target genes for miR-24-3p. Arrowheads represent activating relationships, whereas solid or dotted edges indicate direct and indirect relationships, respectively. b qRT-PCR for SPRY2 in unstimulated MDA-MB-231 cells (CONTROL) or upon nEV, anti-IL-3R-EV, scramble EV, and antago-miRNA-24-3p-EV treatment. Related expression of miR-24-3p for each condition is reported. #$p < 0.05$ anti-IL-3R-EVs vs. nEVs; §$p < 0.05$ antago-miR-24-3p-EVs vs. scramble EVs; *$p < 0.05$ anti-IL-3R-EVs vs. nEVs, and antago-miR-24-3p-EVs vs. scramble. c The apoptotic rate was evaluated after 24 h of treatment of MDA-MB-231 cells untransfected or transfected with scramble or SPRY2 siRNA. Saline or TEC-EVs (nEVs, anti-IL-3R-EVs, scramble EVs, and antago-miR-24-3p-EVs) were used. Data are expressed as the percentage of apoptotic cells ± SD ($n = 6$). ***$p < 0.005$: antago-miR-24-3p-EVs vs. SPRY2-silenced cells + antago-miR-24-3p-EVs; ****$p < 0.0001$: nEVs vs. anti-IL-3R-EVs, scramble EVs vs. antago-miR-24-3p-EVs, and anti-IL-3R-EVs vs. SPRY2-silenced cells + anti-IL-3R-EVs.

treatment. These data suggest that upregulation of SPRY2 may contribute to either anti-IL-3R-EVs or antago-miR-24-3p-EV mechanism of action. Indeed, we found that SPRY2 silencing inhibits anti-IL-3R-EV- and miR-24-3p-EV-mediated apoptosis (Fig. 6c, Supplementary Fig. S9).

Discussion

TNBC is an aggressive highly metastatic breast cancer subtype lacking estrogen, progesterone, and HER-2 receptors[42] and proven target therapies[43]. The identification of molecular markers/effective therapeutics that

impact upon tumor progression is therefore a future clinical challenge.

EVs derived from different TME components, including TEC, influence key aspects of cancer growth/progression, and have recently been recognized as being of great importance for tumor targeting[44]. The goal of this study was to investigate whether IL-3Rα blockade on TEC impacts tumor progression via EVs. A previous study demonstrated that IL-3Rα blockade on TEC, by an anti-IL-3Rα[36], changed the miR-EV cargo and had striking effects on tumor vessel formation[31], suggesting that reprogramming TEC-EVs may also be instrumental in tumor targeting. To provide the rationale for TEC targeting in TNBC, IL-3Rα expression was evaluated in human TNBC samples. We demonstrated that tumor cells highly expressed IL-3Rα in 55.5% of the TNBC examined. Of note, TNBC cell lines, but not MCF10A cells, also expressed IL-3Rα. How the IL-3Rα and its ligand, IL-3, take part in TNBC cell biology is still to be established, and further studies are required to address this issue. However, our data suggest that TNBC may serve as a valuable model with which to investigate the impact of IL-3Rα targeting on cell-to-cell communication in TME, as IL-3Rα was highly expressed in TEC.

We have demonstrated herein that nEV treatment boosts cancer cell viability and migration, while anti-IL-3R-EVs significantly impair both, and induce apoptosis in vitro. E- and N-cadherin expression in cells treated with anti-IL-3R-EVs further sustains their biological activity. EV composition differs significantly in untransformed and transformed cells and accounts for the different biological actions[24]. Accordingly, EVs from normal endothelial cells have no effect on tumor cell growth/migration/apoptosis, whether they were unstimulated or stimulated with IL-3, indicating that the effects of nEVs strictly rely on the unique TEC phenotype.

Intercellular crosstalk can occur via secreted mediators and EVs in the TME[45]. Indeed, tumor-derived EVs and EVs from the TME impact upon tumor progression also by promoting angiogenesis[24]. Furthermore, vessel density in primary tumors correlates with metastasis[46]. We herein demonstrated that, unlike nEVs, anti-IL-3R-EVs inhibit tumor neovascularization without significantly impacting VM[21]. Proteins, mRNAs, and miRs shuttled within TME-derived EVs largely provide services to the tumor[47]. In fact, a previous study of ours demonstrated that miR-214-3p and miR-24-3p, which target the canonical wingless Wnt/β-catenin pathway, were differentially regulated in nEVs and anti-IL-3R-EVs, and mediate their pro- and antiangiogenic effects, respectively[31]. In this study, we have demonstrated that anti-IL-3R-EVs also reduce β-catenin expression in tumor-bearing mice, suggesting that anti-IL-3R-EVs are also able to target the canonical wingless Wnt/β-catenin pathway in neoplastic cells.

β-catenin accumulation and the acquisition of mesenchymal markers, as Vimentin, in tumor cells, are associated with cancer cells' ability to spread to distant sites[48–50]. Indeed, anti-IL-3R-EVs were found effective in reducing the expression of Vimentin, and animals treated with anti-IL-3R-EVs were almost protected from the occurrence of liver and lung metastasis. A harmonized set of transcriptional factors drives the activation of the metastatic program[20], and TWIST1 is one of them[41]. TWIST1 belongs to a family of transcriptional factors highly expressed in most cancers, and particularly in those highly metastatic[20,41]. We demonstrated that TWIST1 was reduced in vitro and more importantly, in mice treated with anti-IL-3R-EVs. TWIST1 expression is strictly controlled at transcriptional and post-transcriptional levels[20]. Several different miRs have been shown to regulate TWIST1 at the post-transcriptional level[20]. Herein, we have demonstrated that, as anti-IL-3R-EVs, EVs depleted of miR-24-3p reduced TWIST1 expression in stimulated cells. miR-214-3p, which was also found enriched in anti-IL-3R-EVs and miR-24-3p-EVs[31], has been involved in TWIST1 post-transcriptional regulation in ovarian cancers[51]. Unfortunately, we failed to detect changes in TWIST1 expression when nEVs enriched in miR-214-3p were used to stimulate MDA-MB-231 and MD-MB-453 cells (data not shown). Vimentin, TWIST1, and β-catenin have been linked through STAT3[52], and more recently, the role of miR-551b-3p in controlling STAT3 transcription and TNBC progression has been documented[53]. Again, we failed to detect miR-551b-3p among miRs differentially expressed in nEVs and anti-IL-3R-EVs[31] and differences in STAT3 expression/activation in our model (data not shown). This suggests that the anti-IL-3R-EV- and antago-miR-24-3p-EV-mediated downregulation of TWIST1 as well as their biological activities may rely on the combined action of a pattern of shared miRs, we have previously described[31]. However, as EVs also induce their biological effects by transferring lipids, proteins, mRNAs, and transcription factors[47,49], it might be necessary to consider the entire EV cargo to explain the anti-IL-3R-EV and miR-24-3p-EV mechanism of action.

Although chemotherapy is still the main modality for TNBC treatment, the recurrence of metastasis hampers the improvement of patient outcomes[54,55]. The development of novel therapeutic options to improve TNBC patient survival is therefore a concrete clinical need. The results in primary tumors and the ability of antago-miR-24-3p-EVs to recapitulate anti-IL-3R-EV action in vitro led us to determine the impact of circulating anti-IL-3R-EVs/antago-miR-24-3p-EVs in preventing the formation of lung metastasis generated by tumor cell intravenous injection. Indeed, we demonstrated that lung metastasis formation was reduced in mice that had been primed with both anti-IL-3R-EVs and antago-miR-24-3p-EVs.

EVs released by cancer stem cells were found to be instrumental for premetastatic niche formation[56]. We herein demonstrate that nEVs are also instrumental for metastasis formation, while anti-IL-3R-EVs and antago-miR-24-3p-EVs were therapeutically effective in reducing their formation. The possibility that this effect relied on their pro-angiogenic/antiangiogenic properties is sustained by the increased/reduced vascular network in the lung of animals primed with nEVs or anti-IL-3R-EVs and antago-miR-24-3p-EVs, respectively.

To gain insight into the potential signaling involved in the anti-IL-3R-EV and antago-miR-24-3p-EV mechanisms of action, IPA was interrogated to identify miR-24-3p-interacting genes. Of the most significant miR-24-3p interactors evaluated, only SPRY2 was found to be upregulated upon anti-IL-3R-EV and antago-miR-24-3p-EV challenge. SPRY2, which belongs to the sprouty gene family, acts as a negative regulator of several receptor tyrosine kinases that are also involved in angiogenesis[57]. Moreover, the expression of the SPRY2 gene was found to be repressed in breast cancers[58]. Accordingly, we found that SPRY2 was downregulated upon nEV treatment, while anti-IL-3R-EVs and antago-miR-24-3p-EVs rescued SPRY2 expression. Moreover, we found that SPRY2 silencing prevented anti-IL-3R-EV- and antago-miR-24-3p-EV-mediated apoptosis.

Overall, this study demonstrates that IL-3Rα blockade on TEC reprograms EVs, which then acquire the ability to change the expression of Vimentin, β-catenin, and TWIST1, and reduce angiogenesis and the metastatic spread of primary tumors. Moreover, anti-IL-3R-EV priming was found to be therapeutically effective in reducing lung metastasis, possibly due to its anti-angiogenic properties and/or interference with cancer cell homing. Moreover, we provide the first evidence that inflammatory cells, TEC, and, more importantly, tumor cells, in human TNBC samples, express IL-3Rα. Finally, since EVs released upon TEC targeting can be considered the leading effectors of IL-3Rα blockade, the results of the present study provide evidence for the therapeutic effectiveness of this antibody-based targeted approach in TNBC.

Materials and methods

Detailed information in this section is reported in Supplementary Information.

Immunohistochemistry and immunofluorescence on human and animal samples

A series of 27 patients diagnosed with TNBC between 2011 and 2012 was retrieved from the files of the Pathology Department of the Città della Salute e della Scienza Hospital (Turin). The study was conducted in accordance with the guidelines and regulations defined by the Research Ethics Committee for human Biospecimen Utilization (Department of Medical Sciences—ChBU) of the University of Turin. Representative blocks were obtained as previously described[59]. Immunohistochemistry was performed using an automated slide-processing platform (Ventana BenchMark AutoStainer, Ventana Medical Systems, Tucson, AZ, USA), with Universal DAB Detection Kit detection systems. In all, 5-μm paraffin-embedded tumor sections were stained with CD31 and PAS to quantify CD31+ vessels and VM expressed as CD31−/PAS+ vessels. Masson's trichrome staining was also used. Ten sections/tumors were analyzed using ImageJ software, and the results were expressed as the number of CD31+/PAS+/fields ± SD. Moreover, tumor sections were analyzed using the ApopTag®Plus Peroxidase In Situ Apoptotic Detection kit (Millipore, #S7101). Immunohistochemistry for the detection of Vimentin, TWIST1, and β-catenin was performed using a monoclonal anti-Vimentin antibody (Sigma #V5255), a polyclonal anti-TWIST1 antibody (Abcam #ab49254), and a polyclonal anti-β-catenin antibody (Abcam #ab16051). Quantifications of Vimentin- and TWIST1-positive area were performed using Fiji software[60]. The analysis of β-catenin-positive cells was performed by two independent pathologists and expressed as Quick score (Q)[61]. MDA-MB-231 cells were detected in livers and lungs by immunofluorescence using anti-HLA I (Santa Cruz Biotechnology, #sc-25619). Details are reported in Supplementary Information.

Cell cultures

The MDA-MB-231, MDA-MB-453, and MCF10A cell lines were purchased from ATCC.

Human-derived TEC was obtained from surgical tumor specimens using anti-CD105-positive selection[62]. Cells were cultured as described previously[11,62].

Primary human umbilical vein endothelial cells, purchased from ATCC and used as controls of nontumoral endothelial cells, were untreated or treated with IL-3 (10 ng/ml) to obtain EVs (EV ctr and EV IL-3, respectively), as previously described[63].

EV isolation and characterization

In selected experiments, starved TEC was cultured for 24 h in the presence of 1 μg/ml Human IL-3Rα/CD123 MAb (R&D Systems, #MAB301-100, Clone 32703). Untreated TEC served as controls. For EV isolation, TEC, untreated or pretreated by blocking IL-3Rα, was cultured for 24 h in fetal bovine serum (FBS)-free EndoGro medium. The conditioned medium was centrifuged for 30 min at 3000 g to remove cell debris and apoptotic bodies, and then submitted to microfiltration with 0.22-μm filters (MF-Millipore™) to remove larger vesicles. The TEC-EV suspension was then stored at −80 °C until further use.

In specific experiments, TEC was transfected with antago-miR-24-3p (Ambion, cat #4464085, assay ID MH1073) or scramble siRNA (Ambion, cat #4464077). Details are reported in Supplementary Information.

EV characterization

EVs were analyzed using NTA, electron microscopy, and FACS analysis. Moreover, EV flow cytometry analysis was performed using the MACSPlex Exosome Kit (human, Miltenyi Biotec), following the manufacturer's protocol[64]. The CD63 exosomal marker was also analyzed by western blot. Details are reported in Supplementary Information.

Cell counting, apoptosis, scratch test, and SPRY2 silencing

Apoptosis assay: cells seeded in 6-well plates were stimulated for 24 h with different types of TEC-EVs (nEVs, anti-IL-3R-EVs, scramble EVs, and antago-miR-24-3p-EVs) $(2 \times 10^8 \, \mathrm{EVs/ml})$ in FBS-free DMEM. The effective dose was selected with reference to the preliminary results obtained using different EV concentrations (data not shown). Treated and untreated cells were analyzed using Muse® Annexin V & Dead Cell Kit (Millipore, #MCH100105). Cell proliferation was assayed by direct cell count by two different operators. Scratch assay: cells seeded in 24-well plates and grown until confluence in DMEM 10% FBS were stimulated with TEC-EVs (as above) in DMEM FBS-free medium and analyzed 24 h later. The results were expressed as mean distance (0–24 h) ± SD. In selected experiments, SPRY2 was silenced in MDA-MB-231 cells by transfecting siRNA scramble (Qiagen, Cat No. 1027310) or siRNA for SPRY2 (Qiagen, Cat No. SI00081788) using HiPerFect Transfection Reagent (Qiagen, Cat No. 301704) (Supplementary Information).

Sphere-formation assay

To test the ability of MDA-MB-231 cells to grow in nonadhesive conditions as floating spheres, cells were plated in 6-well nonadherent plates, at a concentration 50×10^3/well, in 2 ml of sphere-formation medium in the presence of nEVs or anti-IL-3R-EVs $(1 \times 10^8 \, \mathrm{EVs/ml})$. Data are expressed as the number of sphere/sample ± SD (Supplementary Information).

Tumor growth and model of metastasis formation in vivo

Animal studies were conducted in accordance with the Italian National Institute of Health Guide for the Care and Use of Laboratory Animals (protocol No. 944/2015-PR). Mice were housed according to the guidelines of the Federation of European Laboratory Animal Science Association and the Ethical Committee of the University of Turin. The investigators (at least 2) were blinded when assessing the outcome. Tumors were obtained by injecting MDA-MB-231 cells in Matrigel into the mammary fat pad of SCID mice (8 weeks/female) (4 mice/group) $(1 \times 10^6$ cells per injection). After 3 weeks, when tumors became palpable, animals were treated with saline, nEVs, or anti-IL-3R-EVs $(1 \times 10^{10}$ EV/tumor) twice a week for 3 additional weeks (Fig. 3a). At day 45, tumors were embedded in paraffin ($n = 4$/each condition). To evaluate metastasis formation after intravenous tumor injection, EVs $(1 \times 10^{10}$ EV/injection) were intravenously injected for 5 days into SCID mice (Fig. 5a). On day 5, 0.6×10^6 MDA-MB-231 cells were injected intravenously. The mice were sacrificed after 5 weeks and lungs analyzed. Lung metastases were counted using ImageJ in five nonsequential sections. The results were expressed as mean ± SD of metastasis per lung ($n = 4$/each condition)[56]. Lung vessels with red blood cells inside were quantified in lung sections stained with Masson's trichrome and expressed as the number of vessels/field ± SD. Details are reported in Supplementary Information.

Real-time PCR

Real-time polymerase chain reaction (PCR) was performed to detect miR-24-3p, SPRY2, and TWIST1 in TEC-EVs and MDA-MB-231 cells as indicated. Total RNA from TEC-EV samples and MDA-MB-231 cells was extracted using the RNAeasy kit (Qiagen). RNA was reverse-transcribed using miScript II RT Kit (Qiagen).

Western blot

Western blot was performed as previously described[31] and reported in Supplementary Information.

miR-24-3p target validation

Ingenuity pathway analysis (IPA) was used to predict the target genes for miR-24-3p. The miR Target Filter tool was set up on IPA (Qiagen: http://www.qiagenbioinformatics.com/products/ingenuity-pathway-analysis/) to associate miR-24-3p with predicted mRNA targets. miR-24-3p target expression (HNF1B, TAZ, PARP1, HNF1A, SPRY2, MYC, YAP, NET1, and NDST1) was evaluated by RT-PCR using actin-β as the housekeeping transcript. Primer sequences and details are in Supplementary Table S2

Statistical analysis

All data are reported as mean ± SD. Comparison between two groups was carried out by t test. Our data passed normality and equal-variance tests. Comparisons among ≥3 were performed by one- way ANOVA followed by Tukey's multiple-comparison test. The cutoff for statistical significance was set at $p < 0.05$. All in vitro or in vivo results are representative of at least 3 independent experiments. All statistical analyses were carried out on Graph Pad Prism version 5.04 (Graph Pad Software, Inc., USA).

Conflict of interest
G.C. is a component of the Scientific Advisory Board of UNICYTE. The remaining authors declare that they have no conflict of interest.

Publisher's note
Springer Nature remains neutral with regard to jurisdictional claims in published maps and institutional affiliations.

Supplementary Information accompanies this paper at (https://doi.org/10.1038/s41389-020-00274-y).

References
1. McNiece, I. et al. Action of interleukin-3, G-CSF, and GM-CSF on highly enriched human hematopoietic progenitor cells: synergistic interaction of GM-CSF plus G-CSF. *Blood* **74**, 110–114 (1989).
2. Brizzi, M. F. et al. Interleukin 3 stimulates proliferation and triggers endothelial-leukocyte adhesion molecule 1 gene activation of human endothelial cells. *J. Clin. Investig.* **91**, 2887–2892 (1993).
3. Deregibus, M. C. et al. HIV-1-Tat protein activates phosphatidylinositol 3-kinase/AKT-dependent survival pathways in Kaposi's sarcoma cells. *J. Biol. Chem.* **277**, 25195–25202 (2002).
4. Dentelli, P. et al. Human IL-3 stimulates endothelial cell motility and promotes in vivo new vessel formation. *J. Immunol.* **163**, 2151–2159 (1999).
5. Xu, M., Nie, L., Kim, S. H. & Sun, X. H. STAT5-induced Id-1 transcription involves recruitment of HDAC1 and deacetylation of C/EBPbeta. *EMBO J.* **22**, 893–904 (2003).
6. Sadras, T., Kok, C. H., Perugini, M., Ramshaw, H. S. & D'Andrea, R. J. miR-155 as a potential target of IL-3 signaling in primary AML cells. *Leuk. Res.* **57**, 57–59 (2017).
7. Dentelli, P. et al. microRNA-222 controls neovascularization by regulating signal transducer and activator of transcription 5A expression. *Arterioscler. Thromb. Vasc. Biol.* **30**, 1562–1568 (2010).
8. Radpour, R. et al. CD8(+) T cells expand stem and progenitor cells in favorable but not adverse risk acute myeloid leukemia. *Leukemia* **33**, 2379–2392 (2019).
9. Arai, N. et al. Impact of CD123 expression, analyzed by immunohistochemistry, on clinical outcomes in patients with acute myeloid leukemia. *Int. J. Hematol.* **109**, 539–544 (2019).
10. Dentelli, P. et al. IL-3 affects endothelial cell-mediated smooth muscle cell recruitment by increasing TGF beta activity: potential role in tumor vessel stabilization. *Oncogene* **23**, 1681–1692 (2004).
11. Dentelli, P., Rosso, A., Olgasi, C., Camussi, G. & Brizzi, M. F. IL-3 is a novel target to interfere with tumor vasculature. *Oncogene* **30**, 4930–4940 (2011).
12. Hoarau-Vechot, J. et al. Akt-activated endothelium promotes ovarian cancer proliferation through notch activation. *J. Transl. Med.* **17**, 194 (2019).
13. Bussolati, B., Assenzio, B., Deregibus, M. C. & Camussi, G. The proangiogenic phenotype of human tumor-derived endothelial cells depends on thrombospondin-1 downregulation via phosphatidylinositol 3-kinase/Akt pathway. *J. Mol. Med.* **84**, 852–863 (2006).
14. Dudley, A. C. Tumor endothelial cells. *Cold Spring Harb. Perspect. Med.* **2**, a006536 (2012).
15. Dutta, A. et al. Integrin alphavbeta6 promotes an osteolytic program in cancer cells by upregulating MMP2. *Cancer Res.* **74**, 1598–1608 (2014).
16. Hida, K., Ohga, N., Akiyama, K., Maishi, N. & Hida, Y. Heterogeneity of tumor endothelial cells. *Cancer Sci.* **104**, 1391–1395 (2013).
17. Aguilar-Cazares, D. et al. Contribution of angiogenesis to inflammation and cancer. *Front. Oncol.* **9**, 1399–1416 (2019).
18. Maishi, N. & Hida, K. Tumor endothelial cells accelerate tumor metastasis. *Cancer Sci.* **108**, 1921–1926 (2017).
19. van Staalduinen, J., Baker, D., Ten Dijke, P. & van Dam, H. Epithelial-mesenchymal-transition-inducing transcription factors: new targets for tackling chemoresistance in cancer? *Oncogene* **37**, 6195–6211 (2018).
20. Abba, M. L., Patil, N., Leupold, J. H. & Allgayer, H. MicroRNA regulation of epithelial to mesenchymal transition. *J. Clin. Med.* **5**, 8 (2016).
21. Hendrix, M. J., Seftor, E. A., Hess, A. R. & Seftor, R. E. Vasculogenic mimicry and tumour-cell plasticity: lessons from melanoma. *Nat. Rev. Cancer* **3**, 411–421 (2003).
22. Kim, H. S. et al. Morphological characteristics of vasculogenic mimicry and its correlation with EphA2 expression in gastric adenocarcinoma. *Sci. Rep.* **9**, 3414 (2019).
23. Yao, H. et al. Triple-negative breast cancer: is there a treatment on the horizon? *Oncotarget* **8**, 1913–1924 (2017).
24. Wan, Z. et al. Exosome-mediated cell-cell communication in tumor progression. *Am. J. Cancer Res.* **8**, 1661–1673 (2018).
25. Nishida-Aoki, N. & Gujral, T. S. Emerging approaches to study cell-cell interactions in tumor microenvironment. *Oncotarget* **10**, 785–797 (2019).
26. Colombo, M., Raposo, G. & Thery, C. Biogenesis, secretion, and intercellular interactions of exosomes and other extracellular vesicles. *Annu. Rev. Cell Dev. Biol.* **30**, 255–289 (2014).
27. Guo, J. et al. PRAS40 connects microenvironmental stress signaling to exosome-mediated secretion. *Mol. Cell. Biol.* **37**, pii e00171–17 (2017).
28. Shao, C. et al. Role of hypoxia-induced exosomes in tumor biology. *Mol. Cancer* **17**, 120 (2018).
29. Hoshino, A. et al. Tumour exosome integrins determine organotropic metastasis. *Nature* **527**, 329–335 (2015).
30. Conigliaro, A. et al. CD90+ liver cancer cells modulate endothelial cell phenotype through the release of exosomes containing H19 lncRNA. *Mol. Cancer* **14**, 155 (2015).
31. Lombardo, G. et al. IL-3R-alpha blockade inhibits tumor endothelial cell-derived extracellular vesicle (EV)-mediated vessel formation by targeting the beta-catenin pathway. *Oncogene* **37**, 1175–1191 (2018).
32. Scott, A. M., Wolchok, J. D. & Old, L. J. Antibody therapy of cancer. *Nat. Rev. Cancer* **12**, 278–287 (2012).
33. Jordan, C. T. et al. The interleukin-3 receptor alpha chain is a unique marker for human acute myelogenous leukemia stem cells. *Leukemia* **14**, 1777–1784 (2000).
34. Munoz, L. et al. Interleukin-3 receptor alpha chain (CD123) is widely expressed in hematologic malignancies. *Haematologica* **86**, 1261–1269 (2001).
35. Testa, U. et al. Elevated expression of IL-3Ralpha in acute myelogenous leukemia is associated with enhanced blast proliferation, increased cellularity, and poor prognosis. *Blood* **100**, 2980–2988 (2002).
36. He, S. Z. et al. A Phase 1 study of the safety, pharmacokinetics and anti-leukemic activity of the anti-CD123 monoclonal antibody CSL360 in relapsed, refractory or high-risk acute myeloid leukemia. *Leuk. Lymphoma* **56**, 1406–1415 (2015).
37. Bareche, Y. et al. Unravelling triple-negative breast cancer molecular heterogeneity using an integrative multiomic analysis. *Ann. Oncol.* **29**, 895–902 (2018).
38. Graeber, T. G. et al. Hypoxia-mediated selection of cells with diminished apoptotic potential in solid tumours. *Nature* **379**, 88–91 (1996).
39. Dey, N. et al. Wnt signaling in triple negative breast cancer is associated with metastasis. *BMC Cancer* **13**, 537 (2013).
40. Fatima, I. et al. Simultaneous multi-organ metastases from chemo-resistant triple-negative breast cancer are prevented by interfering with WNT-signaling. *Cancers (Basel)* **11**, pii e2039 (2019).
41. Karreth, F. & Tuveson, D. A. Twist induces an epithelial-mesenchymal transition to facilitate tumor metastasis. *Cancer Biol. Ther.* **3**, 1058–1059 (2004).
42. Khaled, N. & Bidet, Y. New insights into the implication of epigenetic alterations in the EMT of triple negative breast cancer. *Cancers (Basel)* **11**, pii e559 (2019).
43. Malla, R. R. et al. A perspective on the diagnostics, prognostics, and therapeutics of microRNAs of triple-negative breast cancer. *Biophys. Rev.* **11**, 227–234 (2019).
44. Mohammadi, S. et al. Exosomes and cancer: from oncogenic roles to therapeutic applications. *IUBMB Life* **72**, 724–748 (2019).
45. Li, L & Nabet, B. Y. Exosomes in the tumor microenvironment as mediators of cancer therapy resistance. *Mol. Cancer* **18**, 32 (2019).
46. Holleb, A. I. & Folkman, J. Tumor angiogenesis. *CA Cancer J. Clin.* **22**, 226–229 (1972).

47. Valadi, H. et al. Exosome-mediated transfer of mRNAs and microRNAs is a novel mechanism of genetic exchange between cells. *Nat. Cell Biol.* **9**, 654–659 (2007).
48. Patel, S., Alam, A., Pant, R. & Chattopadhyay, S. Wnt signaling and its significance within the tumor microenvironment: novel therapeutic insights. *Front. Immunol.* **10**, 2872 (2019).
49. Lamouille, S., Xu, J. & Derynck, R. Molecular mechanisms of epithelial-mesenchymal transition. *Nat. Rev. Mol. Cell Biol.* **15**, 178–196 (2014).
50. Thiery, J. P., Acloque, H., Huang, R. Y. & Nieto, M. A. Epithelial-mesenchymal transitions in development and disease. *Cell* **139**, 871–890 (2009).
51. Fang, Y. Y. et al. miR-214-3p inhibits epithelial-to-mesenchymal transition and metastasis of endometrial cancer cells by targeting TWIST1. *Onco Targets Ther.* **12**, 9449–9458 (2019).
52. Banerjee, K & Resat, H. Constitutive activation of STAT3 in breast cancer cells: a review. *Int. J. Cancer* **138**, 2570–2578 (2016).
53. Parashar, D. et al. miRNA551b-3p activates an oncostatin signaling module for the progression of triple-negative breast cancer. *Cell Rep.* **29**, 4389–4406.e4310 (2019).
54. Foulkes, W. D., Smith, I. E. & Reis-Filho, J. S. Triple-negative breast cancer. *N. Engl. J. Med.* **363**, 1938–1948 (2010).
55. da Silva, J. L. Cardoso, Nunes, N. C., Izetti, P., de Mesquita, G. G. & de Melo, A. C. Triple negative breast cancer: a thorough review of biomarkers. *Crit. Rev. Oncol. Hematol.* **145**, 102855 (2019).
56. Grange, C. et al. Microvesicles released from human renal cancer stem cells stimulate angiogenesis and formation of lung premetastatic niche. *Cancer Res.* **71**, 5346–5356 (2011).
57. Peier, M., Walpen, T., Christofori, G., Battegay, E. & Humar, R. Sprouty2 expression controls endothelial monolayer integrity and quiescence. *Angiogenesis* **16**, 455–468 (2013).
58. Lo, T. L. et al. The ras/mitogen-activated protein kinase pathway inhibitor and likely tumor suppressor proteins, sprouty 1 and sprouty 2 are deregulated in breast cancer. *Cancer Res.* **64**, 6127–6136 (2004).
59. Sapino, A. et al. Routine assessment of prognostic factors in breast cancer using a multicore tissue microarray procedure. *Virchows Arch.* **449**, 288–296 (2006).
60. Ngan, C. Y. et al. Quantitative evaluation of vimentin expression in tumour stroma of colorectal cancer. *Br. J. Cancer* **96**, 986–992 (2007).
61. Liu, H. W. et al. The disruption of the beta-catenin/TCF-1/STAT3 signaling axis by 4-acetylantroquinonol B inhibits the tumorigenesis and cancer stem-cell-like properties of glioblastoma cells, in vitro and in vivo. *Cancers (Basel)* **10**, 491 (2018).
62. Bussolati, B., Deambrosis, I., Russo, S., Deregibus, M. C. & Camussi, G. Altered angiogenesis and survival in human tumor-derived endothelial cells. *FASEB J.* **17**, 1159–1161 (2003).
63. Lombardo, G. et al. Activated Stat5 trafficking via endothelial cell-derived extracellular vesicles controls IL-3 pro-angiogenic paracrine action. *Sci. Rep.* **6**, 25689 (2016).
64. Wiklander, O. P. B. et al. Systematic methodological evaluation of a multiplex bead-based flow cytometry assay for detection of extracellular vesicle surface signatures. *Front. Immunol.* **9**, 1326 (2018).

IL-3 signalling in the tumour microenvironment shapes the immune response *via* tumour endothelial cell-derived extracellular vesicles

Tatiana Lopatina [a,1], Malvina Koni [a,1], Cristina Grange [a,1], Massimo Cedrino [b], Saveria Femminò [a], Giusy Lombardo [a], Enrica Favaro [a], Maria Felice Brizzi [a,*]

[a] *Department of Medical Sciences, University of Turin, Turin, Italy*
[b] *2i3T Scarl University of Turin, Italy*

ABSTRACT

Antibody-based anti-cancer therapy is considered a successful approach to impair tumour progression. This study aimed to investigate the clinical impact of targeting the IL-3 signalling in the microenvironment of solid tumours. We intended to investigate whether the IL-3Rα blockade on tumour-derived endothelial cells (TEC) can modulate PD-L1 expression in tumour cells and peripheral blood mononuclear cells (PBMC) to reshape the anti-tumour immune response. Extracellular vesicles released by TEC after IL-3Rα blockade (aTEV) were used as the ultimate effectors of the antibody-based approach, while naive TEC-derived extracellular vesicles (nTEV) served as control. Firstly, we demonstrated that, either directly or indirectly *via* nTEV, IL-3 controls the expression of its receptor on TEC and PBMC respectively. Moreover, we found that nTEV, moulded by the autocrine secretion of IL-3, increased PD-L1 expression in myeloid cells both *in vitro* and *in vivo*. In addition, we found that nTEV-primed PBMC favour tumour cell growth (TEC and MDA-MB-231 cells), whereas PBMC-primed with aTEV still retain their anti-tumour properties. Isolated T-cells pre-conditioned with nTEV or aTEV and co-cultured with TEC or MDA-MB-231 cells have no effects, thereby sustaining the key role of myeloid cells in tumour immune editing. *In vivo* nTEV, but not aTEV, increased the expression of PD-L1 in primary tumours, lung and liver metastases. Finally, we demonstrated that the enrichment of miR-214 in aTEV impacts on PD-L1 expression *in vivo*. Overall, these data indicate that an approach based on IL-3Rα blockade in TEC rearranges EV cargo and may reshape the anti-tumour immune response.

1. Introduction

Tumour immune regulation leading to tumour tolerance is also orchestrated by tumour-derived extracellular vesicles (TEV) [1,2]. Extracellular vesicles (EV) are heterogenic membrane structures with a specific molecular composition dictated by their cell of origin. TEV have surface receptors and stimulating factors, such as, TLR4, HLA class I, HLA G, as well as inflammatory cytokines (TGFβ1, IFN, IL-6, IL-10) [2]. TEV are also enriched in immune relevant microRNA (miR-146, miR-214 and many others) [3–5].

TEV express tumour-associated antigens and neo-antigens conveyed by the parental tumour cells as well as major histocompatibility complex (MHC) class I and class II molecules [1]. Thus, TEV could present tumour antigens to antigen presenting cells and drive specific immune response [6]. The choice to trigger cytotoxic effect or immunosuppression depends on the presence of co-stimulatory factors. Indeed, it has been extensively reported that TEV promote tumour immune escape through different mechanisms [1,2]. This implies that, since TEV regulate the immune response, by facilitating communication between immune cells and cancer cells, they also impact on tumour progression and metastasis formation.

The programmed cell death-1 receptor (PD-1) is an immune checkpoint inhibitor, expressed on the surface of immune effector cells [7]. PD-1 is mainly activated by the programmed cell death ligand 1 (PD-L1), expressed by several cell types [8]. The PD-1/PD-L1 pathway fine-tunes inflammation also supporting tolerance of circulating T-lymphocyte [8]. In cancer, the expression of PD-L1 is recognized as one of the major immune escape mechanisms [7,9]. Indeed, in several cancers, PD-L1 is highly expressed and the PD-L1/PD-1 signalling is engaged to evade the T-cell-mediated immune regulation [7]. Additionally, PD-L1 was found

in TEV, derived from melanoma [8], prostate cancer [11], glioblastoma [10], and leukaemia [13] and has been detected in blood samples of cancer patients [14]. Recent studies have suggested that EV isolated from the blood samples of cancer patients express PD-L1, and that EV PD-L1 content correlates with patient's pathological features [12,15, 16].

Tumour endothelial cells (TEC) strictly control tumour development and metastasis formation by allowing nutrient and oxygen supply, immune cell entrance, and managing the escape of tumour cells to reach secondary sites [17,18]. TEC are unique and differ from normal endothelial cells in term of proliferation surface protein expression, secretome, and released EV [19,20]. Moreover, naive EV released by TEC (nTEV) share with TEV several activities: the ability to promote vessel formation, the capability to restrain of the immune surveillance, and the enhancement of tumour growth and metastasis formation [2,4]. We have previously shown that TEC also express the receptor for interleukin 3 (IL-3Rα) [21]. More recently we provided evidence that the IL-3Rα blockade on TEC changes the content of their released EV (aTEV), impairing their oncogenic action [3,4]. Due to its highly expression in leukemic cells the impact of the IL-3Rα blockade has been extensively investigated in leukaemia patients [22], while poorly explored in solid tumours. Since nTEV suppress the immune response [2,6], while the impairment of IL-3 signalling in TEC, by the receptor blockade, interferes with tumour progression, we aimed to evaluate whether and how aTEV can also revert the immunosuppressive functions of nTEV in solid tumours. Particular attention has been devoted to investigate the impact of nTEV and aTEV in the regulation of PD-L1 expression.

2. Materials and methods

2.1. nTEV and aTEV isolation

TEC were isolated as previously described [23] and grown in the complete EndoGro medium (Millipore) supplemented with 2% of fetal bovine serum (FBS). TEC were functionally evaluated to form vessel-like structures at different passages. The expression of IL-3Rα on TEC untreated or stimulated with IL-3 was evaluated by Fluorescence-activated cell sorting (FACS) using anti-human IL-3Rα antibody (Miltenyi Biotec, #130–113–322).

For nTEV isolation, confluent TEC were cultured in serum-free DMEM for 18 h. For aTEV collection, TEC were treated with 1 μg/ml of anti-human IL-3Rα mouse antibody (R&D Systems, #MAB301–100, Clone 32703) in serum-free DMEM. The conditioned medium from TEC untreated or treated with the blocking IL-3Rα antibody was centrifuged for 30 min at 3.000 g to remove cell debris and apoptotic bodies. Then the supernatant was filtered with PES membrane filters (0.22 μm, Millipore) and submitted to ultracentrifugation for 2 h at 100.000 g at 4 °C, using the Beckman Coulter Optima L-100 K Ultracentrifuge with the rotor type 45 Ti 45000RPM. The EV pellets were resuspended in DMEM supplemented with 1% of DMSO and stored at − 80 °C until further use. After thawed, EV aliquots were resuspended in PBS and analysed using the Nanoparticle tracking analysis (NTA) by NanoSight NS300 system (Malvern Instruments, Ltd) and transmission electron microscopy (Jeol JEM 1400 Flash electron microscope, Jeol, Tokyo, Japan) [24]. For further characterisation ExoView analysis (NanoView Biosciences), and MACSPlex exosome kit (Miltenyi Biotech) were used according to manufacturer instructions.

Western blot analysis for nTEV and aTEV was performed using 7% sodium dodecyl sulfate–polyacrylamide gel electrophoresis. Immunoblotting with anti-human CD63 (Abcam, #ab134045), CD81 (Abcam, #ab109201), CD9 (Abcam, #ab223052), CD29 (Invitrogen, #Ma5–17103), and GM-130 (Abcam, #ab52649) antibody was performed overnight at 4 °C. Appropriate secondary HRP-labelled anti rabbit or mouse antibody (BioRad) were used at 1:1000 dilution for 1 h at room temperature. The protein bands were visualized with chemiluminescence (ECL) detection kit and ChemiDoc™ XRS + System

(BioRad). Lysates from cells, nTEV, and aTEV were loaded at concentration of 10 μg/well.

2.2. PBMC isolation and treatment with nTEV or aTEV

Fresh human PBMC were isolated by density gradient (Ficoll, Sigma) centrifugation from heparinized blood samples obtained from healthy donors. The use of PBMC was approved by the Ethic Committee of A.O. U. Città della Salute e della Scienza di Torino, Turin, Italy (CS2/1255–Protocol number 0050416, May 16, 2019). PBMC were seeded in 6-well plates at the density of 2×10^7/well in 2 ml of serum-free AIM V medium. nTEV or aTEV were added to PBMC at the concentration of 1×10^{10}/ml (approximately 1×10^3 EV/cell) for at least 24 h. As control, we used non-stimulated PBMC. After 24 h or 5 days, PBMC were counted using Muse® Count & Viability Kit (Luminex), analysed by FACS using the anti-human IL-3Rα antibody (#306014, Biolegend), or used for co-culture experiments or for T-cell isolation. In selected experiments, T-cells were isolated from fresh PBMC (naive) seeded at the density of 1×10^7/well in 2 ml of serum-free AIM V medium and stimulated as indicated.

For PD-L1 analysis, approximately 1×10^6 PBMC, cultured for 48 h in the presence of nTEV or aTEV were resuspended in 100 μl of PBS supplemented with 0.1% bovine serum albumin and incubated with anti-human PD-L1 antibody (Miltenyi Biotec, #130–122–809) or PE non-immune isotypic IgG for 30 min at 4 °C. Then the cells were washed and analysed using CytoFlex from Beckman Coulter.

T-cells were isolated before or after preconditioning PBMC with nTEV or aTEV using Dynabeads™ Untouched™ Human kit (Invitrogen, #11344D) according to the manufacturer instructions.

2.3. ELISA assay

Relative quantification of IL-1β, IL-10, and TGFβ1 secretion by PBMC pre-treated with nTEV or aTEV alone or co-cultured with tumour cells (MDA-MB-231 and TEC) was performed using DuoSet ELISA Development Systems (R&D Systems) according to manufacturer instructions. Naive PBMC served as internal control.

2.4. Co-culture of PBMC and TEC or MDA-MB-231 cells

To study the expression of the IL-3Rα on TEC, 0.4 μm pore transwells (Costar, #3412) were used for co-culture experiments with PBMC pre-treated with nTEV or aTEV. 1×10^5 TEC were seeded in 6-well plates and PBMC were stimulated with nTEV or aTEV as above described. After 24 h pre-stimulated PBMC were plated in the upper chamber of the transwell at the concentration of 5×10^6/well and put onto TEC. After additional 48 h TEC were analysed by FACS using the anti-human IL-3Rα antibody (Miltenyi Biotec, #130–113–322).

To evaluate the cytotoxic effects of PMBC against tumour, a direct cell-to-cell contact cultures were used. To this end, freshly isolated PBMC were stimulated with nTEV or aTEV as above described for 24 h, meanwhile TEC or MDA-MB-231 cells were labelled with CFSE and seeded in 6-well plates, at the concentration of 1×10^5/well. The day after, 5×10^6 of pre-stimulated PBMC were plated on TEC or MDA-MB-231 cells for 48 h. As control, we used TEC or MDA-MB-231 cells cultured alone or co-cultured with untreated PBMC. Six independent experiments were performed in duplicates.

2.5. Tumour in vivo models

Animal studies were conducted in accordance with the Italian National Institute of Health Guide for the Care and Use of Laboratory Animals (protocol No. 833/2020-PR). Mice were housed according to the guidelines of the Federation of European Laboratory Animal Science Association and the Ethical Committee of the University of Turin. The investigators (at least 2) were blinded when assessing the outcome. To
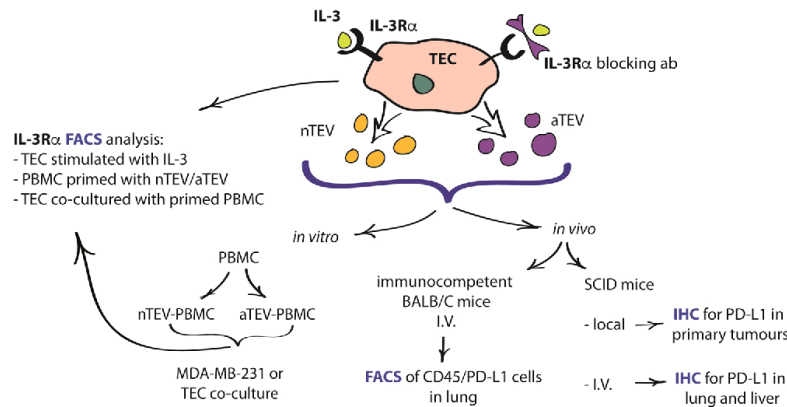
2

Fig. 1. Scheme of the *in vitro* and *in vivo* studies. FACS or IHC were used for PD-L1 detection. FACS analysis for IL-3Rα expression. I.V.: intravenously; IHC: immunohistochemistry.

investigate nTEV- or aTEV-mediated immune regulation *in vivo,* we used the immunocompetent female BALB/C mice. We treated mice intravenously (I.V.) with nTEV or aTEV (1×10^{10}/injection) 5 times during 2 weeks. The day after the last nTEV or aTEV injection, mice were sacrificed and PD-L1 was analysed in different tissues by FACS. To this end, the tissues were homogenized and cells positive for mouse PD-L1 (Biolegend, #124334) and CD45 (Miltenyi Biotec, #130–110–798) were detected.

Primary tumours were obtained by injecting subcutaneously Matrigel containing TEC in SCID mice (8 weeks/female) (4 mice/group) (1×10^6 cells/injection). Matrigel plugs containing TEC were locally injected with saline, nTEV, or aTEV (1×10^{10}/plug) at the third and seventh day after implantation. At day 10, the recovered plugs were embedded in paraffin (n = 4/each condition) and PD-L1 expression was analysed by immunohistochemistry, using the anti-human rabbit PD-L1 antibody (Abcam, #ab233482).

For the metastasis model, SCID mice were pre-treated intravenously with nTEV or aTEV for 5 days (1×10^{10}/injection). On day 5, 0.6×10^6 MDA-MB-231 cells were injected I.V. The mice were sacrificed after 5 weeks and lung and liver tissues analysed for PD-L1 expression. Liver metastases were also counted according to human PD-L1 expression.

2.6. Immunohistochemistry for PD-L1 detection in the lung and liver

Immunohistochemistry was performed using an automated slide-processing platform (Ventana BenchMark AutoStainer, Ventana Medical Systems), with Universal DAB Detection Kit detection systems. The anti-human PD-L1 rabbit polyclonal antibody (Abcam #ab233482) was diluted 1:100. Secondary HRP-labelled anti-rabbit antibody (Goat Anti-Rabbit IgG (H+L)-HRP Conjugate, BioRad) was used at 1:1000 dilution for 1 h at room temperature. Sections were counterstained with haematoxylin, dehydrated, and mounted. Quantification of the PD-L1 expression was performed using Fiji software (ImageJ). The results were expressed as mean ± SD of PD-L1 positive area (related units) per sample (10 images/section, 4 samples/each condition).

2.7. miR-214 enrichment in nTEV

To obtaining nTEV enriched in miR-214, TEC growing in 75 cm cultured flasks were transfected with HiPerfect reagent (Qiagen) using 20 μM hsa-miR-214 Pre-miR™ miRNA Precursor (PM12124, Invitrogen) according to manufacturer instructions. TEC transfected with scramble mimic were used as control. The day after transfection fresh FBS-free DMEM was replaced for additional 24 h and collected for nTEV_miR-

214 or Scramble miRNA_TEV isolation. We used PCR to confirm the enrichment of miR-214 in nTEV_miR-214. Briefly, single-stranded cDNA was generated from total RNA sample (80 ng) by reverse transcription using miScript Reverse Transcription Kit (Qiagen) following the manufacturer's protocol. miR-214 content was measured by qRT-PCR using the miScript SYBR Green PCR Kit (all from Qiagen). All reactions were performed using an Applied Biosystems 7900HT real-time PCR instrument and run in triplicate (3 ng of cDNA for each reaction) as described by the manufacturer's protocol (Qiagen). Relative miR-214 expression was normalized to the mean expression value of RNU6 and actin housekeeping genes. Data were analysed using Expression Suite Software (ThermoFisher).

2.8. Statistical Analysis

All data are reported as mean ± SD. Comparison between two groups was analysed by Student's t-test. Data passed both normality and equal-variance tests. One-way ANOVA followed by Tukey's multiple-comparison test was used for comparison among 3 or more groups; *p*-value < 0.05 was considered as significant. All *in vitro* or *in vivo* data are representative of at least 4 independent experiments. Graph Pad Prism version 5.04 (Graph Pad Software) was used for all statistical analyses.

3. Results

3.1. nTEV and aTEV characterisation

Firstly, nTEV and aTEV were characterized (see the scheme of the study, Fig. 1). As shown by TEM and NanoSight (data not shown), nTEV and aTEV did not differ in size (Supplementary Fig. S1). ExoView (NanoView Biosciences), MACSPlex (Miltenyi Biotech), and Western blot analyses, revealed a similar pattern of surface marker expression (CD9, CD29, CD63, and CD81) (Supplementary Fig. S1). We failed to detect PD-L1 on both nTEV and aTEV (data not shown).

3.2. IL-3Rα expression in TEC

This study has been designed to investigate the potential "clinical" impact of targeting TEC using a blocking IL-3 receptor antibody, and, in particular, the effect on PD-L1 expression. Therefore, the expression of IL-3Rα was first evaluated on naive or IL-3 stimulated TEC. Moreover, since IL-3 is mostly released by activated T-cells [24], to mimic the TME, IL-3Rα was also analysed on TEC stimulated with nTEV-primed PBMC (Fig. 1). As shown by FACS analysis, IL-3 significantly up-regulated the
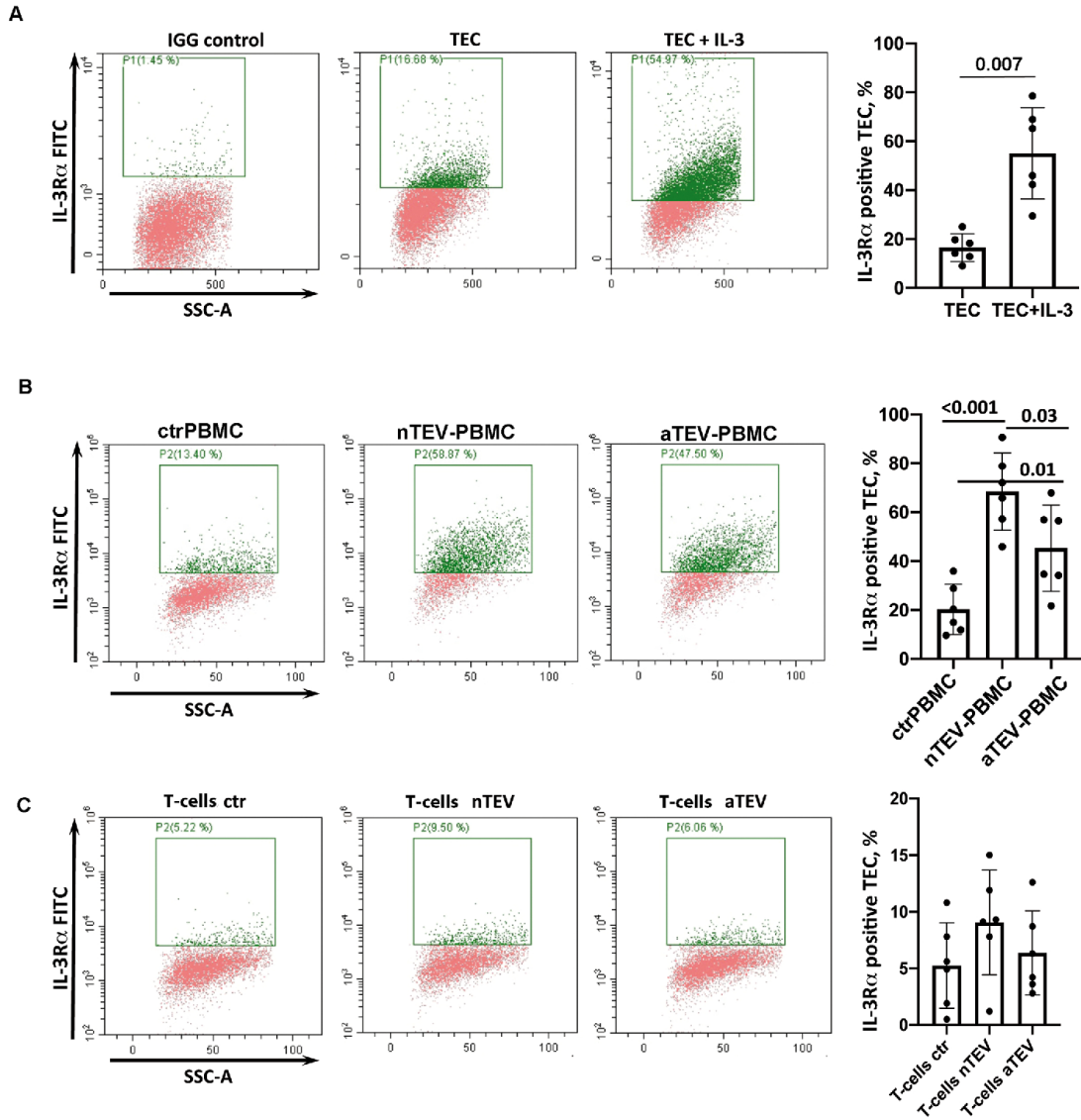
3

Fig. 2. IL-3Rα is up-regulated in TEC co-cultured with primed PBMC and T-cells, and stimulated with IL-3. (A) Representative FACS dot plots of untreated or IL-3 stimulated TEC (24 h). (B) Representative FACS dot plots of TEC co-cultured with control PBMC (ctrPBMC) or PBMC primed with nTEV or aTEV (24 h). (C) Representative FACS dot plots of TEC co-cultured with unstimulated T-cells or T-cells primed with nTEV or aTEV (24 h). Data are presented as the mean ± SD, n 6.

expression of its receptor on TEC (Fig. 2A). No differences in PBMC viability at both 24 h and 5 days, as well as in IL-3Rα expression (24 h) upon nTEV and aTEV priming were detected (Supplementary Fig. S2A-B).

Then we evaluated the expression of IL-3Rα in TEC co-cultured with nTEV or aTEV-primed PBMC. We demonstrated that PBMC primed with nTEV, but not with aTEV, significantly increased the expression of the IL-3Rα (Fig. 2B). Interestingly, naive T-cells (isolated from naive PBMC) pre-treated with nTEV or aTEV failed to induce the expression of IL-3Rα on TEC (Fig. 2C), suggesting a key role of myeloid cells in the transfer of nTEV signals.

3.3. PBMC primed with aTEV retain their anti-tumour properties

TME immunosuppression also stems from EV-mediated communications [1]. Therefore, the effect of nTEV and aTEV in shaping PBMC anti-tumour action was further investigated. To this end, PBMC were pre-stimulated with nTEV or aTEV for 24 h, and the secretion of inflammatory factors was first analysed. We found that nTEV significantly enhance the secretion of IL-10 and TGFβ1, while aTEV increase the release of IL-1β (Fig. 3 A). We then investigated the impact of PBMC, either untreated or primed with nTEV or aTEV, in co-cultures (direct contact) with CSFE-labelled MDA-MB-231 cells or TEC for 48 h. As
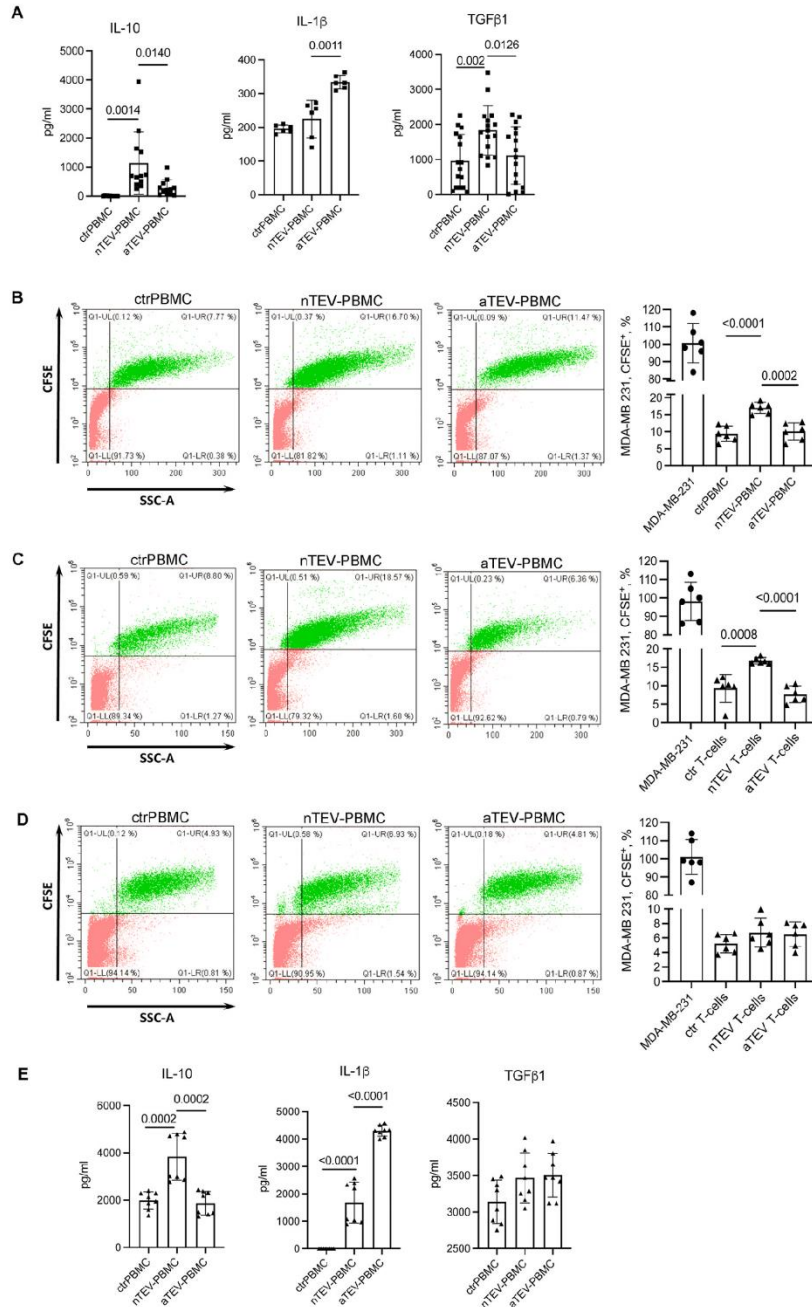
4

Fig. 3. nTEV, unlike aTEV, primed PBMC are impaired in their cytotic activity. (A) Diagrams of IL-1β, IL-10, and TGFβ1 secretion by naive (ctrPBMC) or PBMC pre-treated with nTEV or aTEV. (B) Representative FACS dot plots of MDA-MB-231 cells co-cultured with ctrPBMC or PBMC pre-treated with nTEV or aTEV. Diagram represents data on MDA-MB-231 cells cultured alone (circles) or with the aforementioned PBMC (triangles). (C) Representative FACS dot plots and diagram of MDA-MB-231 cells co-cultured with T-cells, isolated from ctrPBMC or from PBMC pre-treated with nTEV or aTEV. (D) Representative FACS dot plots and diagram of MDA-MB-231 cells co-cultured with naive T-cells (isolated from ctrPBMC) pre-treated with nTEV or aTEV. (E) Diagrams of IL-1β, IL-10, and TGFβ1 secretion by ctrPBMC or PBMC pre-treated with nTEV or aTEV co-cultured with MDA-MB-231 cells. Diagram data are presented as the mean ± SD (at least n = 6 independent experiments).
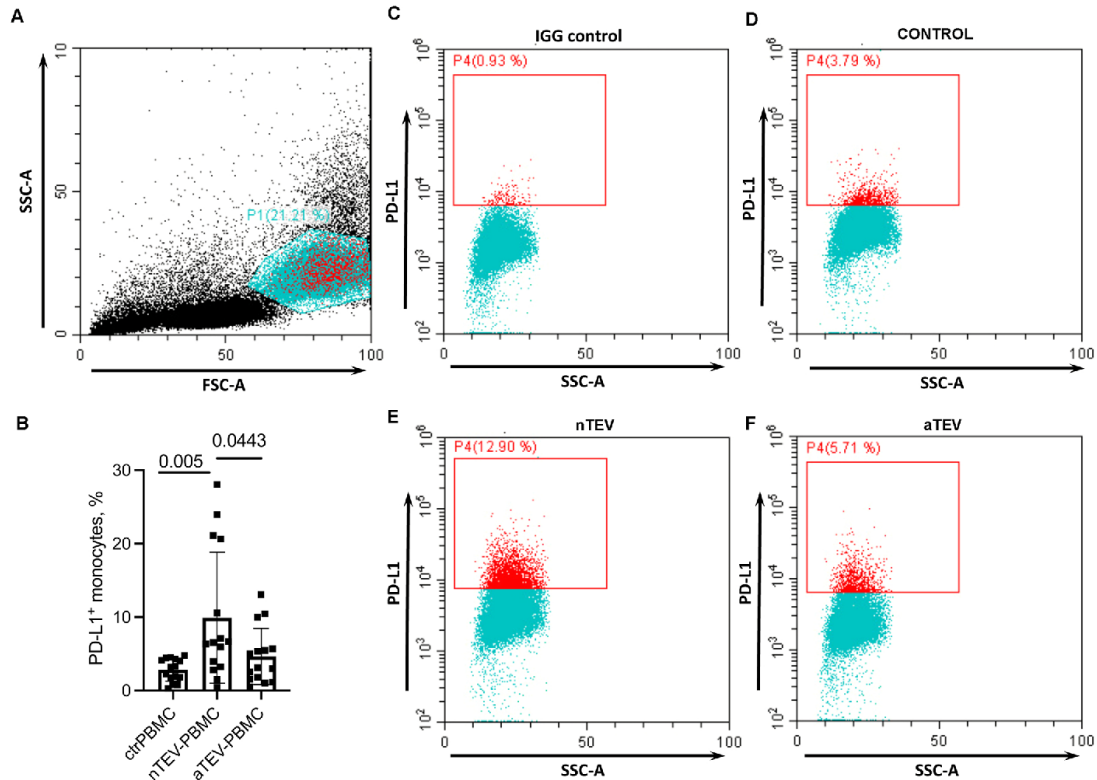
Fig. 4. nTEV, unlike aTEV, upregulated PD-L1 expression on PBMC. (A) Representative FACS dot plot image showing PBMC gating. (B) Diagram of PD-L1 expression on PBMC. Data are presented as the mean $\pm$ SD, n 15 independent experiments. (C-F) Representative FACS dot plot images of ctrPBMC incubated with IGG control antibodies (C), ctrPBMC (D), nTEV primed PBMC (E), and aTEV primed PBMC (F) stained with anti-human PD-L1 PE conjugated antibody. In red are indicated PD-L1$^+$ cells.

shown in Fig. 3B and Supplementary Fig. S3A we demonstrated that, while the percentage of living cells decreases in the presence of PBMC, the cytotoxic activity of nTEV primed PBMC was reduced compared to both naive and aTEV primed PBMC. To investigate whether changes in PBMC secretome may contribute to the different immune response, ELISA assay was also performed on these conditioned media. The results reported in Fig. 3D and Supplementary Fig. S3E revealed that in the presence of nTEV primed PBMC IL-10 secretion was increased. Conversely, and consistent with functional data, a reduced secretion of IL-10 and an increased level of IL-1β were detected in co-cultures containing aTEV primed PBMC. Of note, the release of TGFβ1 did not change (Fig. 3E, Supplementary Fig. S3E). We also investigated the contribute of T-cells. The role of T-cells in mediating the cytotoxic effect was confirmed by the observation that T-cells isolated from aTEV-primed PBMC were still able to exert anti-tumour effect when seeded together with MDA-MB-231 cells (Fig. 3 C) and TEC (Supplementary Fig. S3B). Conversely, no effect was detected when naive T-cells primed with nTEV or aTEV were co-cultured with MDA-MB-231 cells and TEC (Fig. 3D, Supplementary Fig. S3C). These data indicate that nTEV contribute to suppress the immune response and myeloid cells are key supervisors.

3.4. aTEV fine-tune PD-L1 expression

To evaluate if the expression of PD-L1 in myeloid cells may contribute to our observations, FACS analysis was first performed on PBMC primed with nTEV or aTEV. We found that, unlike aTEV, nTEV significantly increased the expression of PD-L1 on myeloid cells (Fig. 4).

Since no data are so far available on the role played by nTEV and, most importantly, by aTEV in an immunocompetent context, *in vivo* experiments were performed in BALB/C mice intravenously injected with nTEV or aTEV for 2 weeks (Fig. 5 A). PD-L1 and CD45 co-expression were evaluated in lung, bone marrow, spleen, and peripheral blood by FACS analysis. As shown in Fig. 5B, the number of PD-L1$^+$/CD45$^+$ cells was significantly increased in the lung of nTEV-treated animals, but not in spleen, bone marrow, and peripheral blood (data not shown). Of note, we found that aTEV *in vivo* administration reduced the percentage of PD-L1$^+$/CD45$^+$ cells isolated from the lung.

Since tumour cells also express PD-L1 and contribute to immune evasion, the ability of nTEV and aTEV to regulate its expression on TEC derived tumours was further evaluated. We demonstrated that intratumour injection of nTEV in Matrigel plugs containing TEC enhanced PD-L1 expression, while aTEV significantly reduced its expression (Fig. 5 C,D). This indicates that nTEV and aTEV can control PDL-1 expression in different cell population in the TME, including, at least, myeloid cells and tumour cells.

Finally, to investigate the possibility that aTEV may also impact on tumour cell recruitment by regulating PD-L1 expression on homed cells, nTEV and aTEV were injected intravenously for 5 consecutive days before MDA-MB-231 cell administration (Fig. 6 A). The expression of
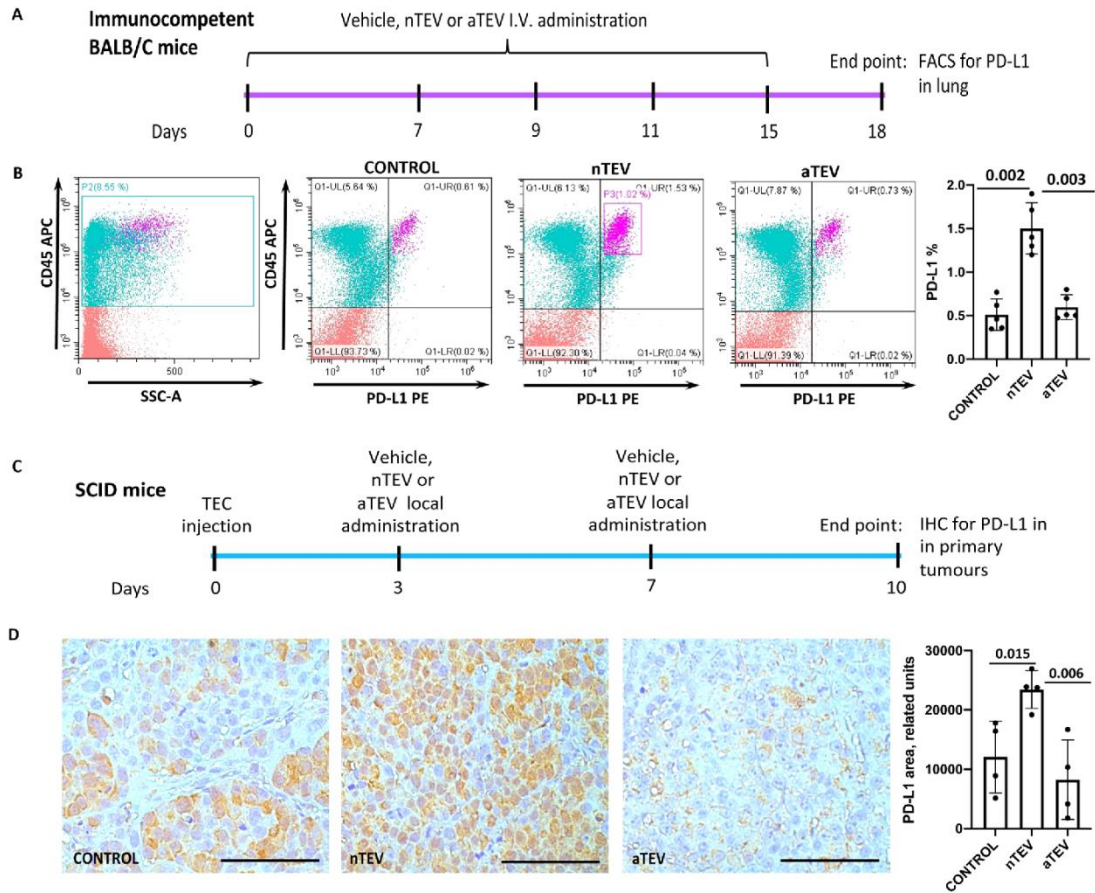
6

60

Fig. 5. nTEV, but not aTEV, increase the expression of PD-L1 in the lung and primary tumours. (A) Schematic representation of the *in vivo* study. (B) Representative FACS dot plot images showing CD45+/PD-L1+ lung-derived cells from control, nTEV, and aTEV treated mice. Data are presented as the mean ± SD, n   5. (C) Schematic representation of the *in vivo* study in SCID mice. (D) Representative images of Matrigel containing TEC treated with nTEV, or aTEV stained with PD-L1 antibody. Saline treatment served as control. Scale bars   100 µm (original magnification, 400X). Diagram data are presented as the mean ± SD, n   4. I.V.: intravenously; IHC: immunohistochemistry.

PD-L1 was analysed in the lung and liver of immune-deficient animals. As shown in Fig. 6B-C, PD-L1+ area were significantly increased in mice primed with nTEV both in the lung and liver tissues. Again, in aTEV treated animals a significant reduction of PD-L1+ area was detected in both organs. Finally, as previously reported in the lung [4] a reduced number of metastatic foci was detected in the liver of aTEV primed animals (Fig. 6 C).

This observation provides evidence that aTEV priming can prevent the recruitment/homing of PD-L1+ tumour cells both in the lung and in the liver. More importantly, these results indicate that disturbing the IL-3 signalling on TEC drives changes on their released aTEV, impacting on the expression of PD-L1 in both tumour and CD45+ cells.

3.5. miR-214 enrichment in aTEV regulates the expression of PD-L1

We have previously shown that aTEV miRNA content is relevant for their biological action [3,4]. It has been shown that miR-214 post--transcriptionally regulate PD-L1 expression in B-cell lymphoma [25]. Since miR-214 was found enriched in aTEV [3], we south to determine whether miR-214 enrichment could also control PD-L1 expression in our

model. To this end, the effect of nTEV enriched in miR-214 (nTEV_-miR-214) was evaluated *in vivo*. Matrigel plugs containing TEC were therefore locally injected with nTEV, aTEV, or nTEV_miR-214. Similarly to aTEV, nTEV_miR-214 treatment reduced the number of PD-L1+ cells in TEC formed tumours (Fig. 7) compared to nTEV. These data further confirm the role of miR-214 in the regulation of PD-L1 expression [25].

4. Discussion

In the present study, we have shown that IL-3 signalling in TEC regulates the release of pro-metastatic nTEV that suppress the immune response by enhancing PD-L1 expression on tumour and myeloid cells. Conversely, an approach based on IL-3Rα blockade on TEC led to the release of aTEV enriched in miR-214 that retune the aberrant anti-tumour immune response reshuffling PD-L1 expression. Overall, these findings provide evidence that blocking IL-3 signalling in the TME amends PD-L1 expression and reshapes the anti-tumour immune response.

Blocking the interaction between PD-1 and PD-L1 became a revolution in cancer therapeutic approaches, particularly for lung, kidney, and
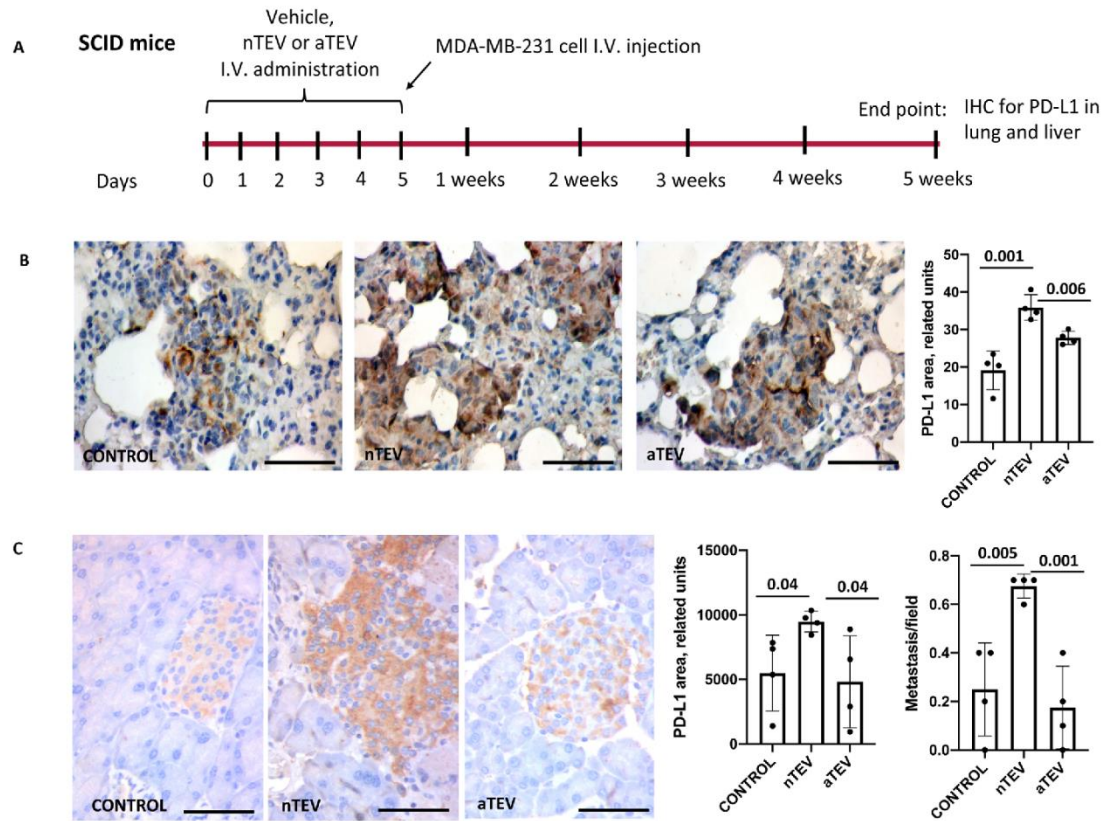
7

Fig. 6. PD-L1 expression is increased in the lung and liver tissues of SCID mice systemically primed with nTEV. (A) Schematic representation of the *in vivo* study. (B) Representative images and diagram of PD-L1 expression in lung tissues of control mice, and mice primed with nTEV or aTEV. Scale bars   100 μm (original magnification, 400X). Diagram data are presented as the mean ± SD, n   4. (C) Representative images of PD-L1 expression in liver tissues of control mice, and mice primed with nTEV or aTEV. Scale bars   100 μm (original magnification, 400X). Diagram data are presented as the mean ± SD, n   4.

bladder cancer, melanoma, and even for breast cancer [26–29]. However, the rate of success of PD-1/PD-L1 blockade in solid tumours is relatively low and mostly accompanied by both immune-related side effects [30] and TME-mediated acquired resistance [31,32]. Herein, an additional mechanism regulating PD-L1 expression in the TME is reported. In particular, we demonstrated that IL-3 signalling in TEC translates in the release of EV displaying immunosuppressive properties.

IL-3 is a hematopoietic factor mostly produced by activated T-cells, but also by monocytes/macrophages and other cell types [24]. According to proteinaltas.org (https://www.proteinatlas.org/ENS-G00000185291-IL3RA/tissue) the IL-3Rα is detected in cerebral cortex and fallopian tubes in healthy subjects, while in several tumour types in cancer patients (https://www.proteinatlas.org/ENSG00000185291-IL3 RA/pathology), thus suggesting the relevance of the IL-3 signalling in solid cancer. IL-3, and in particular its binding subunit, the IL-3Rα, is a well-established acute leukaemia therapeutic target, while its role in solid tumours is yet largely undetermined [33]. The observation that the IL-3Rα is highly expressed in leukaemia stem cells, compared to their normal counterpart, has provided the rational to specifically target tumour cells [22] using an anti-IL-3Rα blocking antibody [34]. In the present study, we demonstrated that a microenvironment containing IL-3 generates a positive loop involving TEC and PBMC resulting in the up regulation of the IL-3Rα in both cell types. This suggests that, as in the leukemic microenvironment, in the TME of solid tumours, the

up-regulation of IL-3Rα may represent a valuable therapeutic target. Therefore, since TEC may be considered the gate for antibody entry in the TME, an antibody-based approach was used to target IL-3Rα on TEC. By means of this approach we investigated whether blocking the IL-3 signalling may "educate" TEC to rearrange the cargo of their derivatives, aTEV, thereby refining the anti-tumour immune response.

TEV are involved in key aspects of cancer growth, metastatic spread, tumour immune editing, thereby considered as relevant anti-tumour targets [2,4,35]. The regulation of TEV molecular composition is highly sensitive and specific. Protein, RNA, and lipid content changes in response to microenvironment cues. We have previously shown that blocking the IL-3 signalling in TEC led to a complex rearrangement of EV molecular composition. This results in the inhibition of their pro-oncogenic functions, according to their angiogenic and metastatic actions [3,4]. Consistent with our previous results, using TEV from tumours of different origin [2], we demonstrated that nTEV impair the anti-tumour effect of PBMC against both TEC and MDA-MB-231 cells. Notably, we demonstrated that the anti-tumour effect of PBMC was retained by aTEV-primed PBMC, indicating that IL-3Rα blockade may also act on PBMC to re-establish their cytotoxic activity. Moreover, unlike T-cells isolated after PBMC pre-conditioning naive T-cells, directly stimulated with nTEV or aTEV, have no effect on tumour cells. This observation strongly supports the notion that nTEV-mediated immune regulation mainly involves mechanisms orchestrated by
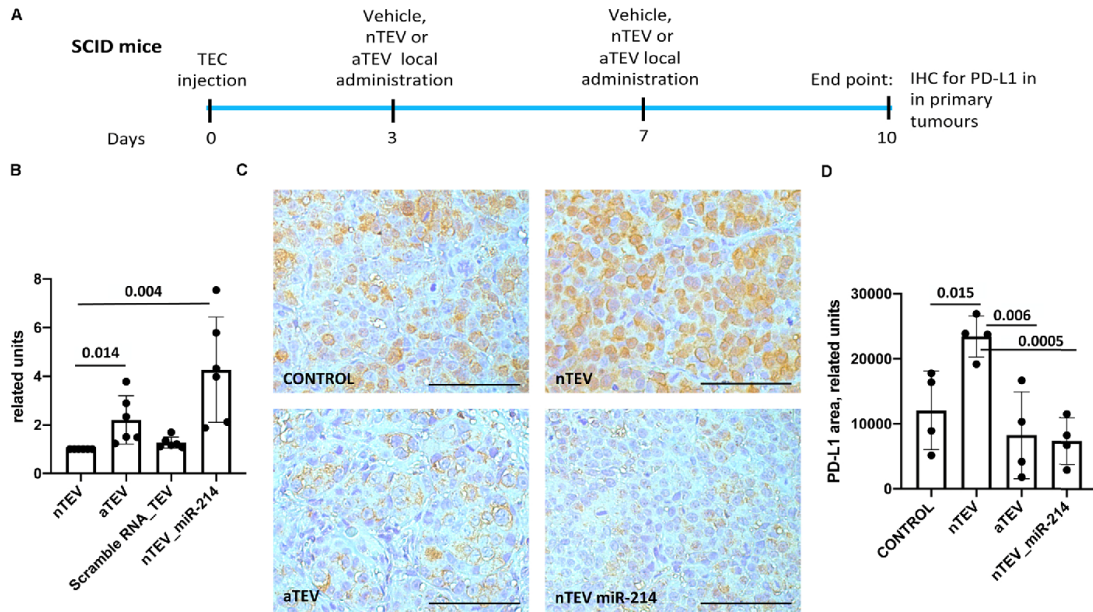
8

Fig. 7. miR-214 controls PD-L1 expression in *vivo*. (A) Schematic representation of the *in vivo* study. (B) Diagram of PCR analysis of miR-214 expression in nTEV, aTEV and nTEV_miR-214. As a control Scramble RNA was used. Data are presented as the mean ± SD, n ≥ 6. Representative images (C) and diagram (D) of PD-L1 staining on TEC in control tumours, and in tumours from mice locally treated with nTEV, aTEV or nTEV_miR-214. Scale bars ≥ 100 μm (original magnification, 400X). Diagram data are presented as the mean ± SD, n ≥ 4.

antigen-presenting cells. As a matter of fact, we demonstrated that nTEV, but not aTEV, increased the expression of PD-L1 on primary myeloid cells *in vitro* and *in vivo* in an immunocompetent model. This observation provides the first evidence that nTEV can control PD-L1 expression in an immunocompetent context.

PD-L1 is expressed by different tumour cell types [36], and its overexpression represents one of the most relevant mechanisms of T-cell exhaustion [37] and tumour progression. We herein demonstrated that intra-tumour nTEV injections was able to increase the expression of PD-L1 on tumour cells, and, more importantly, that aTEV bring back PD-L1 expression to the control level. Using a different mouse model, we also demonstrated that nTEV and aTEV can differently modulate PD-L1 expression in tumour cells engaged into metastatic sites. Of note, in this model we found that the expression of PD-L1 correlated with the number of metastases both in the lung and in the liver. Therefore, these results demonstrate that an antibody-based approach against the IL-3Rα may reshape PD-L1 expression and the anti-tumour immune response, *via* aTEV.

Different mechanisms control PD-L1 expression in cancer [38]. Inflammatory cytokines released in the TME have been reported to boost the expression of PD-L1 in tumour and stromal cells [39,40]. We herein demonstrated that the inflammatory cytokine IL-3, released in the TME, besides controlling the tumour vasculature takes part in cancer immune escape, *via* nTEV. Moreover, the observation that IL-10 was increased when PBMC were primed with nTEV and left in co-cultures with cancer cells, sustains the role of nTEV in the reshuffle of the TME secretome and in tumour immune suppression. The ability of aTEV to reverse PBMC secretome and to re-establish PBMC-mediated anti-tumour cytotoxic activity, further supports the role of IL-3 in tumour immune tolerance.

Several studies have designated EV as PD-L1 delivery system [10]. However, we failed to detect PD-L1 in nTEV suggesting that, rather than transferring PD-L1 to immune or tumour cells, nTEV tune the adaptive immune response by a mechanism involving their cargo.

Epigenetic mechanisms such as histone acetylation/methylation or abnormal miRNA expression are instrumental for cancer immune escape *via* PD-L1 expression [25,38]. miR-200, miR-326, miR-34a and miR-214 are from among the most relevant miRNAs involved in PD-L1 expression [25,38,42]. Consistent with these data, we demonstrated that the enrichment of miR-214 in aTEV down-regulates PD-L1 expression and may conceivably break down tumour immune evasion. However, since EV action rely on their entire cargo we cannot rule out the possibility that cancer microenvironment can hijack the TEV cargo at different level to facilitate discrete mechanisms of the multi-step cancer process.

5. Conclusions

Overall, we provide evidence that interfering with the IL-3 signalling, by blocking the activity of its receptor at the entrance of the TME, may be instrumental for reschedule the anti-tumour immune response. Downregulating PD-L1 expression in myeloid cells also improves the response of combined immune checkpoint approaches [43]. Therefore, our findings offer a new therapeutic window to boost and reshape the aberrant immune response in solid tumour.

CRediT authorship contribution statement

TL was involved in conceptualization, methodology, data curation and writing the original draft; MK provided formal analysis of *in vitro* and *in vivo* experiments; CG performed *in vitro* and *in vivo* experiments and provided formal analysis of the *in vitro* and *in vivo* studies; MC performed the animal studies; SF isolated and characterized extracellular vesicles; GL performed the animal study; EF performed *in vitro* studies; MFB was involved in conceptualization, supervision, writing, review and editing the Ms, as well as in providing resources.

9

Declaration of Competing Interest

The authors declare no conflict of interest.

Acknowledgements

The authors acknowledge the technical support of Dr. Federica Antico, Prof. Stefania Bruno, and Dr. Chiara Gai. A special thanks to Prof. Giovanni Camussi and Dr. Chiara Deregibus for TEM analysis.

Appendix A. Supporting information

Supplementary data associated with this article can be found in the online version at doi:10.1016/j.phrs.2022.106206.

References

[1] T.L. Whiteside, Exosomes and tumor-mediated immune suppression, J. Clin. Invest. vol. 126 (4) (. 2016) 1216–1223, https://doi.org/10.1172/JCI81136.

[2] T. Lopatina, et al., Extracellular vesicles released by tumor endothelial cells spread immunosuppressive and transforming signals through various recipient cells, Front. Cell Dev. Biol. vol. 8 (2020), https://doi.org/10.3389/fcell.2020.00698.

[3] G. Lombardo, et al., IL-3R-alpha blockade inhibits tumor endothelial cell-derived extracellular vesicle (EV)-mediated vessel formation by targeting the β-catenin pathway, Oncogene vol. 37 (9) (. 2018) 1175–1191, https://doi.org/10.1038/s41388-017-0034-x.

[4] T. Lopatina, et al., Targeting IL-3Rα on tumor-derived endothelial cells blunts metastatic spread of triple-negative breast cancer via extracellular vesicle reprogramming, Oncogenesis vol. 9 (10) (10, . 2020), https://doi.org/10.1038/s41389-020-00274-y.

[5] "A miRNA signature in endothelial cell-derived extracellular vesicles in tumor-bearing mice | Scientific Reports."https://www.nature.com/articles/s41598-019-52466-1 (Accessed 22 December 2021).

[6] K. Taguchi, T. Onoe, T. Yoshida, Y. Yamashita, Y. Tanaka, H. Ohdan, Tumor Endothelial Cell-Mediated Antigen-Specific T-cell Suppression via the PD-1/PD-L1 Pathway, Mol. Cancer Res. MCR vol. 18 (9) (. 2020) 1427–1440, https://doi.org/10.1158/1541-7786.MCR-19-0897.

[7] Y. Han, D. Liu, L. Li, PD-1/PD-L1 pathway: current researches in cancer, Am. J. Cancer Res. vol. 10 (3) (. 2020) 727–742.

[8] A.H. Sharpe, K.E. Pauken, The diverse functions of the PD1 inhibitory pathway, Nat. Rev. Immunol. vol. 18 (3) (. 2018) 153–167, https://doi.org/10.1038/nri.2017.108.

[9] V.R. Juneja, et al., PD-L1 on tumor cells is sufficient for immune evasion in immunogenic tumors and inhibits CD8 T cell cytotoxicity, J. Exp. Med. vol. 214 (4) (. 2017) 895–904, https://doi.org/10.1084/jem.20160801.

[10] G. Chen, et al., Exosomal PD-L1 contributes to immunosuppression and is associated with anti-PD-1 response, Nature vol. 560 (7718) (. 2018) 382–386, https://doi.org/10.1038/s41586-018-0392-8.

[11] M. Poggio, et al., Suppression of exosomal PD-L1 induces systemic anti-tumor immunity and memory, e13, Cell vol. 177 (2) (. 2019) 414–427, https://doi.org/10.1016/j.cell.2019.02.016.

[12] F.L. Ricklefs, et al., Immune evasion mediated by PD-L1 on glioblastoma-derived extracellular vesicles, eaar2766, Sci. Adv. vol. 4 (3) (. 2018), https://doi.org/10.1126/sciadv.aar2766.

[13] M.J. Cox, et al., Leukemic extracellular vesicles induce chimeric antigen receptor T cell dysfunction in chronic lymphocytic leukemia, Mol. Ther. J. Am. Soc. Gene Ther. vol. 29 (4) (. 2021) 1529–1540, https://doi.org/10.1016/j.ymthe.2020.12.033.

[14] J. Zhou, et al., Soluble PD-L1 as a biomarker in malignant melanoma treated with checkpoint blockade, Cancer Immunol. Res. vol. 5 (6) (. 2017) 480–492, https://doi.org/10.1158/2326-6066.CIR-16-0329.

[15] M.-N. Theodoraki, S.S. Yerneni, T.K. Hoffmann, W.E. Gooding, T.L. Whiteside, Clinical significance of pd-l1+ exosomes in plasma of head and neck cancer patients, J. Am. Assoc. Cancer Res. vol. 24 (4) (. 2018) 896–905, https://doi.org/10.1158/1078-0432.CCR-17-2664.

[16] S. Ludwig, et al., Suppression of lymphocyte functions by plasma exosomes correlates with disease activity in patients with head and neck cancer, Clin. Cancer Res. . J. Am. Assoc. Cancer Res. vol. 23 (16) (. 2017) 4843–4854, https://doi.org/10.1158/1078-0432.CCR-16-2819.

[17] D.A.-M. Annan, H. Kikuchi, N. Maishi, Y. Hida, K. Hida, Tumor endothelial cell—a biological tool for translational cancer research, Int. J. Mol. Sci. vol. 21 (9) (. 2020), https://doi.org/10.3390/ijms21093238.

[18] H. Ohmura-Kakutani, et al., Identification of tumor endothelial cells with high aldehyde dehydrogenase activity and a highly angiogenic phenotype, PLOS ONE vol. 9 (12) (. 2014), e113910, https://doi.org/10.1371/journal.pone.0113910.

[19] B. Bussolati, I. Deambrosis, S. Russo, M.C. Deregibus, G. Camussi, Altered angiogenesis and survival in human tumor-derived endothelial cells, FASEB J. vol. 17 (9) (2003) 1159–1161, https://doi.org/10.1096/fj.02-0557fje.

[20] D. Lambrechts, et al., Phenotype molding of stromal cells in the lung tumor microenvironment, Nat. Med. vol. 24 (8) (. 2018) 1277–1289, https://doi.org/10.1038/s41591-018-0096-5.

[21] P. Dentelli, A. Rosso, C. Olgasi, G. Camussi, M.F. Brizzi, IL-3 is a novel target to interfere with tumor vasculature, Oncogene vol. 30 (50) (. 2011) 4930–4940, https://doi.org/10.1038/onc.2011.204.

[22] I. Aldoss, M. Clark, J.Y. Song, V. Pullarkat, Targeting the alpha subunit of IL-3 receptor (CD123) in patients with acute leukemia, Hum. Vaccin. Immunother. vol. 16 (10) (. 2020) 2341–2348, https://doi.org/10.1080/21645515.2020.1788299.

[23] T. Lopatina, et al., Extracellular vesicles from human liver stem cells inhibit a angiogenesis, Int. J. Cancer vol. 144 (2) (. 2019) 322–333, https://doi.org/10.1002/ijc.31796.

[24] M.C. Deregibus, et al., Charge-based precipitation of extracellular vesicles,", Int. J. Mol. Med. vol. 38 (5) (. 2016) 1359–1366, https://doi.org/10.3892/ijmm.2016.2759.

[25] S.E. Broughton, et al., The GM-CSF/IL-3/IL-5 cytokine receptor family: from ligand recognition to initiation of signaling, Immunol. Rev. vol. 250 (1) (. 2012) 277–302, https://doi.org/10.1111/j.1600-065X.2012.01164.x.

[26] J.-R. Sun, X. Zhang, Y. Zhang, MiR-214 prevents the progression of diffuse large B-cell lymphoma by targeting PD-L1, Cell. Mol. Biol. Lett. vol. 24 (1) (. 2019) 68, https://doi.org/10.1186/s11658-019-0190-9.

[27] "Pembrolizumab versus Chemotherapy for PD-L1–Positive Non–Small-Cell Lung Cancer | NEJM." https://www.nejm.org/doi/full/10.1056/nejmoa1606774 (Accessed 22 December 2021).

[28] "Nivolumab versus Everolimus in Advanced Renal-Cell Carcinoma | NEJM." https://www.nejm.org/doi/full/10.1056/nejmoa1510665 (Accessed 22 December 2021).

[29] "Pembrolizumab as Second-Line Therapy for Advanced Urothelial Carcinoma | NEJM." https://www.nejm.org/doi/full/10.1056/nejmoa1613683 (Accessed 22 December 2021).

[30] P. Schmid, et al., Atezolizumab and Nab-Paclitaxel in Advanced Triple-Negative Breast Cancer, N. Engl. J. Med. vol. 379 (22) (. 2018) 2108–2121, https://doi.org/10.1056/NEJMoa1809615.

[31] F. Martins, et al., Adverse effects of immune-checkpoint inhibitors: epidemiology, management and surveillance, Nat. Rev. Clin. Oncol. vol. 16 (9) (. 2019) 563–580, https://doi.org/10.1038/s41571-019-0218-0.

[32] R. Pathak, R.R. Pharaon, A. Mohanty, V.M. Villaflor, R. Salgia, E. Massarelli, Acquired resistance to PD-1/PD-L1 blockade in lung cancer: mechanisms and patterns of failure, Cancers vol. 12 (12) (. 2020) 3851, https://doi.org/10.3390/cancers12123851.

[33] Y. Shi. et al. Acquired resistance to PD-L1 inhibition is associated with an enhanced type I IFN-stimulated secretory program in tumor cells 2021.

[34] U. Testa, R. Riccioni, D. Diverio, A. Rossini, F. Lo Coco, C. Peschle, Interleukin-3 receptor in acute leukemia, Leukemia vol. 18 (2) (. 2004) 219–226, https://doi.org/10.1038/sj.leu.2403224.

[35] "Full article: A Phase 1 study of the safety, pharmacokinetics and anti-leukemic activity of the anti-CD123 monoclonal antibody CSL360 in relapsed, refractory or high-risk acute myeloid leukemia." https://www.tandfonline.com/doi/full/10.3109/10428194.2014.956316 (Accessed 22 December 2021).

[36] R. Kalluri, The biology and function of exosomes in cancer, J. Clin. Invest. vol. 126 (4) (. 2016) 1208–1215, https://doi.org/10.1172/JCI81135.

[37] A.H. Sharpe, E.J. Wherry, R. Ahmed, G.J. Freeman, The function of programmed cell death 1 and its ligands in regulating autoimmunity and infection, Nat. Immunol. vol. 8 (3) (. 2007) 239–245, https://doi.org/10.1038/ni1443.

[38] K.E. Pauken, E.J. Wherry, Overcoming T cell exhaustion in infection and cancer, Trends Immunol. vol. 36 (4) (. 2015) 265–276, https://doi.org/10.1016/j.it.2015.02.008.

[39] J.-H. Cha, L.-C. Chan, C.-W. Li, J.L. Hsu, M.-C. Hung, Mechanisms Controlling PD-L1 Expression in Cancer, Mol. Cell vol. 76 (3) (. 2019) 359–370, https://doi.org/10.1016/j.molcel.2019.09.030.

[40] X. Wang, et al., Inflammatory cytokines IL-17 and TNF-α up-regulate PD-L1 expression in human prostate and colon cancer cells, Immunol. Lett. vol. 184 (. 2017) 7–14, https://doi.org/10.1016/j.imlet.2017.02.006.

[42] L. Shao, et al., MicroRNA-326 attenuates immune escape and prevents metastasis in lung adenocarcinoma by targeting PD-L1 and B7-H3, Cell Death Disco vol. 7 (1) (. 2021) 1–10, https://doi.org/10.1038/s41420-021-00527-8.

[43] E. Anastasiadou, et al., MiR-200c-3p Contrasts PD-L1 induction by combinatorial therapies and slows proliferation of epithelial ovarian cancer through downregulation of β-catenin and c-myc, Cells vol. 10 (3) (. 2021) 519, https://doi.org/10.3390/cells10030519.

Review

The Wnt Signalling Pathway: A Tailored Target in Cancer

Malvina Koni, Veronica Pinnarò and Maria Felice Brizzi *

Department of Medical Sciences, University of Turin, Corso Dogliotti 14, 10126 Turin, Italy;
malvina.koni@unito.it (M.K.); veronica.pinnaro@edu.unito.it (V.P.)
* Correspondence: mariafelice.brizzi@unito.it; Tel.: +39-0116706653

check for
updates

Abstract: Cancer is one of the greatest public health challenges. According to the World Health Organization (WHO), 9.6 million cancer deaths have been reported in 2018. The most common cancers include lung, breast, colorectal, prostate, skin (non-melanoma) and stomach cancer. The unbalance of physiological signalling pathways due to the acquisition of mutations in tumour cells is considered the most common cancer driver. The Wingless-related integration site (Wnt)/β-catenin pathway is crucial for tissue development and homeostasis in all animal species and its dysregulation is one of the most relevant events linked to cancer development and dissemination. The canonical and the non-canonical Wnt/β-catenin pathways are known to control both physiological and pathological processes, including cancer. Herein, the impact of the Wnt/β-catenin cascade in driving cancers from different origin has been examined. Finally, based on the impact of Extracellular Vesicles (EVs) on tumour growth, invasion and chemoresistance, and their role as tumour diagnostic and prognostic tools, an overview of the current knowledge linking EVs to the Wnt/β-catenin pathway is also discussed.

Keywords: Wnt/β-catenin dependent pathway; Wnt/β-catenin independent pathway; colorectal cancer; breast cancer; ovarian cancer; extracellular vesicles

1. Introduction

The human wingless-related integration site (Wnt) genes encode 19 evolutionarily conserved glycoproteins with 22-24 Cys residues. In the endoplasmic reticulum (ER), the Wnt ligands are post-translationally acetylated by porcupine, a membrane associated O-acyl transferase. Acetylation leads to palmitoylation, which is required for the release and binding of Wnt to the frizzled (*FZD*) receptors. This, in turn, drives the biological response [1].

The Wnt signalling pathway regulates crucial cellular processes including cell fate determination, organogenesis during embryonic development, normal adult homeostasis, motility, polarity and stem cell renewal [2]. Moreover, its contribution in cancer has been extensively investigated [3].

The Wnt pathway has been widely studied and reviewed, and a general understanding of the transduction cascade has been clarified. The Wnt cascade has been subdivided into different branches due to its complexity [4,5]. They include the canonical Wnt/β-catenin (Wnt/β-catenin dependent pathway) and the non-canonical Wnt/β-catenin pathway (β-catenin-independent pathway). The latter was further allocated into two additional branches, the planar cell polarity (PCP) and the Wnt/calcium pathways [2]. Both of them contribute to cancer development and dissemination.

The aim of the present review is to provide an overview of the current knowledge about the Wnt signalling pathway in tumour development and progression. Tumours from different origin are discussed. Although the canonical and the non-canonical Wnt/β-catenin pathway work together to control physiological and pathological processes [2], data related to each one are independently

debated. Finally, the contribution of extracellular vesicles (EVs) in triggering the Wnt/β-catenin cascade is also analyzed.

2. Wnt Canonical Pathway: β-Catenin Dependent

The canonical pathway turns around the β-catenin intracellular level (Figure 1). In the absence of Wnt proteins, the β-catenin "destruction complex" keeps low β-catenin in the cell. The "destruction complex" mainly consists of two kinases: casein kinase 1α (*CK1α*), glycogen synthase kinase 3 β (*GSK-3β*) and two scaffolds: axis inhibition (*Axin*), and adenomatous polyposis coli (*APC*). Firstly, β-catenin undergoes phosphorylation by *CK1α* at serine 45 (Ser45), Ser33, Ser37 and threonine 41 (Thr41) by *GSK-3β*. Then, the E3 ubiquitin ligase, denoted as β-transducin repeat-containing protein (*βTrCP*), marks β-catenin ubiquitination and degradation [1]. This prevents β-catenin nuclear translocation while allowing histone deacetylation and chromatin compaction by the Groucho repressor, translating into the inhibition of gene transcription [6] (Figure 1a).
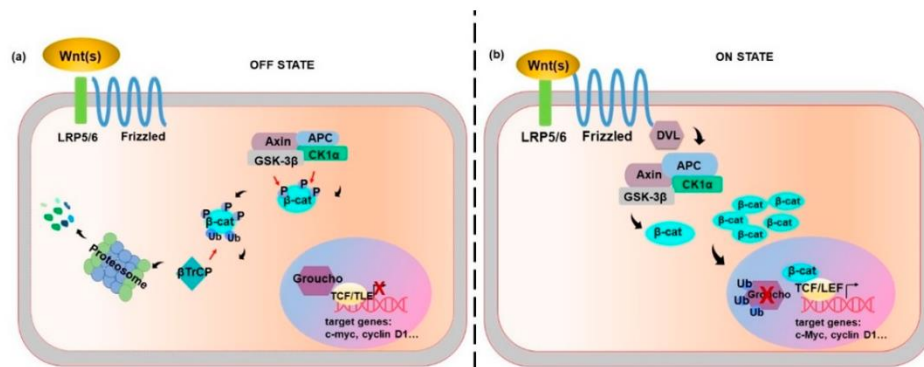

Figure 1. The Canonical Wnt signalling pathway. (**a**) OFF STATE. In the absence of Wnt ligands, β-catenin moves to the "destruction complex" consisting of casein kinase 1α (*CK1α*), glycogen synthase kinase 3 β (*GSK-3β*) and two scaffolds: axis Inhibition (*Axin*), and adenomatous polyposis coli (*APC*). β-catenin undergoes phosphorylation at Ser45 residue by *CK1α* and at Ser33, Ser37 and Thr41 residues by *GSK-3β*. Then, the E3 ubiquitin ligase β-transducin repeat-containing protein (*βTrCP*) marks β-catenin ubiquitination and proteasomal degradation. This prevents β-catenin nuclear accumulation while allowing chromatin compaction and Groucho-mediated promoter repression. (**b**) ON STATE. The Wnt ligands bind to frizzled (*FZD*) receptor and the low-density-lipoprotein-related protein 5/6 (*LRP5/LRP6*); this results in dishevelled (*DVL*) phosphorylation and β-catenin release from the "destruction complex", allowing β-catenin accumulation and nuclear translocation. In the nucleus, the Groucho repressor undergoes displacement, allowing β-catenin to interact with T-cell factor/lymphoid enhancer factor (*TCF/LEF*), chromatin remodeling and transcription of genes such as *c-myc* and *cyclin D1*.

The activation of the canonical Wnt signal requires both the *FZD* family receptors and the low-density-lipoprotein-related protein 5/6 (*LRP5/LRP6*) co-receptors, phosphorylation of which is essential for receptor activation. Wnt binding to its receptor results in dishevelled (*DVL*) phosphorylation, leading to *Axin* de-phosphorylation and decline of its cytoplasmic content [7]. Thereby, β-catenin can be released from the "destruction complex", and its degradation prevented while stabilization is allowed. Accumulation of β-catenin turns into its nuclear translocation [7].

Although several nuclear β-catenin binding partners have been involved in the control of gene transcription, the most relevant β-catenin partners are the members of the T-cell factor/lymphoid enhancer factor (*TCF/LEF*) family of transcription factors [7]. This complex binds to the promoter region of target genes and regulates their transcription.

Once in the nucleus, the engagement of β-catenin transiently converts the *TCF/LEF* into transcriptional activators, which displace Groucho and induce chromatin remodelling and transcriptional activity (Figure 1b).

A number of genes are targeted by Wnt-β-catenin. Among them, genes involved in positive- and negative-feedback regulation, cell-cycle progression, and stem cell homeostasis are the most commonly included genes.

3. Wnt Non-Canonical Pathways: Wnt/Planar Cell Polarity (PCP) and Wnt/Calcium

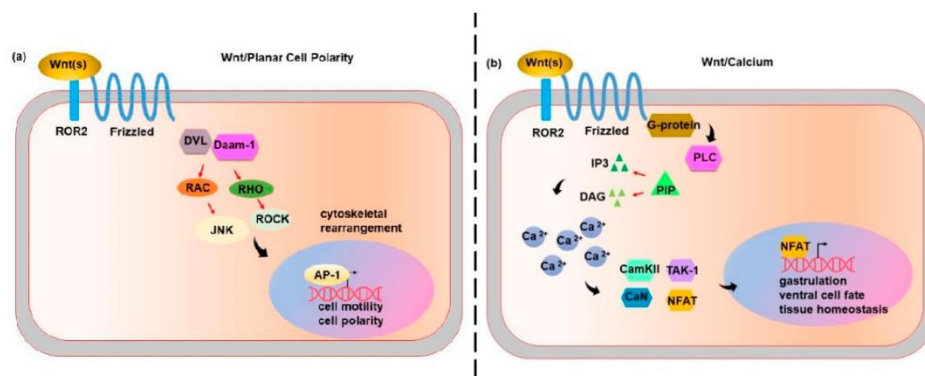To date, the canonical Wnt/β-catenin pathway is much better characterized than the non-canonical one (Figure 2).

Figure 2. The Wnt non-canonical signalling pathways. (**a**) Wnt/planar cell polarity (PCP) pathway. Wnt ligands bind to *FZD* receptors and co-receptor RAR-related orphan receptor (*ROR*) and convey the signal to *DVL*. *DVL* forms the Disheveled associated activator of morphogenesis 1 (*DVL-Daam-1*) complex, which triggers *RhoA*, *RHO* and *ROCK* to control cytoskeletal rearrangement. On the other hand, *DVL* triggers *RAC*, *JNK* and *AP-1* involved in cell motility and polarity. (**b**) Wnt/Calcium pathway. Wnt ligands bind to *FZD* and activate the phospholipase C (*PLC*), which hydrolyses the phosphatidylinositol (4,5)-biphosphates (*PIP2*) to inositol (1,4,5)-triphosphates (*IP3*) and diacylglycerol (*DAG*). This translates into intracellular calcium release and the activation of *CaN* and *CamKII*. The calmodulin activation stimulates *TAK-1* and *NLK* activity. *CaN* activates the *NFAT*, which moves to the nucleus and modulates the expression of genes involved in the control of gastrulation, ventral cell fate and tissue homeostasis.

In the non-canonical PCP pathway, Wnt ligands bind to *FZD* receptors and co-receptor protein tyrosine kinase 7 (*PTK7*), RAR-related orphan receptor (*ROR*) or the receptor like tyrosine kinase (*RYK*) and convey the signal to DVL. On the one side, *DVL* forms the disheveled associated activator of morphogenesis 1 (*DVL-Daam-1*) complex, which triggers a small guanosine-5'-triphosphate (GTP) GTPase, such as ras homolog gene family member A (*RhoA*), RHO and RHO-associated kinase (*ROCK*). *DVL* also triggers ras-related C3 botulinum toxin substrate (*RAC*), JUN-N-terminal kinase (*JNK*) and the activator protein-1 (*AP-1*). [7] The PCP pathway is involved in the cytoskeletal rearrangement, cell motility and co-ordinates cell polarity. In vertebrates, the PCP pathway is also required for morphology and migration of dorsal mesodermal cells undergoing gastrulation, hair follicle organization, and orientation of stereocilia in the sensory epithelium of the inner ear [8] (Figure 2a).

In the calcium-dependent pathway, Wnt ligands bind to *FZD* and activate the phospholipase C (*PLC*), which hydrolyses the phosphatidylinositol (4,5)-biphosphates (*PIP2*) to inositol (1,4,5)-triphosphates (*IP3*) and diacylglycerol (*DAG*). This translates into the release of the intracellular calcium and the activation of both calcineurin (*CaN*) and calcium/calmodulin-dependent kinase II

(*CamKII*). Moreover, the activation of calmodulin promotes the activation of the TGF-β-Activated kinase 1 (*TAK-1*) and nemo-like kinase (*NLK*), thereby antagonizing and neutralizing the canonical Wnt/β-catenin cascade. *CaN* activates the nuclear factor of activated T-cells (*NFAT*), which moves to the nucleus and regulates the expression of target genes [7] (Figure 2b). The calcium-dependent pathway plays a crucial role in several processes, including early pattern formation during gastrulation [2], ventral cell fate [9], dorsal axis formation [10], and tissue homeostasis [11].

4. Colorectal Cancer

Colorectal cancer (CRC) is one of most common cancers worldwide and represents a deep cause of cancer mortality [12] with a rapid increase in incidence and death rate [13]. Dienstmann et al. [14] established a new classification of CRCs into four consensus molecular subtypes (*CMSs*). Among them *CMS2*, *CMS3*, and *CMS4* have a higher rate of *APC* mutations (over 50%) compared to *CMS1*. Each *CMS* has unique features: *CMS1* (MSI Immune, 14%): hyper- mutated, microsatellite instability, strong immune activation; *CMS2* (Canonical, 37%): epithelial, chromosomally unstable, marked Wnt and myc signalling activation; *CMS3* (Metabolic, 13%): epithelial, metabolic dysregulation; and *CMS4* (Mesenchymal, 23%): a prominent transforming growth factor β (*TGFβ*) activation, stromal invasion, and angiogenesis. Samples with combined features (13%) represent transition phenotypes or are supposed to reflect the intra-tumour heterogeneity [14].

The heterogeneous genetic ground underlying CRC initiation and progression mainly involves gene fusion, deletion or amplification, somatic gene mutations and epigenetic alterations. Wnt/β-catenin signalling has emerged as one of the most significant biological pathways in both the physiological setting and in CRC development. Almost all CRCs are characterized by a hyper-active Wnt/β-catenin pathway, which, in many cases, is considered the most critical cancer initiating and driving event. Proteins and miRNAs guiding the Wnt/β-catenin pathway and proposed as potential CRC therapeutic targets are discussed.

5. Canonical Wnt/β-Catenin Pathway and CRC

Ring finger protein 6 (*RNF6*) is an oncogene frequently upregulated by gene amplification in primary CRC. Moreover, *APC* mutation and *RNF6* copy number amplification were commonly found in CRC patients. *RNF6* is a RING-domain E3 ubiquitin ligase and exerts its pro-metastatic effects by promoting CRC cell growth, cell-cycle progression, and epithelial to mesenchymal transition (EMT). Furthermore, *RNF6* expression and its gene amplification have been considered independent patients' prognostic factors. *RNF6* mediates the polyubiquitination of the transducin-like enhancer of split 3 (*TLE3*), a transcriptional repressor of the β-catenin/*TCF4* complex, and its proteasome degradation. The lack of *TLE3/TCF4/LEF* interaction enhances the Wnt/β-catenin transcriptional activity, and the expression of its downstream target genes [15] (Table 1).

The leucine-rich repeat-containing G-protein coupled receptor 5 (*LGR5*) is a Wnt/β-catenin target gene implicated in cancer cell proliferation and migration. It has been reported that *LGR5* is highly expressed in CRC tissues compared to the healthy ones. A decline in β-catenin and *c-myc* mRNA expression were detected by knocking-down *LGR5* expression, suggesting that it may regulate the Wnt/β-catenin activity by modulating the expression of β-catenin. Furthermore, since targeting *LGR5* improves the response to chemotherapy, *LGR5* has been proposed as a novel therapeutic target in CRC [16] (Table 1).

Table 1. Proteins involved in several tumours, their alteration, targets, and impact on tumours.

Protein	Related Cancers	Expression Level	Pathway Interaction	Impact on Tumour	Ref.
RNF6	CRC	Upregulated	β-catenin	cell growth cell cycle progression EMT metastasis	[15]
LGR5	CRC, BC	Upregulated	β-catenin	proliferation migration	[16,17]
TNIK	Gastric	Upregulated	β-catenin	cell growth	[18,19]
KYA1797K	CRC	Upregulated	β-catenin	tumour growth stem cell features	[20]
BCL6	CRC	Upregulated	β-catenin	cellular proliferation tumour development tumour progression	[21–23]
ZEB2 and ZEB1	CRC	Upregulated	β-catenin	tumour progression invasion	[17,24–26]
XIAP	CRC	Upregulated	β-catenin	proliferation chemoresistance	[24,25]
RHBDD1	CRC	Upregulated	β-catenin	metastasis stemness EMT migration invasiveness	[27]
SLC35C1	CRC	Downregulated	β-catenin	cell proliferation cell progression	[28]
NPTX2	CRC	Upregulated	β-catenin	tumour stages lymphatic invasion metastasis	[29]
KLHL22	CRC	Downregulated	β-catenin	invasion migration	[30]
CCL2	CRC	Upregulated	Non-canonical	progression	[31]
LGR4	BC	Upregulated	β-catenin	tumorigenesis metastasis CSC maintenance	[17,26,32,33]
ST7L	BC	Downregulated	GSK-3β	proliferation invasion	[34]
TMED	BC	Upregulated	β-catenin	cell cycle progression colony formation migration	[35]
Wnt5a	BC	Downregulated	β-catenin	migration lactate production invasion	[36,37]
Wnt5a	BC	Downregulated	β-catenin -cyclin D1 -TGF-β	cell proliferation aggressiveness	[38,39]
Wnt5a	BC	Upregulated	ALCAM	vessel invasion tumour size migration	[40]
Nek2B	TNBC	Upregulated	β-catenin	chemoresistance	[41]
VANGL2	TNBC	Upregulated	p62/SQSTM1 (PCP)	migration anchorage-dependent and independent cell proliferation	[42]
HePTP	TNBC	Upregulated	-GSK-3β β-catenin	metastasis	[43]

Table 1. *Cont.*

Protein	Related Cancers	Expression Level	Pathway Interaction	Impact on Tumour	Ref.
DLC-3	TNBC	Downregulated	β-catenin	proliferation colony formation migration invasion	[44]
DKK1	OC	Downregulated	β-catenin	stemness	[45]
SFRP1	OC	Downregulated	β-catenin	cell growth stem-like phenotype	[46]
AXIN2	OC	Downregulated	β-catenin	stem-like phenotype	[46]
LGR6	OC	Upregulated	β-catenin	stemness chemoresistance	[47,48]
RAB14	OC	Upregulated	β-catenin	proliferation chemoresistance invasion	[49,50]
FZD7	OC	Upregulated	Non-canonical	EMT cell cycle progression migration	[51]
ITGBL1	OC	Upregulated	Non-canonical	migration adhesion	[52]
ALPL	OC	Upregulated	Non-canonical	EMT migration invasion	[53]
VDR	Melanoma	Upregulated	β-catenin	tumour growth immune response	[54]

The β-catenin and RAS signalling pathways are frequently associated with the development and progression of several different cancers. They mainly act on cancer stem cell (CSC) expansion. High levels of β-catenin and RAS proteins are considered the major drivers of CSC expansion and cancer dissemination and are associated with poor patient's outcome [55].

Targeting the CSC pool without affecting the somatic stem cell (SSC) niche is one of the major goals of recent decades. As reported by Lenz et al. [56], the β-catenin antagonist molecule, ICG-001, effectively prevented the interplay between β-catenin and its coactivator cAMP response element binding protein (CREB)-binding protein (*CBP*). Moreover, ICG-001 effectively and without side effects abrogated drug-resistant cells. On the same line, PRI-724, a second generation of *CBP*/β-catenin antagonist, was found safe in pre-clinical studies and displayed an acceptable toxicity profile.

Yu et al. [18] investigated the traf2- and nck-interacting kinase (*TNIK*) amplification and its role in tumor progression by applying siRNA technology, while Masuda et al. [19] have generated a small molecule denoted as NCB-0846 acting as *TNIK* inhibitor. *TNIK* selectively binds both to *TCF4* and β-catenin in order to promote cancer cell growth via Wnt/β-catenin cascade and drives colorectal CSC expansion. The NCB-0846 inhibitor was effective in interfering with *TNIK* activity tumour growth.

KYA1797K, a small molecule identified by Cha et al. [57], was found effective in suppressing CRC growth due to the activation of *GSK-3β* via Axin binding and β-catenin/RAS destabilization. In line with this observation, treatment with KYA1797K abrogated CRC stem cell features both in vitro and in vivo. Mechanistically, KYA1797K pushes β-catenin and RAS towards the *Axin* binding [20] (Table 1).

In the last decade, miRNAs have gained particular attention in cancer [58]. miRNA profiling has been linked to cancer types, stage, and invasion [59]. Moreover, oncogenic or tumour suppressive actions have been linked to miRNA expression. For these reasons, miRNAs are considered valuable tools for cancer diagnosis and prognosis and therefore useful therapeutic targets (Table 2).

Table 2. miRNAs involved in the tumours, their alteration and tumour impact.

miRNA	Related Cancer	Expression Level	Impact on Tumour	Ref.
miR-144-3p	CRC	Downregulated	cell proliferation	[21–23]
miR-377-3p	CRC	Upregulated	cell expansion EMT repression of apoptosis	[60]
miR-377-3p	CRC	Downregulated	proliferation migration chemoresistance	[61]
miR-520e	CRC	Downregulated	cell proliferation colony formation invasion	[62,63]
miR106a	BC	Upregulated	cell growth cisplatin sensitivity	[64]
miR-5188	BC	Upregulated	tumour cell proliferation metastasis formation EMT chemoresistance	[65]
miR-148a	BC	Downregulated	cell migration invasion	[66]
miR-6838-5p	BC	Downregulated	cell invasion migration EMT	[42,67]
miR-27a-3p	BC	Upregulated	proliferation migration.	[68]
miR-1207	OC	Upregulated	tumorigenicity stem cell-like traits stemness	[46]
miR-590-3p	OC	Upregulated	cell growth migration, invasion	[69,70]
miR-1180	OC	Upregulated	cell proliferation glycolysis	[71]
miR-939	PCa	Downregulated	tumour stage metastasis	[72]
miR-92a-3p	CRC EVs	Upregulated	cancer progression stemness EMT drug resistance	[73]
miR-1273f	HCC EVs	Upregulation	cell proliferation migration invasiveness EMT	[74]
miR-1260b	LAC EVs	Upregulation	cell invasion metastasis	[75]
miR-214-3p	TEC EVs	Upregulation	neovessel formation	[76]
miR-24-3p	TEC EVs	Downregulation	neovessel formation	[76]

Sun and co-workers [21] identified miR-144-3p as a new biomarker for CRC diagnosis and response to treatment. miR-144-3p was found downregulated and associated with CRC pathological stages in CRC patients. Interestingly, miR-144-3p overexpression reduced CRC cell proliferation by delaying G1/S phase transition in tumour cells. On the contrary, the B-cell lymphoma 6 protein (*BCL6*), a nuclear protein belonging to the BTB/POZ/zinc finger (*ZF*) family of transcription factors,

was found upregulated and surprisingly post-transcriptionally regulated by miR-144-3p. Previous studies revealed that *BCL6* is involved in the control of cell cycle progression and differentiation [22,23]. Indeed, miR-144-3p/*BCL6* co-operate to inhibit cellular proliferation, development, and progression of CRC by interfering with *c-myc* and *cyclin D1* expression [21] (Table 1).

miR-377-3p displays an ambiguous role in CRC. Liu and colleagues [60] uncovered that upregulation of miR-377-3p promotes G1-S phase transition, cell expansion and EMT, while repressing apoptosis in CRC patients. Moreover, *GSK-3β*, a direct miR-377-3p target, was found upregulated upon miR-377-3p overexpression. These data suggest that a complex regulatory network boosting tumour progression is associated with the expression of miR-377-3p in CRC.

Conversely, in a recent study, Huang et al. [61] have shown that miR-377-3p, significantly reduced in CRC patients, is involved in the control of proliferation, migration and chemo resistance, particularly at advanced tumour stage. The authors investigated miR-377 functions and mechanism of action in CRC cells. The zinc finger E-box binding homeobox 2 (*ZEB2*) and the X-linked inhibitor of apoptosis protein (*XIAP*) are two positive regulators of the Wnt/β-catenin cascade [24,25]. In CRC, *ZEB2* enables tumour progression and invasion, whereas *XIAP* promotes cell proliferation and chemoresistance. De facto, miR-377-3p overexpression was found to suppress the malignant CRC phenotype, as well as cell proliferation, invasion and drug resistance by directly targeting the 3′ UTR sequence of both *ZEB2* and *XIAP* mRNAs. Since miR-377-3p/*ZEB2-XIAP* inhibited CRC progression by reducing Wnt/β-catenin-associated gene expression (e.i. *cyclin D1*, *Axin2*, *TCF1*, *SOX2*, *c-myc*, matrix metalloproteinase-2 (*MMP-2*), *MMP-9*, CD44, vascular endothelial growth factor (*VEGF*), and Twist), approaches involving increasing its expression have been proposed for novel therapeutic options (Table 1).

Functional experiments showed that miR-520e plays a pivotal role in regulating CRC cell proliferation, colony formation and invasion [62]. Moreover, it has been reported that low miR-520e expression is associated with the increased CRC growth and migration. The astrocyte elevated gene-1 (*AEG-1*), which acts as an oncogene [63], is a direct miR-520e target in CRC. Cells overexpressing miR-520e displayed lower *GSK-3β* phosphorylation and β-catenin expression. Mechanistically, it was found that miR-520e regulates cancer cell behaviour by targeting *AEG-1*, which in turn inactivates the Wnt/β-catenin signalling and the transcription of its downstream genes. Hence, miR-520e overexpression could represent a promising therapeutic target in CRC by *AEG-1* suppression.

Approximately 40–50% of CRC patients develop metastasis, mostly to the liver and lung. In cancer patients, metastases are associated with 90% of all cancer-related death; thereby, the mechanisms accounting for the metastatic spread have been deeply investigated. Zhang et al. [27] demonstrated that the rhomboid domain containing 1 (*RHBDD1*) plays a crucial role in driving metastasis formation in CRC patients, via the Wnt/β-catenin pathway. It has been shown that *RHBDD1* is able to influence the Wnt/β-catenin cascade by increasing the phosphorylation of β-catenin at the Ser552 and Ser675 residue without affecting its nuclear translocation. Moreover, it promotes EMT, stemness, migration and invasiveness. *RHBDD1* also improves the expression of the β-catenin target gene, *ZEB1*. Furthermore, the protein level of *RHBDD1* positively correlated with *ZEB1*. Thereby, *RHBDD1* has been proposed as a novel therapeutic target and/or a clinically useful biomarker for metastatic CRC (Table 1).

SLC35C1, or GDP-fucose transporter 1, is a member of the solute carrier (*SLC*) superfamily of solute carriers. Deng's group [28] explored the mechanism throughout *SLC35C1* that regulates the canonical Wnt/β-catenin pathway in CRC. They demonstrated a reduction in *SLC35C1* and an increase in β-catenin at all tumour stages. Indeed, silencing *SLC35C1* resulted in the increased release of Wnt3a and *c-myc*, *Axin2* and *cyclin-D1* expression. This suggests that *SLC35C1* is involved in the control of the canonical Wnt/β-catenin pathway, and thereby in tumour cell proliferation and tumour progression (Table 1).

Neuronal pentraxin 2 (*NPTX2*) is a member of the neuronal pentraxin family and is essential for the formation of synapsis. *NPTX2* was found overexpressed at both mRNA and protein level in CRC, particularly in metastatic lesions [29]. *NPTX2*, which was found to positively correlate with tumour

stages, lymphatic invasion, distant metastasis, and poor patients' outcome, promotes β-catenin nuclear translocation and the expression of *c-myc, cyclin D1, Snail*, and *N-cadherin*. No *NPTX2* receptors have been identified in CRC; however, its cellular internalization was found mediated by the Wnt/β-catenin receptor, *FZD6*. Additionally, it has been reported that *NPTX2/FZD6* interaction translates in cancer cell proliferation and metastasis formation by triggering the Wnt/β-catenin pathway [29] (Table 1).

Aberrant gene expression and DNA methylation profiles are considered hallmarks of CRC initiation and progression [77]. Due to the *APC* inactivating mutations, the Wnt/β-catenin pathway plays a key role in CRC metastatic spread [78]. Bruschi el al. [79] investigated the early transcriptional and epigenetic changes resulting from *APC* inactivation in intestinal crypts in crypt base columnar (*CBC*) cells. The authors have found that *APC* disruption rapidly induces changes in DNA methylation, indicating that focal remodelling of the DNA methylation profile occurs early and concomitantly with the first oncogenic event. Moreover, it has been demonstrated that the hyper-activation of the Wnt/β-catenin pathway associated with the *APC* loss-of-function turns out in a rapid increase in intestinal stem cell commitment towards differentiation. Again, it was correlated with the remodelling of the DNA methylation profile. This study unveils that early changes in DNA methylation are crucial for the impaired fate decision program associated with *APC* loss-of-function.

The kelch-like family member 22 (*KLHL22*) is a tumour suppressor protein involved in the development/progression of several cancers [30]. Low expression of *KLHL22* was found in CRC tissues. *KLHL22* overexpression was associated with decreased migration, invasion and reduced expression of the EMT markers, vimentin, N-cadherin, Twist1 and Snail1. Intriguingly, *KLHL22* knockdown led to increased expression of β-catenin and *LEF*, while *KLHL22* overexpression translates into *GSK-3β* upregulation and β-catenin downregulation [30] (Table 1).

6. Non-Canonical Wnt Pathway and CRC

The canonical and non-canonical Wnt family members play discrete roles in CRC. The activation of the Wnt/calcium pathway turns into stimulation of sensitive proteins such as *CamKII* and *PKC* [80]. A Ror family of receptor tyrosine kinases, the *ROR2* has been shown to act as a Wnt5a receptor or co-receptor [81]. Wnt5a has different roles in CRC. It can act as an antagonist or agonist of the canonical Wnt/β-catenin pathway, depending on the cellular context. Lee et al. [82] noticed that the antagonism between the canonical and the non-canonical Wnt/β-catenin signalling pathways is linked to Wnt5a. Mechanistically, Wnt5a suppressed the canonical Wnt/β-catenin cascade by acting as a ligand on the *RORα* [81]. After *PKCα*-mediated phosphorylation, RORα modifies its affinity and interacts with the armadillo repeat domains of β-catenin, thus supressing its transcriptional activity.

Three relevant goals have been recently achieved by Voloshanenko et al. [83] supporting the role of Wnt5a/b in cell growth, via the non-canonical β-catenin pathway. First, they identified the procollagen-lysine,2-oxoglutarate 5-dioxygenase 2 (*PLOD2*), the hydroxyacyl-CoA dehydrogenase (*HADH*), ligand-dependent corepressor (*LCOR*) and the receptor expression-enhancing protein 1 (*REEP1*) as candidate genes regulated by the non-canonical Wnt/β-catenin pathway. Second, these genes were found regulated by Wnt5a/b, as well as by *ROR2*, the *DVL2*, the activating transcription factor 2 (*ATF2*) and *ATF4* in a non-canonical Wnt/β-catenin independent manner. Lastly, Wnt5a/b silencing was found to impair cancer cell proliferation.

Among several soluble Wnt proteins, Wnt11 was found to be upregulated in CRC patients [84]. Recently, Gorroño-Etxebarria and colleagues [85] have shown that increased Wnt11, and its *FZD6, RYK, PTK7* receptors, positively correlate with poor prognosis. Additionally, Wnt11 downregulated β-catenin transcriptional activity and increased *ATF2* via the non-canonical Wnt signalling pathway. Thereby, Wnt11 has been proposed as a prognostic biomarker and therapeutic target in CRC patients.

Tumour micro environment (TME) has a pivotal role in cancer development [86]. Liu et al. [31] reported that, unlike CRC cells, tumour associate macrophages (TAMs), and, in particular, M2-like cells, express Wnt5a. Furthermore, it has been shown that Wnt5a positive TAMs regulate macrophages infiltration, tumour cell proliferation and migration. Wnt5a pro-tumour activity was found to be

associated with the overexpression of the C-C motif chemokine ligand 2 (*CCL2*) in Wnt5a-treated macrophages. Consistently, Wnt5a knockdown reduced *CCL2* expression in TAMs and their cancer-promoting activity. In Wnt5a-treated macrophages, both *CaMKII* and ERK1/2 undergo phosphorylation and lead to *CCL2* secretion. This study provided evidence for a new role of Wnt5a in CRC and describes a potential novel therapeutic target (Table 1).

7. Breast Cancer

Breast cancer (BC) is the most diagnosed cancer in women [87], the first cause of cancer death in women worldwide [88], and one of the most expensive in terms of health care costs [87]. Both the canonical and non-canonical Wnt/β-catenin pathways are essential for mammary gland development [89] and for BC growth and dissemination [90]. Hyper-active Wnt/β-catenin was reported in breast tumours [91]. In human BC, elevated intracellular β-catenin level has been associated with high tumour grade [92] and poor prognosis. In addition, up to 90% of metaplastic carcinomas and non-metastasizing fibromatosis have been associated with the highest β-catenin expression level [93]. Moreover, proteins such as Wnt3a [94] and xenopus frizzled 7 (*Xfz7*) [95] have been involved in the activation of both the canonical and the non-canonical Wnt signalling pathways.

8. Canonical Wnt Pathway and BC

Dysregulation of the Wnt/β-catenin cascade has been associated with cancer initiation and metastasis formation [96]. Moreover, high β-catenin expression has been reported in basal-like BC subtype [91]. Additionally, it has been demonstrated that loss of secreted frizzled-related protein 1 (*sFRP1*) is an early event in BC patients and is associated with poor prognosis [97]. Furthermore, the activation of the Wnt/β-catenin cascade has been associated with radio resistance of progenitor cells. Thereby, the Wnt/β-catenin pathway has been proposed as a target to harm the self-renewal potential of stem/progenitors [98].

A recent study demonstrated that high β-catenin level is associated with miR106a overexpression and involved in BC cell growth. Additionally, high levels of miR106a were reported to reduce cisplatin sensitivity. Major results were obtained exploiting the Wnt inhibitor, FH535. In fact, FH535 treatment reduced the expression of β-catenin, *cyclin D1*, *c-myc* and *Ki67*, impaired tumour growth and induced apoptosis [64].

In a different study [99], the impact of the Wnt/β-catenin canonical pathway in cisplatin resistance was investigated by silencing β-catenin via small interfering RNA (siRNA). The authors demonstrated that upon β-catenin silencing, the cells become more sensitive to cisplatin treatment. These effects were associated with the increased expression of the apoptotic proteins caspase 3/9.

A recent study demonstrated that miR-5188, aberrantly expressed in breast cancer patients, positively correlates with poor prognosis. The molecular analyses revealed that miR-5188 directly targets the forkhead box protein O1 (*FOXO1*). In the physiological setting, *FOXO1* binds β-catenin and induces its degradation. This implies that miR-5188 overexpression leads to β-catenin nuclear accumulation and transcription of its downstream target genes, mainly involved in EMT, tumour cell proliferation, metastasis formation and chemo resistance. Moreover, the authors elegantly showed that miR-5188 expression is under the control of c-Jun, which directly binds to its promoter region. This in turn generates a positive loop, accelerating tumour progression. Clinically, miR-5188 has been proposed as a diagnostic or prognostic factor and/or a direct target for anti-cancer therapy [65].

The upregulation of the lncRNA hoxa transcript at the distal tip (*HOTTIP*) has also been linked to poor prognosis in BC patients. Overexpression of *HOTTIP* correlates with the expansion of breast CSCs (BCSCs) and the expression of the stem cell markers, *OCT4* and *SOX2*. Han et al. [66] demonstrated a reduced expression of differentiation markers, such as *CK18* and *CK14* and that miR-148a inhibits BC cell migration and invasion by directly targeting Wnt1. Moreover, it has been reported that *HOTTIP* controls miR-148a-3p by acting as a competing endogenous RNA (ceRNA). Thereby, *HOTTIP* promotes

expansion of CSCs in vitro and tumorigenesis in vivo by regulating the miR-148a-3p/Wnt1/β-catenin axis [66]. These data are summarized in Table 2.

The *LGR4* was identified as a prognostic marker in breast tumours displaying poor prognosis [32]. A tight molecular interplay between *LGR4* and Wnt/β-catenin signalling has been reported to control stemness. Indeed, *LGR4* binding to the soluble R-spondin proteins eases the Wnt/β-catenin cascade [33]. Previous studies have proven that upregulation of *ZEB1* by *SLUG* (the protein product of *SNAI2*), increased EMT [26]. As a matter of fact, *LGR4* knockdown leads to *SLUG* and *ZEB1* downregulation, thereby impairing invasion and metastasis [17]. A correlation with poor outcome and the expression of the *LGR4* homolog *LGR5* was also reported. *LGR5* maintains the pool of BCSCs and promotes tumour progression and invasiveness by activating the Wnt/β-catenin canonical pathway [17] (Table 1).

Wang et al. [34] first demonstrated that the expression of the suppression of tumorigenicity 7 like (*ST7L*) is downregulated in BC cells, and more importantly, that *ST7L* acts as an antitumor supervisor by reducing *GSK-3β* phosphorylation and inducing β-catenin degradation. However, the mechanisms through which *ST7L* controls *GSK-3β* phosphorylation are still missing (Table 1).

A recent study [35] reported the overexpression of the transmembrane emp24 domain (*TMED*) in BC and its correlation to poor prognosis. An aberrant level of *TMED* boosts cell cycle progression, colony formation, migration and invasion and the expression of *CDK2*, *CDK4*, *CDK6*, cyclin E, β-catenin, *cyclin D1*, *c-myc*, *MMP-7* and *TCF4*. Conversely, silencing *TMED3* drastically reduced migration and invasion. Moreover, the observation that β-catenin knockdown translates in the reduction of its regulated genes supports the notion that the oncogenic effect of *TMED* goes through the Wnt/β-catenin pathway (Table 1).

Cryptotanshinone (CTS) is an herbal medicine derived from roots of salvia miltiorrhiza, which displays anti-tumour properties. It has been shown that in vitro CTS reduces tumour cell growth, migration and invasion by downregulating the pyruvate kinase muscle isozyme M2 (*PKM2*), a protein involved in glycolysis, and more importantly in β-catenin activation [100].

9. Wnt Non-Canonical Pathway and BC

Among the Wnt ligands, the most extensively studied ligand, activating the β-catenin independent pathway, is Wnt5a. However, its different biological actions are enlightened by the observation that it can also initiate the canonical β-catenin signalling cascade [101].

Wnt5a is an evolutionarily conserved Wnt ligand, which plays an important role in developmental processes. Wnt5a$^{-/-}$ knockout mice showed perinatal lethality, due to developmental defects [102].

In tumorigenesis, Wnt5a signalling is central and displays multiple intriguing and opposite roles, mainly acting as a β-catenin antagonist. These data are discussed.

The Wnt5a suppressive properties detected in tumours connoted by β-catenin hyper-activation have been linked to the shift towards the stimulation of the β-catenin independent signalling pathway.

Foxy5 is a Wnt5a mimicking hexapeptide able to decrease BC cell migration and invasion [103]. More recently, Prasad et al. [36] confirmed these data and added new information on the role of Wnt5a in the regulation of the expression of the phosphofructokinase platelet-type (*PFKP*). They have shown that low *PFKP* level correlates to cancer cell migration and poor patients' survival. The growth and expansion of tumour cells also rely on glucose consumption, resulting in the accumulation of lactate. Cancer cell metabolism was also associated with β-catenin activation [37]. In this regard, it has been shown that Wnt5a affects the aerobic glycolysis by inhibiting the activation of β-catenin. Therefore, an onco-suppressive role was proposed for *PFKP*.

According to the study of Borcherding et al. [104], Roarty et al. [105] demonstrated that the paracrine activity of Wnt5a suppresses the expression of both β-catenin and *cyclin D1*. The authors have shown that Wnt5a supports *TGF-β*-mediated tumour suppressive functions by antagonising Wnt/β-catenin signalling and limiting tumour cell proliferation.

Moreover, Leris and colleagues [38] proved that Wnt5a mRNA level was significantly lower in tumour than in normal tissues, particularly in those displaying a more aggressive behaviour. Again,

this observation has suggested a suppressive role of Wnt5a in cancers. It has also been reported that loss of Wnt5a is associated with a higher histological tumour grade, increased risk of recurrence, and a shorter recurrence-free survival in invasive BC [39] (Table 1).

On the contrary, Kobayashi et al. [40] reported that Wnt5a is expressed in ER-positive BC cells and positively associates to vessel invasion, tumour size and migration. Mechanistically, Wnt5a induces the expression of the activated leukocyte cell adhesion molecule (*ALCAM*), a protein involved in migration and invasion. Knockdown of either Wnt5a or *ALCAM* inhibited tumour cell migration, confirming the role of the Wnt5a/*ALCAM* axis in the migratory phenotype of ER-positive BC (Table 1).

A relevant role of Wnt5a in reprogramming the TME was also described [106]. It has been shown that under pro-inflammatory conditions the non-canonical Wnt protein induces the expansion of the CD163(+) immunosuppressive macrophages translating in the release of IL-10 and the inhibition of the classical *TLR4*-NF-kB signalling pathway [106].

Moreover, higher level of Wnt5a was found in human monocyte-derived myeloid dendritic cells (Mo-mDCs) than in normal monocytes and macrophages. Wnt5a was found to inhibit the generation of Mo-mDCs by stimulating BC cells to produce IL-6. In addition, the presence of IL-6 in the conditioned media of Wnt5a stimulated BC cells was found to be involved in the inhibition of Mo-mDC differentiation [107]. Consistently, overexpression of Wnt5a mRNA was detected in metastases derived from primary BC cells and in BC cell lines [108].

Wnt5a signalling is also able to modify the CD44-AKT signalling pathway, leading to a reduced BC cell migration and invasion. In epithelial BC cells, silencing of Wnt5a drives EMT-like changes without altering the expression of common EMT markers. On the contrary, it interferes with CD44 expression and induces pAKT downregulation, thereby acting via a EMT-independent mechanism [109].

The dual activity of Wnt5a has also been ascribed to the Wnt5a isoforms. Bauer et al. [110] have shown that the Wnt5a gene encodes for two distinct isoforms: the Wnt5a-long (*Wnt5a-L*) and Wnt5a-short (*Wnt5a-S*) isoform. When analysed in several cell lines, *Wnt5a-L* reduced tumour progression, while *Wnt5a-S* promoted tumour growth.

Overall, Wnt5a may play multiple roles. Whether it acts as a tumour suppressor or a tumour promoter remains elusive and depends on the availability of essential receptors, the TME, and the activation of discrete signalling pathways.

10. Triple-Negative Breast Cancer

Triple-Negative Breast Cancer (TNBC) is an invasive type of breast carcinoma that lacks the expression of estrogen and progesteron receptor as well of the human epidermal growth factor receptor 2 (HER2) [111] and accounts from 10 to 15% of all BC [112].

TNBC patients have poor outcome due to the high grade of proliferation, early tumour dissemination, and the lack of targeting approaches [113,114]. The malignancy is associated with earlier age of onset, aggressive clinical course, and dismal prognosis [112]. TNBC gained attention due to the aggressiveness and the lack of effective treatment options. Therefore, the most relevant data on this breast cancer subtype are independently discussed.

Gene expression omnibus (GEO) databases were applied by Shen et al. [41] to gather gene expression data in TNBC patients who underwent chemotherapy. They reported that co-expression of NIMA-related kinase 2 (*Nek2*) and β-catenin correlated with patients' poor prognosis. β-catenin binds to and is phosphorylates by the *Nek2B* isomer. Thereby, in TNBC, *Nek2B* functions as a β-catenin regulator by activating the Wnt signalling pathway and its downstream target genes. In addition, it has been suggested that *Nek2B* and β-catenin may synergize to promote resistance to chemotherapy. However, further studies are required to better elucidate the relationship between β-catenin and *Nek2* and its possible implications in cancer development (Table 1).

TNBC aggressiveness also relies on the activation of the non-canonical Wnt/PCP pathway. Indeed, the aberrant activation of downstream genes activated by the non-canonical Wnt/PCP pathway has been implicated in tumour growth and poor prognosis. Results from Puvirajesinghe and

colleagues [42] revealed that Van Gogh-like 2 (*VANGL2*), a core Wnt/PCP component, plays a crucial role in cancer cell migration, anchorage-dependent and independent cell proliferation, as well as in tumour growth. Since the scaffold p62/SQSTM1 protein, a *VANGL2*-binding partner, has a key role in the *VANGL2*–p62/SQSTM1–*JNK* pathway, the possibility to exploit p62/SQSTM1 as a potential therapeutic target has been proposed. This would be of particular relevance since the *JNK* targeting approaches are associated with major side effects in the clinical setting (Table 1).

Yu and colleagues [43] demonstrated that the hematopoietic protein tyrosine phosphatase (*HePTP*) stabilizes β-catenin in the cytoplasm and allows its nuclear translocation by regulating the phosphorylation of *GSK-3β*. This results in the transcriptional activation of target genes, leading to cell migration and invasion. Since knockdown of *HePTP* significantly suppresses metastases formed by TNBC cells, *HePTP* has also been proposed for therapeutic approaches in TNBC (Table 1).

Recently, Kong et al. [44] have shown that a Rho-GTPase-activating protein, the deleted in liver cancer gene 3 (*DLC-3*), is downregulated in TNBC and its expression is linked to lymphatic metastases. *DLC-3* overexpression leads to β-catenin and *c-myc* downregulation as well as in reduced in vitro cell proliferation, colony formation, migration, and invasion. Hence, a tumour-suppressor role related to the inhibition of the Wnt/β-catenin signalling pathway has been postulated (Table 1).

Liu and colleagues [67] have reported a low expression of miR-6838-5p in TNBC compared to normal cells. miR-6838-5p overexpression reduced cell invasion, migration, EMT, β-catenin, *c-myc* and *cyclin D1* expression by post-transcriptionally controlling Wnt3a expression.

Recently, miR-27a-3p was found overexpressed in tumour cells and linked to poor prognosis in TNBC patients. miR-27a-3p leads to the activation of Wnt/β-catenin cascade and enhances cell proliferation and migration by directly targeting the 3′-UTR region of *GSK-3β* [68] (Table 2).

11. Ovarian Cancer

Ovarian Cancer (OC) is a global issue representing the fourth most common cancer in the female population, particularly in developed countries [115]. The poor survival rate is mainly due to the lack of screening methods at the early stages along with the absence of effective treatment options for advanced stages [116]. Among different OC subtypes, the epithelial subtype (EOC) holds about 90% of the overall ovarian malignancies [117].

12. Canonical Wnt Pathway and OC

The Wnt/β-catenin signalling pathways play a crucial role in carcinogenesis of all OC subtypes [118]. In particular, several transcription factors, proteins and miRNAs acting on this pathway have been explored [119].

Chen and co-workers [45] investigated the role of the Wnt/β-catenin pathway antagonist dickkopf-related protein 1 (*DKK1*). They showed that *DKK1* is involved in the control of OC stemness. Mechanistically, it has been shown that STAT3 directly activates the transcription of miRNA-92a, translating in *DKK1* downregulation [45]. Moreover, overexpression of miR-1207 was found to correlate with high nuclear β-catenin level [46]. Wu et al. [46] investigated the effects of miR-1207 on the expression of the *SFRP1-AXIN2* and the inhibitor of β-catenin and T cell factor 4 (*ICAT*). They found that miR-1207 overexpression was associated with a reduced *SFRP1-AXIN2* and *ICAT* expression and the appearance of a stem-like phenotype (Table 1).

Salem et al. [69] proved that miR-590-3p promotes OC growth and metastasis, by targeting *FOXA2*. Moreover, it has been shown that miR-590-3p upregulation significantly increases cell growth, migration, and invasion in EOC cells, both in vitro and in vivo [70]. Similarly, *FOXA2*, which exhibits suppressive activity on EOC cells, has been identified as a miR-590-3p target [70]. The cyclin G2 gene (*CCNG2*) has also been reported to display several repressive actions on EOC-derived tumour cell lines. It inhibits cell proliferation, migration, invasion and EMT. Thereby, since miR-590-3p post-transcriptionally regulates *FOXA2, FOXO3, CCNG2* and *DDK1* expression, miR-590-3p has been proposed as a potential target in EOC patients [70]. A crucial role of *SFRP1* in OC growth has also

been proposed. Since miR-1180 is highly expressed in neoplastic tissues, Hu et al. [71] explored the relationship between miR-1180 and the *SFRP1*/Wnt/β-catenin signalling pathway in this context, demonstrating that miR-1180 triggers the activation of the Wnt/β-catenin cascade by targeting *SFRP1*.

The members of the R-spondin ligand family have been reported as positive effectors of Wnt/β-catenin signalling [47]. *LGR4-6* plays crucial roles in the activation of the Wnt/β-catenin cascade [47,48]. Moreover, Ruan et al. [47] have reported that LGR6 induces stemness and chemo resistance via the Wnt/β-catenin pathway in OC cells. Restrain of the stem phenotype and increased sensitivity to chemotherapy have been proved by *LGR6* silencing (Table 1).

A recent study established that the overexpression of the Rab GTPase family member, *Rab14*, regulates *GSK-3β* phosphorylation and β-catenin nuclear accumulation [49,50]. Moreover, high levels of *Rab14* were found to be associated with higher expression of Wnt/β-catenin target genes including *MMP-7* and *c-myc* [50] (Table 1).

Jiang et al. [115] have demonstrated that tetrandrine (TET) enhances the anti-tumour effect of paclitaxel (PTX) by decreasing *c-myc* and *cyclin D1* and increasing p21 expression, resulting in cell cycle arrest. The pro-apoptotic effects of PTX+TET have also been investigated. TET was found to inhibit β-catenin downstream target genes by enhancing PTX activity and conferring sensitivity to PTX in resistant cells [115].

Barghout and co-workers [120] demonstrated a more active Wnt/β-catenin signalling in carboplatin-resistant cells than in sensitive ones. Unlike the Wnt ligands, the negative Wnt regulators *DKK1*, *SFRP1*, and the *FRZB* have been found downregulated in cisplatin-resistant cells. These findings suggest that Wnt/β-catenin blockade may be effective on resistant EOC.

13. Non-Canonical Wnt Pathway and OC

FZD7 is highly expressed in OC [51], and its overexpression in mesenchymal (Mes) and Stem-A OC subtypes has been associated with the induction of EMT. The PCP pathway, which activates the *Rho–ROCK* axis, was found to be involved in the activation of actomyosin contractility, cadherin-based cell-cell adhesion and migration, while the Wnt/calcium pathway in the metastatic spread and cytoskeleton changes in this clinical setting [51]. Therefore, it has been proposed that the *FZD7* controls both cell cycle progression and cell migration via the non-canonical Wnt/PCP pathway (Table 1).

The integrin beta like 1 subunit (*ITGBL1*) was found to be highly overexpressed in OC [52]. It has been shown that *ITGBL1* promotes cell migration and adhesion via Wnt/PCP, *RhoA*, the focal adhesion kinase, and the steroid receptor coactivator (*FAK/src*) pathway (Table 1).

The *PTK7*, which interacts with Wnt5A, *LRP6* and *FZD7* [121,122], may act as a tumour suppressor or oncogene [123,124]. In EOC, *PTK7* downregulation is indeed associated with a poor prognosis [123].

Luo and colleagues [53] have investigated the role of the alkaline phosphatase (*ALPL*) in OC. They demonstrated that *ALPL* overexpression inhibits EMT, migration and invasion of high grade serous OCs (HGSOC) and *FZD2* correlates with a poor survival rate [53]. Mechanistically, they have shown that ALPL overexpression represses Wnt5a/*FZD2*–mediated EMT activation, possibly by interfering with STAT3 activation [53] (Table 1).

14. Wnt Pathway and Other Cancers

Glioma is an aggressive tumour of the nervous system displaying rapid progression and poor prognosis. Zhao et al. [125] have found that overexpression of β-catenin and *cyclin D1* is associated with high level of the long noncoding RNA, *FGD5* antisense RNA 1 (lncRNA FGD5-AS1). A close relationship between them was straitened by the observations that inhibition of FGD5-AS1 reduced β-catenin and *cyclin D1* expression while β-catenin downregulation decrease lncRNA FGD5-AS1 expression. This results in the impaired tumour cell migration and invasion.

Prostate cancer (PCa) is among the most common tumour in male. A recent study by Situ et al. [72] provided evidence for the involvement of the microRNA-939 (miR-939) in PCa. Downregulation of miR-939 was found in tumour tissues at advanced tumour stage, in distant lesions, as well as being

associated with poor prognosis. Molecularly, it was demonstrated that miR-939 upregulation interferes with the Wnt/β-catenin cascade by directly targeting the hepatoma-derived growth factor (*HDGF*).

Osteosarcoma (OS) is a common bone paediatric tumour displaying high rates of lung metastasis. The inhibition of β-catenin activation, metastasis formation and chemo-resistance were found modulated by tegavivint (a Wnt/β-catenin inhibitor), which has been proposed as an alternative therapeutic option in OS [126].

Melanoma is among the most immunogenic tumours displaying increased lymphocytic infiltration. Low 1α,25-dihydroxyvitamin D3 and vitamin D receptor (*VDR*) level correlates to increased cancer incidence and melanoma progression, respectively. Recently, it has been shown that high *VDR* expression correlated with the inhibition of tumour growth, low Wnt/β-catenin activation and the induction of the immune response [54] (Table 1).

The long non-coding RNA00261 (Linc00261) has been shown to display onco-suppressor properties in Pancreatic Cancer (PC). Linc00261 overexpression inhibits PC cell proliferation, invasion, EMT and metastasis. Bioinformatics analysis revealed that Linc0026 inhibits the activation of the β-catenin/*TCF4* cascade and the metastatic spread by regulating the miR-552 5p/*FOXO3* axis [127].

15. Extracellular Vesicles and the Wnt Pathway

EVs are heterogeneous small membrane-bound carriers with complex cargoes released under both physiological and pathological conditions. Almost any cell can release EVs, which act as inter-cellular mediators modifying target cell fate at closed or distant sites [128].

Based on the biogenesis, size, content, mechanisms of release and function, three discrete EV subtypes are recognized: microvesicles (MVs), exosomes, and apoptotic bodies [128].

EVs-mediated transfers of specific molecules are known to dictate the phenotype of the recipient cell. They can act on proliferation, motility, EMT, migration, invasion, immune evasion, chemo-resistance, and TME reprogramming (Figure 3).
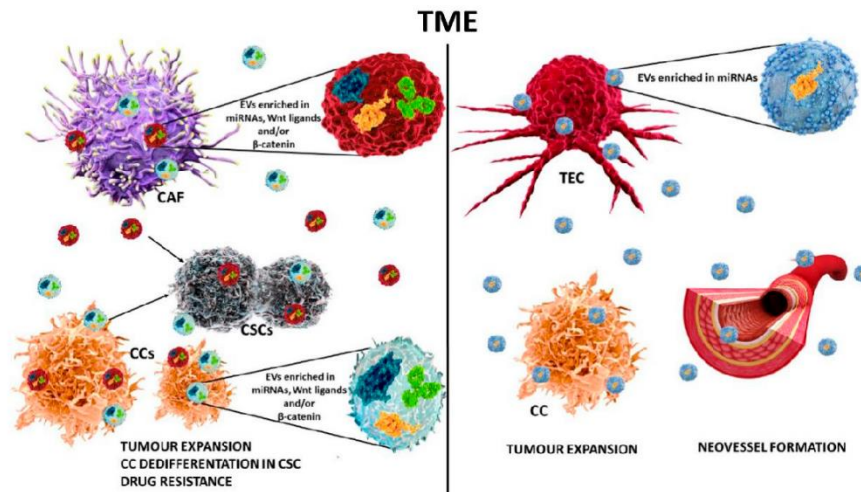

Figure 3. Schematic representation of cell-to-cell communication in the TME by EVs. EVs are released by almost all cell types in the TME. EVs serve as inter-cellular mediators transferring specific molecules (proteins including Wnt ligands and β-catenin, and miRNAs) to recipient cells, thus promoting tumour expansion, cancer cell dedifferentiation in CSCs, chemo-resistance, and neovessel formation. CCs: cancer cells; CSCs: cancer stem cells; TEC: tumour-derived endothelial cell; CAF: cancer associated fibroblasts.

Moreover, EVs derived from serum or other biological fluids have been proposed as tumour biomarkers. More importantly, EVs have gained attention as anti-cancer tools. Indeed, EVs can be used as drug delivery systems or potential cancer vaccines. Moreover, the transfer of Wnt ligands or β-catenin via EVs has been proposed as a Wnt signalling activation mechanism.

Kalra et al. [129] have shown that EVs released by CRC cells and containing the mutant β-catenin and high Wnt/β-catenin activity boost the expression of target genes as *c-myc* and *cyclin D1* when transferred to recipient cells (Table 3).

Table 3. EVs involved in several tumours, their alteration, targets, and impact on tumours.

EV Cargo	EV Source	Target Cells	Related Cancers	Expression Level	Pathway Interaction	Impact on Tumour Cells	Ref.
Mutant β-catenin in EVs	LIM1215	RKO	CRC	Upregulated	β-catenin	migration, metastasis tumour growth	[129]
14-3-3ζ in EVs	HEK293T	COS-7, SW480	CRC	Upregulated	β-catenin GSK-3β DVL2	survival migration	[130]
Wnt ligands in EVs	CAFs	CRC	CRC	Upregulated	β-catenin	dedifferentiation drug resistance colony formation	[131,132]
β-catenin in EVs	milk	HCC	HCC	Silenced	β-catenin	proliferation tumour growth	[133,134]
DKK-1 in EVs	MM	MM	MM	Upregulated	β-catenin	osteoclast activity osteoblast differentiation	[135]
EVs	OSCC	OSCC	OSCC	Upregulated	β-catenin	metastasis stemness chemoresistance	[136]
Wnt5b in EVs	Caco-2 and PANC-1	A549	Lung cancer	Upregulated	β-catenin dependent and independent pathways	proliferation migration	[137]
EVs	CAFs	BC	BC	Upregulated	Wnt-PCP	cell growth and motility	[138]

The *14-3-3* are conserved molecules displaying regulatory functions and promoting cancer progression [130]. The *14-3-3ζ* isoform, which binds both β-catenin and *GSK-3β*, leads to the nuclear translocation and accumulation of β-catenin and enhances cell motility. Moreover, EVs enriched in *14-3-3ζ* and β-catenin, after internalization, promote cell survival and migration by activating the Wnt/β-catenin cascade [130] (Table 3).

Hu et al. [131] have investigated the mechanism of drug resistance in CRC and have proven that EVs released by fibroblasts drive dedifferentiation of CRC cells towards CSCs (Figure 3a). Additionally, they found that EVs derived from fibroblasts contain the Wnt ligands that activate the Wnt/β-catenin pathway in target cells, induce transdifferentiation of CRC cells into CSCs and increase drug resistance. Furthermore, it has been reported that collagen accumulation and the *APC* mutation in CRC cells stimulate the release of EVs and, under hypoxia conditions, fibroblast derived EVs boost CRC colony formation [132] (Table 3).

Accumulating evidence shows that EVs enriched in miRNAs are key determinants of human cancer cell growth, invasion and metastasis [73]. CAF-derived EVs enclose miR-92a-3p, which contributes to cancer progression, stemness, EMT, and drug resistance. Moreover, miR-92a-3p enriched EVs correlated with the activation of the Wnt/β-catenin pathway [73] (Figure 3a).

Long non-coding RNA-*APC1* (lncRNA-APC1) is a negative regulator of CRC. Low levels of lncRNA-APC1 correlate with metastasis, advanced clinical stage and poor prognosis in CRC patients. *APC*, via lncRNA-APC1, promotes cell-cycle arrest and suppresses angiogenesis by lowering the

release of CRC cell-derived EVs. Finally, it has been shown that EV-derived from CRC are enriched in Wnt1 and enhance CRC cell proliferation and migration via non-canonical Wnt/PCP signalling [139].

Hepatocellular carcinoma (HCC) is one of the most common causes of cancer-related deaths worldwide. Constitutive activation of the Wnt/β-catenin pathway turns into the expression of the epithelial cell adhesion molecule (*EpCAM*) [133]. Ishiguro et al. [134] provided evidence that loss in β-catenin and reduced proliferation and invasion can be obtained by *EpCAM* positive liver cancer stem cells (LCSC) targeted by EVs engineered with a β-catenin specific siRNA (Table 3).

Multiple myeloma (MM) is a hematopoietic malignancy associated with an altered homeostasis of bone formation/resorption. MM-derived EVs enriched in *DKK-1* were found to boost the Wnt/β-catenin signalling and contribute to the abnormal osteogenesis. The inhibition of EV shedding, combined to chemotherapy, was found to impair tumour load, angiogenesis and osteolysis [135] (Table 3).

Furthermore, a recent study noticed that the release of EVs from HCC cells is increased in hypoxic conditions and linked to cancer cell proliferation, migration, invasiveness and EMT. Mechanistically, they have shown that miR-1273f enriched in EVs activates the Wnt/β-catenin signalling cascade by targeting the Wnt/β-catenin inhibitor LHX6 [74].

Chen et al. [136] proved that EVs released from oral squamous cell carcinoma (OSCC) cells correlate with an increased level of β-catenin, the expression of several oncogenic markers, the reprogramming of normal gingival fibroblasts into CAFs, increased metastasis, stemness reprogramming, chemoresistance, and poor patients' survival (Table 3).

Xia et al. [75] have demonstrated the uptake of EVs and the delivery of functional miRNAs in different cell lines. The exosomal-miR-1260b was found to be crucial for the activation of the Wnt/β-catenin signalling and the invasivness of lung adenocarcinoma cells.

Harada et al. [137] purified and characterized Wnt5b-associated EVs. In pancreatic PANC-1 and colorectal Caco-2 cell lines, Wnt5a carried by EVs displays the ability to enhance cancer progression (Table 3).

Luga et al. [138] demonstrated that EV shedding by fibroblasts boosts BC cell growth and motility via Wnt/PCP signalling. CAF-derived EVs were found to be crucial drivers of cell migration during metastasis formation. Moreover, they found that EVs secreted from fibroblast L cells promote the autocrine Wnt11-PCP cascade in tumour cells, increasing their motility and metastatic properties (Table 3).

Lombardo et al. [76] provided evidence that EVs released by tumour-derived endothelial cells (TECs-EVs) boost in vivo TEC-derived neovessels. Mechanistically, they showed that EVs released by naive TECs-EVs regulate the expression of *APC*, *GSK-3β* and drive β-catenin nuclear accumulation via miR-214-3p and miR-24-3p (Figure 3b). Overall, this study revealed a key role of the Wnt/β-catenin cascade in TEC-derived neovessel formation. Moreover, they recently showed that naïve TEC-EVs were also able to boost TNBC metastatic spread and lung metastasis formation when injected intravenously [140] (Table 2).

Overall, these data indicate a crucial contribution of EVs released by different cell sources in driving tumor development and dissemination. Several data suggest that these effects mainly rely on the transfer of their specific cargo into target cells. Therefore, approaches able to modify their cargo, particularly miRs and proteins involved in their tumor promoting action, have been proposed as useful therapeutic options. EV engineering by using siRNA for mutated protein has been tested and its effectiveness demonstrated in pancreatic cancer [141]. This suggests that using siRNA for mutant β catenin should be considered as an alternative option for CRC. Likewise, siRNA for different Wnt proteins or rearrangement of dysregulated EV miRs can be used to target the Wnt/β catenin cascade. Alternatively, EVs loaded with Wnt/β catenin inhibitors can be used as natural delivery tools.

16. Conclusions

Cell-to cell communication is part of the evolutional processes. Wnt ligands are essential for homeostasis and, in the last 30 years, genetic, biochemical, and molecular investigations have uncovered several Wnt signalling components [2,3]. Driving interest on this topic mainly relies on dysregulation of the Wnt/β-catenin signalling and cancer development/progression [3]. Moreover, Wnt/β-catenin cascade seems to contribute to the TME shape, which plays a crucial role in the control of tumour progression and immune regulation. Many different Wnt proteins have been described, and, among them, Wnt5a plays a critical role, taking part in both the canonical and the non-canonical Wnt/β-catenin pathway [104,105].

The identification of specific tools able to interfere with the Wnt/β-catenin cascade has been a hotspot for many years. This is particularly true for CRC, in which almost 70% of CRC patients display *APC* mutations [15]. Apart from CRC, the Wnt/β-catenin pathway is gaining attention in several malignancies, such as breast, ovarian, melanoma, prostate and paediatric osteosarcoma [53,124,125]. In this regard, BC and in particular TNBC are featured by the abnormal activation of both the canonical and non-canonical Wnt/β-catenin pathway [113,114]. Likewise, a hyper-active Wnt/β-catenin cascade has been shown to play a crucial role in the progression, stemness, and drug resistance in OC [70,119]. Several miRNAs have been identified to modulate this cascade and thereby widely studied as screening markers or targets in different tumour settings [142].

In the TME, intercellular communication has been recently reported as mediated by the transfer of EV molecular cargo and revised in [143]. Their cargo also includes a number of Wnt components. Of note, wild-type and mutant β-catenin, able to promote survival and proliferation of recipient cells and, in several instances, dedifferentiation towards a CSC phenotype, have been detected in EVs (Figure 3a). Moreover, their role in mediating drug resistance has been reported. Furthermore, since EVs are released within the TME, their contribution in cancer growth and progression has been extensively investigated [144]. EV shedding, blockade, or engineering have been proposed as innovative anti-tumour instruments for fine-tuning the Wnt/β catenin pathway [142,145].

In recent decades, several efforts have been directed to the development of Wnt/β catenin targeting approaches in order to interfere with tumour progression. However, these efforts have been limited by the crucial role of the Wnt/β catenin pathway in preserving tissue homeostasis. Therefore, future energies should be directed to clearly dissect the mechanisms driving the unbalanced Wnt/β catenin pathway in cancer, and the EV mechanism of action should be considered amid them. Should they be identified, targeting approaches would become a suitable anti-cancer option.

References

1. Jackstadt, R.; Hodder, M.C.; Sansom, O.J. WNT and β-Catenin in Cancer: Genes and Therapy. *Annu. Rev. Cancer Biol.* **2020**, *4*, 177–196. [CrossRef]
2. Komiya, Y.; Habas, R. Wnt signal transduction pathways. *Organogenesis* **2008**, *4*, 68–75. [CrossRef] [PubMed]
3. Duchartre, Y.; Kim, Y.M.; Kahn, M. The Wnt signaling pathway in cancer. *Crit. Rev. Oncol. Hematol.* **2016**, *99*, 141–149. [CrossRef]
4. Thrasivoulou, C.; Millar, M.; Ahmed, A. Activation of intracellular calcium by multiple Wnt ligands and translocation of β-catenin into the nucleus: A convergent model of Wnt/Ca2+and Wnt/β-catenin pathways. *J. Biol. Chem.* **2013**, *288*, 35651–35659. [CrossRef]

5. Florian, M.C.; Nattamai, K.J.; Dörr, K.; Marka, G.; Überle, B.; Vas, V.; Eckl, C.; Andrä, I.; Schiemann, M.; Oostendorp, R.A.J.; et al. A canonical to non-canonical Wnt signalling switch in haematopoietic stem-cell ageing. *Nature* **2013**, *503*, 392–396. [CrossRef] [PubMed]

6. MacDonald, B.T.; Tamai, K.; He, X. Wnt/β-Catenin Signaling: Components, Mechanisms, and Diseases. *Dev. Cell* **2009**, *17*, 9–26. [CrossRef] [PubMed]

7. Gajos-Michniewicz, A.; Czyz, M. WNT Signaling in Melanoma. *Int. J. Mol. Sci.* **2020**, *21*, 4852. [CrossRef]

8. Wang, Y.; Nathans, J. Tissue/planar cell polarity in vertebrates: New insights and new questions. *Development* **2007**, *134*, 647–658. [CrossRef]

9. Saneyoshi, T.; Kume, S.; Amsaki, Y.; Mikoshiba, K. The wnt/calcium pathway activates nf-at and promotes ventral cell fate in xenopus embryos. *Nature* **2002**, *417*, 295–299. [CrossRef]

10. Tao, Q.; Yokota, C.; Puck, H.; Kofron, M.; Birsoy, B.; Yan, D.; Asashima, M.; Wylie, C.C.; Lin, X.; Heasman, J. Maternal Wnt11 activates the canonical Wnt signaling pathway required for axis formation in Xenopus embryos. *Cell* **2005**, *120*, 857–871. [CrossRef]

11. Steinhart, Z.; Angers, S. Wnt signaling in development and tissue homeostasis. *Development* **2018**, *145*, 1–8. [CrossRef] [PubMed]

12. Rawla, P.; Sunkara, T.; Barsouk, A. Epidemiology of colorectal cancer: Incidence, mortality, survival, and risk factors. *Prz. Gastroenterol.* **2019**, *14*, 89–103. [CrossRef]

13. Bhandari, A.; Woodhouse, M.; Gupta, S. Colorectal cancer is a leading cause of cancer incidence and mortality among adults younger than 50 years in the USA: A SEER-based analysis with comparison to other young-onset cancers. *J. Investig. Med.* **2017**, *65*, 311–315. [CrossRef]

14. Dienstmann, R.; Wang, X.; de Reyni, A.; Schlicker, A.; Soneson, C.; Marisa, L.; Roepman, P.; Nyamundanda, G.; Angelino, P.; Bot, B.M.; et al. The consensus molecular subtypes of colorectal cancer. *Nat. Med.* **2015**. [CrossRef]

15. Liu, L.; Zhang, Y.; Wong, C.C.; Zhang, J.; Dong, Y.; Li, X.; Kang, W.; Chan, F.K.L.; Sung, J.J.Y.; Yu, J. RNF6 promotes colorectal cancer by activating the Wnt/b-catenin pathway via ubiquitination of TLE3. *Cancer Res.* **2018**, *78*, 1958–1971. [CrossRef]

16. Study of the Role of Leucine-rich Repeat-Containing g-protein Coupled Receptor 5 (LGR5) and WNT Pathway in Colon Cancer. *Egypt. J. Biochem. Mol. Biol.* Available online: https://www.ajol.info/index.php/ejbmb/article/view/191481 (accessed on 11 September 2020).

17. Yang, L.; Xie, X.; Tang, H.; Kong, Y.; Xie, X.; Chen, J.; Song, C.; Liu, X.; Ye, F.; Li, N.; et al. LGR5 promotes breast cancer progression and maintains stem-like cells through activation of wnt/β-catenin signaling. *Stem Cells* **2015**, *33*, 2913–2924. [CrossRef]

18. Yu, D.H.; Zhang, X.; Wang, H.; Zhang, L.; Chen, H.; Hu, M.; Dong, Z.; Zhu, G.; Qian, Z.; Fan, J.; et al. The essential role of TNIK gene amplification in gastric cancer growth. *Oncogenesis* **2014**, *3*. [CrossRef]

19. Masuda, M.; Uno, Y.; Ohbayashi, N.; Ohata, H.; Mimata, A.; Kukimoto-Niino, M.; Moriyama, H.; Kashimoto, S.; Inoue, T.; Goto, N.; et al. TNIK inhibition abrogates colorectal cancer stemness. *Nat. Commun.* **2016**, *7*, 1–7. [CrossRef]

20. Cho, Y.H.; Ro, E.J.; Yoon, J.S.; Kwak, D.K.; Cho, J.; Kang, D.W.; Lee, H.Y.; Choi, K.Y. Small molecule-induced simultaneous destabilization of β-catenin and RAS is an effective molecular strategy to suppress stemness of colorectal cancer cells. *Cell Commun. Signal.* **2020**, *18*, 1–11. [CrossRef]

21. Sun, N.; Zhang, L.; Zhang, C.; Yuan, Y. MiR-144-3p inhibits cell proliferation of colorectal cancer cells by targeting BCL6 via inhibition of Wnt/β-catenin signaling. *Cell. Mol. Biol. Lett.* **2020**, *25*. [CrossRef] [PubMed]

22. Polo, J.M.; Dell'Oso, T.; Ranuncolo, S.M.; Cerchietti, L.; Beck, D.; Da Silva, G.F.; Prive, G.G.; Licht, J.D.; Melnick, A. Specific peptide interference reveals BCL6 transcriptional and oncogenic mechanisms in B-cell lymphoma cells. *Nat. Med.* **2004**, *10*, 1329–1335. [CrossRef]

23. Shaffer, A.L.; Yu, X.; He, Y.; Boldrick, J.; Chan, E.P.; Staudt, L.M. BCL-6 represses genes that function in lymphocyte differentiation, inflammation, and cell cycle control. *Immunity* **2000**, *13*, 199–212. [CrossRef]

24. Qi, S.; Song, Y.; Peng, Y.; Wang, H.; Long, H.; Yu, X.; Li, Z.; Fang, L.; Wu, A.; Luo, W.; et al. ZEB2 mediates multiple pathways regulating cell proliferation, migration, invasion, and apoptosis in glioma. *PLoS ONE* **2012**, *7*, 1–12. [CrossRef] [PubMed]

25. Ng, V.H.; Hang, B.I.; Sawyer, L.M.; Neitzel, L.R.; Crispi, E.E.; Rose, K.L.; Popay, T.M.; Zhong, A.; Lee, L.A.; Tansey, W.P.; et al. Phosphorylation of XIAP at threonine 180 controls its activity in Wnt signaling. *J. Cell Sci.* **2018**. [CrossRef]

26.　Wels, C.; Joshi, S.; Koefinger, P.; Bergler, H. Transcriptional Activation of ZEB1 by Slug Leads to Cooperative Regulation of the EMT like Phenotype in Melanoma. *J. Invest. Dermatol.* **2011**, *131*, 1877–1885. [CrossRef]

27.　Zhang, M.; Miao, F.; Huang, R.; Liu, W.; Zhao, Y.; Jiao, T.; Lu, Y.; Wu, F.; Wang, X.; Wang, H.; et al. RHBDD1 promotes colorectal cancer metastasis through the Wnt signaling pathway and its downstream target ZEB1. *J. Exp. Clin. Cancer Res.* **2018**, *37*, 1–14. [CrossRef]

28.　Deng, M.; Chen, Z.; Tan, J.; Liu, H. Down-regulation of SLC35C1 induces colon cancer through over-activating Wnt pathway. *J. Cell. Mol. Med.* **2020**, *24*, 3079–3090. [CrossRef]

29.　Xu, C.; Tian, G.; Jiang, C.; Xue, H.; Kuerbanjiang, M.; Sun, L.; Gu, L.; Zhou, H.; Liu, Y.; Zhang, Z.; et al. NPTX2 promotes colorectal cancer growth and liver metastasis by the activation of the canonical Wnt/β-catenin pathway via FZD6. *Cell Death Dis.* **2019**, *10*. [CrossRef] [PubMed]

30.　Song, Y.; Yuan, H.; Wang, J.; Wu, Y.; Xiao, Y.; Mao, S. KLHL22 regulates the EMT and proliferation in colorectal cancer cells in part via the Wnt/β-catenin signaling pathway. *Cancer Manag. Res.* **2020**, *12*, 3981–3993. [CrossRef]

31.　Liu, Q.; Song, J.; Pan, Y.; Shi, D.; Yang, C.; Wang, S.; Xiong, B. Wnt5a/caMKII/ERK/CCL2 axis is required for tumor-associated macrophages to promote colorectal cancer progression. *Int. J. Biol. Sci.* **2020**, *16*, 1023–1034. [CrossRef]

32.　Yue, Z.; Yuan, Z.; Zeng, L.; Wang, Y.; Lai, L.; Li, J.; Sun, P.; Xue, X.; Qi, J.; Yang, Z.; et al. LGR4 modulates breast cancer initiation, metastasis, and cancer stem cells. *FASEB J.* **2018**, *32*, 2422–2437. [CrossRef]

33.　Ruffner, H.; Lle Sprunger, J.; Charlat, O.; Leighton-Davies, J.; Grosshans, B.; Salathe, A.; Zietzling, S.; Rie Beck, V.; Therier, M.; Isken, A.; et al. R-Spondin Potentiates Wnt/b-Catenin Signaling through Orphan Receptors LGR4 and LGR5. *PLoS ONE* **2012**. [CrossRef] [PubMed]

34.　Wang, H.; Sun, L.; Jiang, J.; Yu, S.; Zhou, Q. Suppression of the proliferation and invasion of breast cancer cells by ST7L occurs through inhibition of activation of Wnt/GSK-3β/β-catenin signalling. *Clin. Exp. Pharmacol. Physiol.* **2020**, *47*, 119–126. [CrossRef]

35.　Zhang, X.; Luo, Y.; Li, Q. TMED3 promotes proliferation and migration in breast cancer cells by activating Wnt/β-catenin signaling. *Onco. Targets. Ther.* **2020**, *13*, 5819–5830. [CrossRef]

36.　Prasad, C.P.; Södergren, K.; Andersson, T. Reduced production and uptake of lactate are essential for the ability of WNT5A signaling to inhibit breast cancer cell migration and invasion. *Oncotarget* **2017**, *8*, 71471–71488. [CrossRef]

37.　Lee, S.Y.; Jeon, H.M.; Ju, M.K.; Kim, C.H.; Yoon, G.; Han, S.I.; Park, H.G.; Kang, H.S. Wnt/snail signaling regulates cytochrome c oxidase and glucose metabolism. *Cancer Res.* **2012**, *72*, 3607–3617. [CrossRef] [PubMed]

38.　Leris, A.C.A.; Roberts, T.R.; Jiang, W.G.; Newbold, R.F.; Mokbel, K. WNT5A expression in human breast cancer. *Anticancer Res.* **2005**, *25*, 731–734.

39.　Jönsson, M.; Dejmek, J.; Bendahl, P.O.; Andersson, T. Loss of Wnt-5a protein is associated with early relapse in invasive ductal breast carcinomas. *Cancer Res.* **2002**, *62*, 409–416. [PubMed]

40.　Kobayashi, Y.; Kadoya, T.; Amioka, A.; Hanaki, H.; Sasada, S.; Masumoto, N.; Yamamoto, H.; Arihiro, K.; Kikuchi, A.; Okada, M. Wnt5a-induced cell migration is associated with the aggressiveness of estrogen receptor-positive breast cancer. *Oncotarget* **2018**, *9*, 20979–20992. [CrossRef]

41.　Shen, H.; Yan, W.; Yuan, J.; Wang, Z.; Wang, C. Nek2B activates the wnt pathway and promotes triple-negative breast cancer chemothezrapy-resistance by stabilizing β-catenin. *J. Exp. Clin. Cancer Res.* **2019**, *38*, 1–17. [CrossRef]

42.　Puvirajesinghe, T.M.; Bertucci, F.; Jain, A.; Scerbo, P.; Belotti, E.; Audebert, S.; Sebbagh, M.; Lopez, M.; Brech, A.; Finetti, P.; et al. Identification of p62/SQSTM1 as a component of non-canonical Wnt VANGL2-JNK signalling in breast cancer. *Nat. Commun.* **2016**, *7*. [CrossRef]

43.　Yu, L.; Wang, C.; Pan, F.; Liu, Y.; Ren, X.; Zeng, H.; Shi, Y. HePTP promotes migration and invasion in triple-negative breast cancer cells via activation of Wnt/β-catenin signaling. *Biomed. Pharmacother.* **2019**, *118*. [CrossRef] [PubMed]

44.　Kong, B.; Lv, Z.-D.; Xia, J.; Jin, L.-Y.; Yang, Z.-C. DLC-3 suppresses cellular proliferation, migration, and invasion in triple-negative breast cancer by the Wnt/β-catenin pathway. *Int. J. Clin. Exp. Pathol.* **2019**, *12*, 1224–1232. [PubMed]

45. Chen, M.W.; Yang, S.T.; Chien, M.H.; Hua, K.T.; Wu, C.J.; Hsiao, S.M.; Lin, H.; Hsiao, M.; Su, J.L.; Wei, L.H. The STAT3-miRNA-92-Wnt signaling pathway regulates spheroid formation and malignant progression in ovarian cancer. *Cancer Res.* **2017**, *77*, 1955–1967. [CrossRef] [PubMed]

46. Wu, G.; Liu, A.; Zhu, J.; Lei, F.; Wu, S.; Zhang, X.; Ye, L.; Cao, L.; He, S. MiR-1207 overexpression promotes cancer stem cell-like traits in ovarian cancer by activating the Wnt/β-catenin signaling pathway. *Oncotarget* **2015**, *6*, 28882–28894. [CrossRef]

47. Ruan, X.; Liu, A.; Zhong, M.; Wei, J.; Zhang, W.; Rong, Y.; Liu, W.; Li, M.; Qing, X.; Chen, G.; et al. Silencing LGR6 Attenuates Stemness and Chemoresistance via Inhibiting Wnt/β-Catenin Signaling in Ovarian Cancer. *Mol. Ther. Oncolytics* **2019**, *14*, 94–106. [CrossRef]

48. Park, S.; Cui, J.; Yu, W.; Wu, L.; Carmon, K.S.; Liu, Q.J. Differential activities and mechanisms of the four r-spondins in potentiating wnt/-catenin signaling. *J. Biol. Chem.* **2018**, *293*, 9759–9769. [CrossRef]

49. Nguyen, V.H.L.; Hough, R.; Bernaudo, S.; Peng, C. Wnt/β-catenin signalling in ovarian cancer: Insights into its hyperactivation and function in tumorigenesis. *J. Ovarian Res.* **2019**, *12*, 1–17. [CrossRef]

50. Hou, R.; Jiang, L.; Yang, Z.; Wang, S.; Liu, Q. Rab14 is overexpressed in ovarian cancers and promotes ovarian cancer proliferation through Wnt pathway. *Tumor Biol.* **2016**, *37*, 16005–16013. [CrossRef]

51. Asad, M.; Wong, M.K.; Tan, T.Z.; Choolani, M.; Low, J.; Mori, S.; Virshup, D.; Thiery, J.P.; Huang, R.Y.J. FZD7 drives in vitro aggressiveness in stem-A subtype of ovarian cancer via regulation of non-canonical wnt/PCP pathway. *Cell Death Dis.* **2014**, *5*, e1346. [CrossRef]

52. Sun, L.; Wang, D.; Li, X.; Zhang, L.; Zhang, H.; Zhang, Y. Extracellular matrix protein ITGBL1 promotes ovarian cancer cell migration and adhesion through Wnt/PCP signaling and FAK/SRC pathway. *Biomed. Pharmacother.* **2016**, *81*, 145–151. [CrossRef] [PubMed]

53. Luo, M.; Zhou, L.; Zhan, S.J.; Cheng, L.J.; Li, R.N.; Wang, H.; Liu, B.; Linghu, H. ALPL regulates the aggressive potential of high grade serous ovarian cancer cells via a non-canonical WNT pathway. *Biochem. Biophys. Res. Commun.* **2019**, *513*, 528–533. [CrossRef] [PubMed]

54. Muralidhar, S.; Filia, A.; Nsengimana, J.; Pozniak, J.; O'Shea, S.J.; Diaz, J.M.; Harland, M.; Randerson-Moor, J.A.; Reichrath, J.; Laye, J.P.; et al. Vitamin D–VDR signaling inhibits Wnt/b-catenin–mediated melanoma progression and promotes antitumor immunity. *Cancer Res.* **2019**, *79*, 5986–5998. [CrossRef] [PubMed]

55. Moon, B.S.; Jeong, W.J.; Park, J.; Kim, T.I.; Min, D.S.; Choi, K.Y. Role of oncogenic K-Ras in cancer stem cell activation by aberrant wnt/β-catenin signaling. *J. Natl. Cancer Inst.* **2014**, *106*, 1–10. [CrossRef]

56. Lenz, H.J.; Kahn, M. Safely targeting cancer stem cells via selective catenin coactivator antagonism. *Cancer Sci.* **2014**, *105*, 1087–1092. [CrossRef] [PubMed]

57. Cha, P.H.; Cho, Y.H.; Lee, S.K.; Lee, J.; Jeong, W.J.; Moon, B.S.; Yun, J.H.; Yang, J.S.; Choi, S.; Yoon, J.; et al. Small-molecule binding of the axin RGS domain promotes β-catenin and Ras degradation. *Nat. Chem. Biol.* **2016**, *12*, 593–600. [CrossRef] [PubMed]

58. Tan, W.; Liu, B.; Qu, S.; Liang, G.; Luo, W.; Gong, C. MicroRNAs and cancer: Key paradigms in molecular therapy (Review). *Oncol. Lett.* **2018**, *15*, 2735–2742. [CrossRef] [PubMed]

59. Lee, Y.S.; Dutta, A. MicroRNAs in Cancer Contents. *Annu. Rev. Pathol.* **2009**, *4*, 199–227. [CrossRef]

60. Liu, W.Y.; Yang, Z.; Sun, Q.; Yang, X.; Hu, Y.; Xie, H.; Gao, H.J.; Guo, L.M.; Yi, J.Y.; Liu, M.; et al. miR-377-3p drives malignancy characteristics via upregulating GSK-3β expression and activating NF-κB pathway in hCRC cells. *J. Cell. Biochem.* **2018**, *119*, 2124–2134. [CrossRef]

61. Huang, L.; Liu, Z.; Hu, J.; Luo, Z.; Zhang, C.; Wang, L.; Wang, Z. MiR-377-3p suppresses colorectal cancer through negative regulation on Wnt/β-catenin signaling by targeting XIAP and ZEB2. *Pharmacol. Res.* **2020**, *156*, 104774. [CrossRef]

62. Lv, S.; Zhang, J.; He, Y.; Liu, Q.; Wang, Z.; Liu, B.; Shi, L.; Wu, Y. MicroRNA-520e targets AEG-1 to suppress the proliferation and invasion of colorectal cancer cells through Wnt/GSK-3β/β-catenin signalling. *Clin. Exp. Pharmacol. Physiol.* **2020**, *47*, 158–167. [CrossRef]

63. Hu, G.; Wei, Y.; Kang, Y. The multifaceted role of MTDH/AEG-1 in cancer progression. *Clin. Cancer Res.* **2009**, *15*, 5615–5620. [CrossRef] [PubMed]

64. You, F.; Li, J.; Zhang, P.; Zhang, H.; Cao, X. MiR106a promotes the growth of transplanted breast cancer and decreases the sensitivity of transplanted tumors to cisplatin. *Cancer Manag. Res.* **2020**, *12*, 233–246. [CrossRef] [PubMed]

65. Zou, Y.; Lin, X.; Bu, J.; Lin, Z.; Chen, Y.; Qiu, Y.; Mo, H.; Tang, Y.; Fang, W.; Wu, Z. Timeless-Stimulated miR-5188-FOXO1/β-Catenin-c-Jun Feedback Loop Promotes Stemness via Ubiquitination of β-Catenin in Breast Cancer. *Mol. Ther.* **2019**, *28*, 313–327. [CrossRef]

66. Han, L.; Yan, Y.; Zhao, L.; Liu, Y.; Lv, X.; Zhang, L.; Zhao, Y.; Zhao, H.; He, M.; Wei, M. LncRNA HOTTIP facilitates the stemness of breast cancer via regulation of miR-148a-3p/WNT1 pathway. *J. Cell. Mol. Med.* **2020**, *24*, 6242–6252. [CrossRef] [PubMed]

67. Liu, G.; Wang, P.; Zhang, H. MiR-6838-5p suppresses cell metastasis and the EMT process in triple-negative breast cancer by targeting WNT3A to inhibit the Wnt pathway. *J. Gene Med.* **2019**, *21*, 1–8. [CrossRef]

68. Wu, R.; Zhao, B.; Ren, X.; Wu, S.; Liu, M.; Wang, Z.; Liu, W. Mir-27a-3p targeting gsk3β promotes triple-negative breast cancer proliferation and migration through wnt/β-catenin pathway. *Cancer Manag. Res.* **2020**, *12*, 6241–6249. [CrossRef] [PubMed]

69. Salem, M.; Shan, Y.; Bernaudo, S.; Peng, C. miR-590-3p Targets Cyclin G2 and FOXO3 to Promote Ovarian Cancer Cell Proliferation, Invasion, and Spheroid Formation. *Int. J. Mol. Sci.* **2019**, *20*, 1810. [CrossRef]

70. Salem, M.; O'brien, J.A.; Bernaudo, S.; Shawer, H.; Ye, G.; Brki, J.; Amleh, A.; Vanderhyden, B.C.; Refky, B.; Yang, B.B.; et al. miR-590-3p Promotes Ovarian Cancer Growth and Metastasis via a Novel FOXA2-Versican Pathway. *Cancer Res.* **2018**. [CrossRef]

71. Hu, J.; Zhao, W.; Huang, Y.; Wang, Z.; Jiang, T.; Wang, L. MiR-1180 from bone marrow MSCs promotes cell proliferation and glycolysis in ovarian cancer cells via SFRP1/Wnt pathway. *Cancer Cell Int.* **2019**, *19*, 66. [CrossRef]

72. Situ, J.; Zhang, H.; Jin, Z.; Li, K.; Mao, Y.; Huang, W. MicroRNA-939 directly targets HDGF to inhibit the aggressiveness of prostate cancer via deactivation of the WNT/β-catenin pathway. *Onco. Targets. Ther.* **2020**, *13*, 4257–4270. [CrossRef] [PubMed]

73. Hu, J.L.; Wang, W.; Lan, X.L.; Zeng, Z.C.; Liang, Y.S.; Yan, Y.R.; Song, F.Y.; Wang, F.F.; Zhu, X.H.; Liao, W.J.; et al. CAFs secreted exosomes promote metastasis and chemotherapy resistance by enhancing cell stemness and epithelial-mesenchymal transition in colorectal cancer. *Mol. Cancer* **2019**, *18*, 1–15. [CrossRef] [PubMed]

74. Yu, Y.; Min, Z.; Linhong, M.; Tao, R.; Yan, L.; Song, H. Hypoxia-induced exosomes promote hepatocellular carcinoma proliferation and metastasis via miR-1273f transfer. *Exp. Cell Res.* **2019**, *385*. [CrossRef] [PubMed]

75. Xia, Y.; Wei, K.; Hu, L.Q.; Zhou, C.R.; Lu, Z.B.; Zhan, G.S.; Pan, X.L.; Pan, C.F.; Wang, J.; Wen, W.; et al. Exosome-mediated transfer of miR-1260b promotes cell invasion through Wnt/β–catenin signaling pathway in lung adenocarcinoma. *J. Cell. Physiol.* **2020**, *235*, 6843–6853. [CrossRef]

76. Lombardo, G.; Gili, M.; Grange, C.; Cavallari, C.; Dentelli, P.; Togliatto, G.; Taverna, D.; Camussi, G.; Brizzi, M.F. IL-3R-alpha blockade inhibits tumor endothelial cell-derived extracellular vesicle (EV)-mediated vessel formation by targeting the β-catenin pathway. *Oncogene* **2018**, *37*, 1175–1191. [CrossRef] [PubMed]

77. Vymetalkova, V.; Vodicka, P.; Vodenkova, S.; Alonso, S.; Schneider-Stock, R. DNA methylation and chromatin modifiers in colorectal cancer. *Mol. Aspects Med.* **2019**, *69*, 73–92. [CrossRef] [PubMed]

78. Tanaka, N.; Mashima, T.; Mizutani, A.; Sato, A.; Aoyama, A.; Gong, B.; Yoshida, H.; Muramatsu, Y.; Nakata, K.; Matsuura, M.; et al. APC mutations as a potential biomarker for sensitivity to tankyrase inhibitors in colorectal cancer. *Mol. Cancer Ther.* **2017**, *16*, 752–762. [CrossRef]

79. Bruschi, M.; Garnier, L.; Cleroux, E.; Giordano, A.; Dumas, M.; Bardet, A.F.; Kergrohen, T.; Quesada, S.; Cesses, P.; Weber, M.; et al. Loss of Apc Rapidly Impairs DNA Methylation Programs and Cell Fate Decisions in Lgr5+ Intestinal Stem Cells. *Cancer Res.* **2020**, *80*. [CrossRef]

80. Proto, M.C.; Fiore, D.; Piscopo, C.; Franceschelli, S.; Bizzarro, V.; Laezza, C.; Lauro, G.; Feoli, A.; Tosco, A.; Bifulco, G.; et al. Inhibition of Wnt/β-Catenin pathway and Histone acetyltransferase activity by Rimonabant: A therapeutic target for colon cancer. *Sci. Rep.* **2017**, *7*, 1–14. [CrossRef]

81. Liu, Y.; Rubin, B.; Bodine, P.V.N.; Billiard, J. Wnt5a induces homodimerization and activation of Ror2 receptor tyrosine kinase. *J. Cell. Biochem.* **2008**, *105*, 497–502. [CrossRef]

82. Lee, J.M.; Kim, I.S.; Kim, H.; Lee, J.S.; Kim, K.; Yim, H.Y.; Jeong, J.; Kim, J.H.; Kim, J.Y.; Lee, H.; et al. RORα Attenuates Wnt/β-Catenin Signaling by PKCα-Dependent Phosphorylation in Colon Cancer. *Mol. Cell* **2010**, *37*, 183–195. [CrossRef]

83. Voloshanenko, O.; Schwartz, U.; Kranz, D.; Rauscher, B.; Linnebacher, M.; Augustin, I.; Boutros, M. β-catenin-independent regulation of Wnt target genes by RoR2 and ATF2/ATF4 in colon cancer cells. *Sci. Rep.* **2018**, *8*, 1–14. [CrossRef] [PubMed]

84. Nishioka, M.; Ueno, K.; Hazama, S.; Okada, T.; Sakai, K.; Suehiro, Y.; Okayama, N.; Hirata, H.; Oka, M.; Imai, K.; et al. Possible involvement of Wnt11 in colorectal cancer progression. *Mol. Carcinog.* **2013**, *52*, 207–217. [CrossRef] [PubMed]

85. Gorroño-Etxebarria, I.; Aguirre, U.; Sanchez, S.; González, N.; Escobar, A.; Zabalza, I.; Quintana, J.M.; dM Vivanco, M.; Waxman, J.; Kypta, R.M. Wnt-11 as a potential prognostic biomarker and therapeutic target in colorectal cancer. *Cancers (Basel)* **2019**, *11*, 1–19. [CrossRef] [PubMed]

86. Vitale, I.; Manic, G.; Coussens, L.M.; Kroemer, G.; Galluzzi, L. Macrophages and Metabolism in the Tumor Microenvironment. *Cell Metab.* **2019**, *30*, 36–50. [CrossRef]

87. Bray, F.; Ferlay, J.; Soerjomataram, I.; Siegel, R.L.; Torre, L.A.; Jemal, A. Global cancer statistics 2018: GLOBOCAN estimates of incidence and mortality worldwide for 36 cancers in 185 countries. *CA. Cancer J. Clin.* **2018**, *68*, 394–424. [CrossRef]

88. Du, X.L.; Fox, E.E.; Lai, D. Competing Causes of Death for Women With Breast Cancer and Change Over Time From 1975 to 2003 NIH Public Access. *Am. J. Clin. Oncol.* **2008**, *31*, 105–116. [CrossRef]

89. Yu, Q.C.; Verheyen, E.M.; Zeng, Y.A. Mammary development and breast cancer: A Wnt perspective. *Cancers* **2016**, *8*, 65. [CrossRef]

90. Katoh, M. Canonical and non-canonical WNT signaling in cancer stem cells and their niches: Cellular heterogeneity, omics reprogramming, targeted therapy and tumor plasticity (Review). *Int. J. Oncol.* **2017**, *51*, 1357–1369. [CrossRef]

91. Khramtsov, A.I.; Khramtsova, G.F.; Tretiakova, M.; Huo, D.; Olopade, O.I.; Goss, K.H. Wnt/β-catenin pathway activation is enriched in basal-like breast cancers and predicts poor outcome. *Am. J. Pathol.* **2010**, *176*, 2911–2920. [CrossRef] [PubMed]

92. Sormunen, R.T.; Leong, A.S.Y.; Vääräniemi, J.P.; Fernando, S.S.E.; Eskelinen, S.M. Immunolocalization of the fodrin, E-cadherin, and β-catenin adhesion complex in infiltrating ductal carcinoma of the breast—Comparison with an in vitro model. *J. Pathol.* **1999**, *187*, 416–423. [CrossRef]

93. Lacroix-Triki, M.; Geyer, F.C.; Lambros, M.B.; Savage, K.; Ellis, I.O.; Lee, A.H.S.; Reis-Filho, J.S. β-Catenin/Wnt signalling pathway in fibromatosis, metaplastic carcinomas and phyllodes tumours of the breast. *Mod. Pathol.* **2010**, *23*, 1438–1448. [CrossRef]

94. Samarzija, I.; Sini, P.; Schlange, T.; MacDonald, G.; Hynes, N.E. Wnt3a regulates proliferation and migration of HUVEC via canonical and non-canonical Wnt signaling pathways. *Biochem. Biophys. Res. Commun.* **2009**, *386*, 449–454. [CrossRef] [PubMed]

95. Medina, A.; Reintsch, W.; Steinbeisser, H. Xenopus frizzled 7 can act in canonical and non-canonical Wnt signaling pathways: Implications on early patterning and morphogenesis. *Mech. Dev.* **2000**, *92*, 227–237. [CrossRef]

96. Michaelson, J.S.; Leder, P. β-catenin is a downstream effector of Wnt-mediated tumorigenesis in the mammary gland. *Oncogene* **2001**, *20*, 5093–5099. [CrossRef]

97. Klopocki, E.; Kristiansen, G.; Wild, P.J.; Klaman, I.; Castanos-Velez, E.; Singer, G.; Stöhr, R.; Simon, R.; Sauter, G.; Leibiger, H.; et al. Loss of SFRP1 is associated with breast cancer progression and poor prognosis in early stage tumors. *Int. J. Oncol.* **2004**, *25*, 641–649. [CrossRef]

98. Woodward, W.A.; Chen, M.S.; Behbod, F.; Alfaro, M.P.; Buchholz, T.A.; Rosen, J.M. WNT/β-catenin mediates radiation resistance of mouse mammary progenitor cells. *Proc. Natl. Acad. Sci. USA* **2007**, *104*, 618–623. [CrossRef]

99. Zhu, X.; Feng, J.; Fu, W.; Shu, X.; Wan, X.; Liu, J. Effects of cisplatin on the proliferation, invasion and apoptosis of breast cancer cells following β-catenin silencing. *Int. J. Mol. Med.* **2020**, *45*, 1838–1850. [CrossRef]

100. Zhou, J.; Su, C.M.; Chen, H.A.; Du, S.; Li, C.W.; Wu, H.; Tsai, S.H.; Yeh, Y.T. Cryptanshinone inhibits the glycolysis and inhibits cell migration through PKM2/β-catenin axis in breast cancer. *Onco. Targets. Ther.* **2020**, *13*, 8629–8639. [CrossRef] [PubMed]

101. Mikels, A.J.; Nusse, R. Purified Wnt5a protein activates or inhibits β-catenin-TCF signaling depending on receptor context. *PLoS Biol.* **2006**, *4*, 570–582. [CrossRef] [PubMed]

102. Yamaguchi, T.P.; Bradley, A.; McMahon, A.P.; Jones, S. A Wnt5a pathway underlies outgrowth of multiple structures in the vertebrate embryo. *Development* **1999**, *126*, 1211–1223. [PubMed]

103. Säfholm, A.; Tuomela, J.; Rosenkvist, J.; Dejmek, J.; Härkönen, P.; Andersson, T. The wnt-5a-derived hexapeptide Foxy-5 inhibits breast cancer metastasis in vivo by targeting cell motility. *Clin. Cancer Res.* **2008**, *14*, 6556–6563. [CrossRef] [PubMed]

104. Borcherding, N.; Kusner, D.; Kolb, R.; Xie, Q.; Li, W.; Velez, G.; Askeland, R.; Weigel, R.J.; Zhang, W.; City, I. Paracrine WNT5A signaling inhibits expansion of tumor-initiating cells. *Cancer Res.* **2015**, *75*, 1972–1982. [CrossRef] [PubMed]

105. Roarty, K.; Baxley, S.E.; Crowley, M.R.; Frost, A.R.; Serra, R. Loss of TGF-β or Wnt5a results in an increase in Wnt/β-catenin activity and redirects mammary tumour phenotype. *Breast Cancer Res.* **2009**, *11*, 1–11. [CrossRef] [PubMed]

106. Bergenfelz, C.; Medrek, C.; Ekström, E.; Jirström, K.; Janols, H.; Wullt, M.; Bredberg, A.; Leandersson, K. Wnt5a Induces a Tolerogenic Phenotype of Macrophages in Sepsis and Breast Cancer Patients. *J. Immunol.* **2012**, *188*, 5448–5458. [CrossRef]

107. Bergenfelz, C.; Janols, H.; Wullt, M.; Jirström, K.; Bredberg, A.; Leandersson, K. Wnt5a Inhibits Human Monocyte-Derived Myeloid Dendritic Cell Generation. *Scand. J. Immunol.* **2013**, *78*, 194–204. [CrossRef]

108. Fernandez-Cobo, M.; Zammarchi, F.; Mandeli, J.; Holland, J.F.; Pogo, B.G.T. Expression of Wnt5A and Wnt10B in non-immortalized breast cancer cells. *Oncol. Rep.* **2007**, *17*, 903–907. [CrossRef]

109. Prasad, C.P.; Chaurasiya, S.K.; Guilmain, W.; Andersson, T. WNT5A signaling impairs breast cancer cell migration and invasion via mechanisms independent of the epithelial-mesenchymal transition. *J. Exp. Clin. Cancer Res.* **2016**, *35*, 1–15. [CrossRef]

110. Bauer, M.; Bénard, J.; Gaasterland, T.; Willert, K.; Cappellen, D. WNT5A encodes two isoforms with distinct functions in cancers. *PLoS ONE* **2013**, *8*, 1–14. [CrossRef]

111. Abramson, V.G.; Lehmann, B.D.; Ballinger, T.J.; Pietenpol, J.A. Subtyping of triple-negative breast cancer: Implications for therapy. *Cancer* **2015**, *121*, 8–16. [CrossRef]

112. Marra, A.; Viale, G.; Curigliano, G. Recent advances in triple negative breast cancer: The immunotherapy era. *BMC Med.* **2019**, *17*, 1–9. [CrossRef] [PubMed]

113. Dent, R.; Trudeau, M.; Pritchard, K.I.; Hanna, W.M.; Kahn, H.K.; Sawka, C.A.; Lickley, L.A.; Rawlinson, E.; Sun, P.; Narod, S.A. Triple-negative breast cancer: Clinical features and patterns of recurrence. *Clin. Cancer Res.* **2007**, *13*, 4429–4434. [CrossRef]

114. Geyer, F.C.; Pareja, F.; Weigelt, B.; Rakha, E.; Ellis, I.O.; Schnitt, S.J.; Reis-Filho, J.S. The Spectrum of Triple-Negative Breast Disease: High- and Low-Grade Lesions. *Am. J. Pathol.* **2017**, *187*, 2139–2151. [CrossRef] [PubMed]

115. Jiang, L.; Hou, R. Tetrandrine Reverses Paclitaxel Resistance in Human Ovarian Cancer via Inducing Apoptosis, Cell Cycle Arrest Through β-Catenin Pathway. *Onco. Targets. Ther.* **2020**, *13*, 3631–3639. [CrossRef] [PubMed]

116. Nagaraj, A.B.; Joseph, P.; Kovalenko, O.; Singh, S.; Armstrong, A.; Redline, R.; Resnick, K.; Zanotti, K.; Waggoner, S.; Di Feo, A. Critical role of Wnt/ß-catenin signaling in driving epithelial ovarian cancer platinum resistance. *Oncotarget* **2015**, *6*, 23720–23734. [CrossRef] [PubMed]

117. Sauriol, A.; Simeone, K.; Portelance, L.; Meunier, L.; Leclerc-Desaulniers, K.; De Ladurantaye, M.; Chergui, M.; Kendall-Dupont, J.; Rahimi, K.; Carmona, E.; et al. Modeling the diversity of epithelial ovarian cancer through ten novel well characterized cell lines covering multiple subtypes of the disease. *Cancers* **2020**, *12*, 2222. [CrossRef]

118. Jeong, J.W.; Lee, H.S.; Franco, H.L.; Broaddus, R.R.; Taketo, M.M.; Tsai, S.Y.; Lydon, J.P.; DeMayo, F.J. B-Catenin Mediates Glandular Formation and Dysregulation of B-Catenin Induces Hyperplasia Formation in the Murine Uterus. *Oncogene* **2009**, *28*, 31–40. [CrossRef]

119. Ryland, G.L.; Bearfoot, J.L.; Doyle, M.A.; Boyle, S.E.; Choong, D.Y.H.; Rowley, S.M.; Tothill, R.W.; Gorringe, K.L.; Campbell, I.G. MicroRNA Genes and Their Target 3'-Untranslated Regions Are Infrequently Somatically Mutated in Ovarian Cancers. *PLoS ONE* **2012**, *7*, e35805. [CrossRef]

120. Barghout, S.H.; Zepeda, N.; Xu, Z.; Steed, H.; Lee, C.H.; Fu, Y. Elevated β-catenin activity contributes to carboplatin resistance in A2780cp ovarian cancer cells. *Biochem. Biophys. Res. Commun.* **2015**, *468*, 173–178. [CrossRef]

121. Shin, W.S.; Gim, J.; Won, S.; Lee, S.T. Biphasic regulation of tumorigenesis by PTK7 expression level in esophageal squamous cell carcinoma. *Sci. Rep.* **2018**, *8*, 1–9. [CrossRef]

122. Berger, H.; Breuer, M.; Peradziryi, H.; Podleschny, M.; Jacob, R.; Borchers, A. PTK7 localization and protein stability is affected by canonical Wnt ligands. *J. Cell Sci.* **2017**. [CrossRef] [PubMed]

123. Wang, H.; Li, G.; Yin, Y.; Wang, J.; Wang, H.; Wei, W.; Guo, Q.; Ma, H.; Shi, Q.; Zhou, X.; et al. PTK7 protein is decreased in epithelial ovarian carcinomas with poor prognosis. *Int. J. Clin. Exp. Pathol.* **2014**, *7*, 7881–7889. [PubMed]

124. Golubkov, V.S.; Chekanov, A.V.; Cieplak, P.; Aleshin, A.E.; Chernov, A.V.; Zhu, W.; Radichev, I.A.; Zhang, D.; Dong, P.D.; Strongin, A.Y. The Wnt/planar cell polarity protein-tyrosine kinase-7 (PTK7) is a highly efficient proteolytic target of membrane type-1 matrix metalloproteinase: Implications in cancer and embryogenesis. *J. Biol. Chem.* **2010**, *285*, 35740–35749. [CrossRef]

125. Zhao, J.B.; Xue, J.F.; Zhang, W.Z.; Ren, Y.L.; Yan, D.M. Long noncoding RNA FGD5-AS1 promotes glioma cell proliferation, migration and invasion by regulating wnt/β-catenin pathway. *Cancer Manag. Res.* **2020**, *12*, 6187–6193. [CrossRef]

126. Nomura, M.; Rainusso, N.; Lee, Y.C.; Dawson, B.; Coarfa, C.; Han, R.; Larson, J.L.; Shuck, R.; Kurenbekova, L.; Yustein, J.T. Tegavivint and the β-Catenin/ALDH Axis in Chemotherapy-Resistant and Metastatic Osteosarcoma. *J. Natl. Cancer Inst.* **2019**, *111*, 1216–1227. [CrossRef]

127. Chen, T.; Lei, S.; Zeng, Z.; Zhang, J.; Xue, Y.; Sun, Y.; Lan, J.; Xu, S.; Mao, D.; Guo, B. Linc00261 inhibits metastasis and the WNT signaling pathway of pancreatic cancer by regulating a miR-552-5p/FOXO3 axis. *Oncol. Rep.* **2020**, *43*, 930–942. [CrossRef] [PubMed]

128. Joshi, B.S.; De Beer, M.A.; Giepmans, B.N.G.; Zuhorn, I.S. Endocytosis of Extracellular Vesicles and Release of Their Cargo from Endosomes. *ACS Nano* **2020**, *14*, 4444–4455. [CrossRef]

129. Kalra, H.; Gangoda, L.; Fonseka, P.; Chitti, S.V.; Liem, M.; Keerthikumar, S.; Samuel, M.; Boukouris, S.; Al Saffar, H.; Collins, C.; et al. Extracellular vesicles containing oncogenic mutant β-catenin activate Wnt signalling pathway in the recipient cells. *J. Extracell. Vesicles* **2019**, *8*. [CrossRef]

130. Dovrat, S.; Caspi, M.; Zilberberg, A.; Lahav, L.; Firsow, A.; Gur, H.; Rosin-Arbesfeld, R. 14-3-3 and β-catenin are secreted on extracellular vesicles to activate the oncogenic Wnt pathway. *Mol. Oncol.* **2014**, *8*, 894–911. [CrossRef]

131. Hu, Y.B.; Yan, C.; Mu, L.; Mi, Y.L.; Zhao, H.; Hu, H.; Li, X.L.; Tao, D.D.; Wu, Y.Q.; Gong, J.P.; et al. Exosomal Wnt-induced dedifferentiation of colorectal cancer cells contributes to chemotherapy resistance. *Oncogene* **2019**, *38*, 1951–1965. [CrossRef]

132. Szvicsek, Z.; Oszvald, Á.; Szabó, L.; Sándor, G.O.; Kelemen, A.; Soós, A.Á.; Pálóczi, K.; Harsányi, L.; Tölgyes, T.; Dede, K.; et al. Extracellular vesicle release from intestinal organoids is modulated by Apc mutation and other colorectal cancer progression factors. *Cell. Mol. Life Sci.* **2019**, *76*, 2463–2476. [CrossRef]

133. Yamashita, T.; Budhu, A.; Forgues, M.; Xin, W.W. Activation of hepatic stem cell marker EpCAM by Wnt-β-catenin signaling in hepatocellular carcinoma. *Cancer Res.* **2007**, *67*, 10831–10839. [CrossRef]

134. Ishiguro, K.; Yan, I.K.; Lewis-Tuffin, L.; Patel, T. Targeting Liver Cancer Stem Cells Using Engineered Biological Nanoparticles for the Treatment of Hepatocellular Cancer. *Hepatol. Commun.* **2020**, *4*, 298–313. [CrossRef] [PubMed]

135. Faict, S.; Muller, J.; De Veirman, K.; De Bruyne, E.; Maes, K.; Vrancken, L.; Heusschen, R.; De Raeve, H.; Schots, R.; Vanderkerken, K.; et al. Exosomes play a role in multiple myeloma bone disease and tumor development by targeting osteoclasts and osteoblasts. *Blood Cancer J.* **2018**, *8*. [CrossRef] [PubMed]

136. Chen, J.H.; Wu, A.T.H.; Bamodu, O.A.; Yadav, V.K.; Chao, T.Y.; Tzeng, Y.M.; Mukhopadhyay, D.; Hsiao, M.; Lee, J.C. Ovatodiolide suppresses oral cancer malignancy by down-regulating exosomal mir-21/STAT3/β-catenin cargo and preventing oncogenic transformation of normal gingival fibroblasts. *Cancers (Basel)* **2020**, *12*. [CrossRef] [PubMed]

137. Harada, T.; Yamamoto, H.; Kishida, S.; Kishida, M.; Awada, C.; Takao, T.; Kikuchi, A. Wnt5b-associated exosomes promote cancer cell migration and proliferation. *Cancer Sci.* **2017**, *108*, 42–52. [CrossRef] [PubMed]

138. Luga, V.; Zhang, L.; Viloria-Petit, A.M.; Ogunjimi, A.A.; Inanlou, M.R.; Chiu, E.; Buchanan, M.; Hosein, A.N.; Basik, M.; Wrana, J.L. Exosomes mediate stromal mobilization of autocrine Wnt-PCP signaling in breast cancer cell migration. *Cell* **2012**, *151*, 1542–1556. [CrossRef] [PubMed]

139. Wang, F.W.; Cao, C.H.; Han, K.; Zhao, Y.X.; Cai, M.Y.; Xiang, Z.C.; Zhang, J.X.; Chen, J.W.; Zhong, L.P.; Huang, Y.; et al. APC-activated long noncoding RNA inhibits colorectal carcinoma pathogenesis through reduction of exosome production. *J. Clin. Investig.* **2019**, *129*, 727–743. [CrossRef] [PubMed]

140. Lopatina, T.; Grange, C.; Cavallari, C.; Navarro-Tableros, V.; Lombardo, G.; Rosso, A.; Cedrino, M.; Pomatto, M.A.C.; Koni, M.; Veneziano, F.; et al. Targeting IL-3Rα on tumor-derived endothelial cells blunts metastatic spread of triple-negative breast cancer via extracellular vesicle reprogramming. *Oncogenesis* **2020**, *9*, 90. [CrossRef] [PubMed]

141. Kamerkar, S.; Lebleu, V.S.; Sugimoto, H.; Yang, S.; Ruivo, C.F.; Melo, S.A.; Lee, J.J.; Kalluri, R. Exosomes facilitate therapeutic targeting of oncogenic KRAS in pancreatic cancer. *Nature* **2017**, *546*, 498–503. [CrossRef]

142. Matsuda, A.; Ishiguro, K.; Yan, I.K.; Patel, T. Extracellular Vesicle-Based Therapeutic Targeting of β-Catenin to Modulate Anticancer Immune Responses in Hepatocellular Cancer. *Hepatol. Commun.* **2019**, *3*, 525–541. [CrossRef]

143. Cavallari, C.; Camussi, G.; Brizzi, M.F. Extracellular Vesicles in the Tumour Microenvironment: Eclectic Supervisors. *Int. J. Mol. Sci.* **2020**, *21*, 6768. [CrossRef] [PubMed]

144. Han, L.; Lam, E.W.F.; Sun, Y. Extracellular vesicles in the tumor microenvironment: Old stories, but new tales. *Mol. Cancer* **2019**, *18*, 1–14. [CrossRef] [PubMed]

145. Lucchetti, D.; Tenore, C.R.; Colella, F.; Sgambato, A. Extracellular Vesicles and Cancer: A Focus on Metabolism, Cytokines, and Immunity. *Cancers* **2020**, *12*, 171. [CrossRef]

90

Conclusions:

The aim of my thesis was to explore the role of the IL-3/IL-Rα in the context of TNBC.

We demonstrated:

- For the first time that IL-3Rα is expressed by TNBC samples and correlates with metastatic nodes and with a poor overall survival. IL-3 stimulation induces vascular mimicry and a general increase of cancer aggressiveness.

- The use of an antibody blocking IL-3Rα on TEC reprograms their EVs. anti-IL-3R-EV alter angiogenesis and the metastasis of primary tumors. Importantly, anti-IL-3R-EV *in vivo* priming reduced lung metastasis, probably because of its antiangiogenic functions and/or interference with cancer cell homing.

- The blockade of IL-3Rα is a tool for anti-tumor immune therapy. The combination of immune checkpoint targeting drugs and PD-L1 downregulation in myeloid and tumor cells can ameliorate the response to immune therapy.

References:

1.   Katsura, C.; Ogunmwonyi, I.; Kankam, H.K.N.; Saha, S. Breast Cancer: Presentation, Investigation and Management. *Br J Hosp Med (Lond)* **2022**, *83*, doi:10.12968/HMED.2021.0459.

2.   Medina, M.A.; Oza, G.; Sharma, A.; Arriaga, L.G.; Hernández, J.M.H.; Rotello, V.M.; Ramirez, J.T. Triple-Negative Breast Cancer: A Review of Conventional and Advanced Therapeutic Strategies. *Int J Environ Res Public Health* **2020**, *17*, doi:10.3390/IJERPH17062078.

3.   KB, K.; JL, H.; DR, B.; KA, P.; TM, M.; MJ, R.-B.; S, J.; FE, van L.; RL, M.; N, A.; et al. Risks of Breast, Ovarian, and Contralateral Breast Cancer for BRCA1 and BRCA2 Mutation Carriers. *JAMA* **2017**, *317*, 2402–2416, doi:10.1001/JAMA.2017.7112.

4.   Mersch, J.; Jackson, M.A.; Park, M.; Nebgen, D.; Peterson, S.K.; Singletary, C.; Arun, B.K.; Litton, J.K. Mersch J, Jackson MA, Park M, Nebgen D, Peterson SK, Singletary C, Arun BK and Litton JK. Cancers Associated with BRCA1 and BRCA2 Mutations Other than Breast and Ovarian. Cancer. 2015;121:269-275. *Cancer* **2015**, *121*, 2474–2475, doi:10.1002/CNCR.29357.

5.   Haddad, C.F. Hereditary Breast Cancer: Review and Current Approach. *Mastology* **2020**, *30*, 20200042, doi:10.29289/25945394202020200042.

6.   Pharoah, P.D.P.; Guilford, P.; Caldas, C. Incidence of Gastric Cancer and Breast Cancer in CDH1 (E-Cadherin) Mutation Carriers from Hereditary Diffuse Gastric Cancer Families. *Gastroenterology* **2001**, *121*, 1348–1353, doi:10.1053/gast.2001.29611.

7.   Chen, J.; Lindblom, A. Germline Mutation Screening of the STK11/LKB1 Gene in Familial Breast Cancer with LOH on 19p. *Clin Genet* **2000**, *57*, 394–397, doi:10.1034/J.1399-0004.2000.570511.X.

8.   Rahman, N.; Seal, S.; Thompson, D.; Kelly, P.; Renwick, A.; Elliott, A.; Reid, S.; Spanova, K.; Barfoot, R.; Chagtai, T.; et al. PALB2, Which Encodes a BRCA2-Interacting Protein, Is a Breast Cancer Susceptibility Gene. *Nat Genet* **2007**, *39*, 165–167, doi:10.1038/NG1959.

9.   Fakhri, N.; Chad, M.A.; Lahkim, M.; Houari, A.; Dehbi, H.; Belmouden, A.; el Kadmiri, N. Risk Factors for Breast Cancer in Women: An Update Review. *Med Oncol* **2022**, *39*, doi:10.1007/S12032-022-01804-X.

10.   Kashyap, D.; Pal, D.; Sharma, R.; Garg, V.K.; Goel, N.; Koundal, D.; Zaguia, A.; Koundal, S.; Belay, A. Global Increase in Breast Cancer Incidence: Risk Factors and Preventive Measures. *Biomed Res Int* **2022**, *2022*, doi:10.1155/2022/9605439.

11. Pizot, C.; Boniol, M.; Mullie, P.; Koechlin, A.; Boniol, M.; Boyle, P.; Autier, P. Physical Activity, Hormone Replacement Therapy and Breast Cancer Risk: A Meta-Analysis of Prospective Studies. *Eur J Cancer* **2016**, *52*, 138–154, doi:10.1016/J.EJCA.2015.10.063.

12. Beral, V.; Bull, D.; Doll, R.; Peto, R.; Reeves, G. Breast Cancer and Breastfeeding: Collaborative Reanalysis of Individual Data from 47 Epidemiological Studies in 30 Countries, Including 50302 Women with Breast Cancer and 96973 Women without the Disease. *Lancet* **2002**, *360*, 187–195, doi:10.1016/S0140-6736(02)09454-0.

13. Prentice, R.L.; Caan, B.; Chlebowski, R.T.; Patterson, R.; Kuller, L.H.; Ockene, J.K.; Margolis, K.L.; Limacher, M.C.; Manson, J.A.E.; Parker, L.M.; et al. Low-Fat Dietary Pattern and Risk of Invasive Breast Cancer: The Women's Health Initiative Randomized Controlled Dietary Modification Trial. *JAMA* **2006**, *295*, 629–642, doi:10.1001/JAMA.295.6.629.

14. Hardefeldt, P.J.; Penninkilampi, R.; Edirimanne, S.; Eslick, G.D. Physical Activity and Weight Loss Reduce the Risk of Breast Cancer: A Meta-Analysis of 139 Prospective and Retrospective Studies. *Clin Breast Cancer* **2018**, *18*, e601–e612, doi:10.1016/J.CLBC.2017.10.010.

15. Bedrosian, I.; Hu, C.Y.; Chang, G.J. Population-Based Study of Contralateral Prophylactic Mastectomy and Survival Outcomes of Breast Cancer Patients. *J Natl Cancer Inst* **2010**, *102*, 401–409, doi:10.1093/JNCI/DJQ018.

16. Visvanathan, K.; Fabian, C.J.; Bantug, E.; Brewster, A.M.; Davidson, N.E.; DeCensi, A.; Floyd, J.D.; Garber, J.E.; Hofstatter, E.W.; Khan, S.A.; et al. Use of Endocrine Therapy for Breast Cancer Risk Reduction: ASCO Clinical Practice Guideline Update. *J Clin Oncol* **2019**, *37*, 3152–3165, doi:10.1200/JCO.19.01472.

17. King, M.C.; Wieand, S.; Hale, K.; Lee, M.; Walsh, T.; Owens, K.; Tait, J.; Ford, L.; Dunn, B.K.; Costantino, J.; et al. Tamoxifen and Breast Cancer Incidence among Women with Inherited Mutations in BRCA1 and BRCA2: National Surgical Adjuvant Breast and Bowel Project (NSABP-P1) Breast Cancer Prevention Trial. *JAMA* **2001**, *286*, 2251–2256, doi:10.1001/JAMA.286.18.2251.

18. Cserni, G. Histological Type and Typing of Breast Carcinomas and the WHO Classification Changes over Time. *Pathologica* **2020**, *112*, 25–41, doi:10.32074/1591-951X-1-20.

19. Weigelt, B.; Horlings, H.M.; Kreike, B.; Hayes, M.M.; Hauptmann, M.; Wessels, L.F.A.; de Jong, D.; van de Vijver, M.J.; Van't Veer, L.J.; Peterse, J.L. Refinement of Breast Cancer Classification by Molecular Characterization of Histological Special Types. *J Pathol* **2008**, *216*, 141–150, doi:10.1002/PATH.2407.

20. Publication of the WHO Classification of Tumours, 5th Edition, Volume 2: Breast Tumours – IARC Available online: https://www.iarc.who.int/news-events/who-classification-of-tumours-5th-edition-volume-2-breast-tumours/ (accessed on 3 November 2022).

21. Hu, Z.; Fan, C.; Oh, D.S.; Marron, J.S.; He, X.; Qaqish, B.F.; Livasy, C.; Carey, L.A.; Reynolds, E.; Dressler, L.; et al. The Molecular Portraits of Breast Tumors Are Conserved across Microarray Platforms., doi:10.1186/1471-2164-7-96.

22. Sørlie, T.; Perou, C.M.; Tibshirani, R.; Aas, T.; Geisler, S.; Johnsen, H.; Hastie, T.; Eisen, M.B.; van de Rijn, M.; Jeffrey, S.S.; et al. Gene Expression Patterns of Breast Carcinomas Distinguish Tumor Subclasses with Clinical Implications. *Proc Natl Acad Sci U S A* **2001**, *98*, 10869–10874, doi:10.1073/PNAS.191367098.

23. Almansour, N.M. Triple-Negative Breast Cancer: A Brief Review About Epidemiology, Risk Factors, Signaling Pathways, Treatment and Role of Artificial Intelligence. *Front Mol Biosci* **2022**, *9*, doi:10.3389/FMOLB.2022.836417.

24. Hammond, M.E.H.; Hayes, D.F.; Dowsett, M.; Allred, D.C.; Hagerty, K.L.; Badve, S.; Fitzgibbons, P.L.; Francis, G.; Goldstein, N.S.; Hayes, M.; et al. American Society of Clinical Oncology/College Of American Pathologists Guideline Recommendations for Immunohistochemical Testing of Estrogen and Progesterone Receptors in Breast Cancer. *J Clin Oncol* **2010**, *28*, 2784–2795, doi:10.1200/JCO.2009.25.6529.

25. Howard, F.M.; Olopade, O.I. Epidemiology of Triple-Negative Breast Cancer: A Review. *Cancer J* **2021**, *27*, 8–16, doi:10.1097/PPO.0000000000000500.

26. Perou, C.M.; Sørile, T.; Eisen, M.B.; van de Rijn, M.; Jeffrey, S.S.; Ress, C.A.; Pollack, J.R.; Ross, D.T.; Johnsen, H.; Akslen, L.A.; et al. Molecular Portraits of Human Breast Tumours. *Nature* **2000**, *406*, 747–752, doi:10.1038/35021093.

27. Hammond, M.E.H.; Hayes, D.F.; Dowsett, M.; Allred, D.C.; Hagerty, K.L.; Badve, S.; Fitzgibbons, P.L.; Francis, G.; Goldstein, N.S.; Hayes, M.; et al. American Society of Clinical Oncology/College of American Pathologists Guideline Recommendations for Immunohistochemical Testing of Estrogen and Progesterone Receptors in Breast Cancer. *Journal of Clinical Oncology* **2010**, *28*, 2784, doi:10.1200/JCO.2009.25.6529.

28. Nielsen, T.O.; Parker, J.S.; Leung, S.; Voduc, D.; Ebbert, M.; Vickery, T.; Davies, S.R.; Snider, J.; Stijleman, I.J.; Reed, J.; et al. A Comparison of PAM50 Intrinsic Subtyping with Immunohistochemistry and Clinical Prognostic Factors in Tamoxifen-Treated Estrogen Receptor-Positive Breast Cancer. *Clin Cancer Res* **2010**, *16*, 5222–5232, doi:10.1158/1078-0432.CCR-10-1282.

29. Lehmann, B.D.; Bauer, J.A.; Chen, X.; Sanders, M.E.; Chakravarthy, A.B.; Shyr, Y.; Pietenpol, J.A. Identification of Human Triple-Negative Breast Cancer Subtypes and

Preclinical Models for Selection of Targeted Therapies. *J Clin Invest* **2011**, *121*, 2750–2767, doi:10.1172/JCI45014.

30.   Lehmann, B.D.; Jovanović, B.; Chen, X.; Estrada, M. v.; Johnson, K.N.; Shyr, Y.; Moses, H.L.; Sanders, M.E.; Pietenpol, J.A. Refinement of Triple-Negative Breast Cancer Molecular Subtypes: Implications for Neoadjuvant Chemotherapy Selection. *PLoS One* **2016**, *11*, doi:10.1371/JOURNAL.PONE.0157368.

31.   Burstein, M.D.; Tsimelzon, A.; Poage, G.M.; Covington, K.R.; Contreras, A.; Fuqua, S.A.W.; Savage, M.I.; Osborne, C.K.; Hilsenbeck, S.G.; Chang, J.C.; et al. Comprehensive Genomic Analysis Identifies Novel Subtypes and Targets of Triple-Negative Breast Cancer. *Clin Cancer Res* **2015**, *21*, 1688–1698, doi:10.1158/1078-0432.CCR-14-0432.

32.   Viallard, C.; Larrivée, B. Tumor Angiogenesis and Vascular Normalization: Alternative Therapeutic Targets. *Angiogenesis* **2017**, *20*, 409–426, doi:10.1007/S10456-017-9562-9.

33.   Nishida, N.; Yano, H.; Nishida, T.; Kamura, T.; Kojiro, M. Angiogenesis in Cancer. *Vasc Health Risk Manag* **2006**, *2*, 213–219, doi:10.2147/VHRM.2006.2.3.213.

34.   Hanahan, D.; Weinberg, R.A. Hallmarks of Cancer: The next Generation. *Cell* **2011**, *144*, 646–674, doi:10.1016/J.CELL.2011.02.013.

35.   Weidner, N.; Semple, J.P.; Welch, W.R.; Folkman, J. Tumor Angiogenesis and Metastasis--Correlation in Invasive Breast Carcinoma. *N Engl J Med* **1991**, *324*, 1–8, doi:10.1056/NEJM199101033240101.

36.   Uzzan, B.; Nicolas, P.; Cucherat, M.; Perret, G.Y. Microvessel Density as a Prognostic Factor in Women with Breast Cancer: A Systematic Review of the Literature and Meta-Analysis. *Cancer Res* **2004**, *64*, 2941–2955, doi:10.1158/0008-5472.CAN-03-1957.

37.   Mohammed, R.A.A.; Ellis, I.O.; Mahmmod, A.M.; Hawkes, E.C.; Green, A.R.; Rakha, E.A.; Martin, S.G. Lymphatic and Blood Vessels in Basal and Triple-Negative Breast Cancers: Characteristics and Prognostic Significance. *Mod Pathol* **2011**, *24*, 774–785, doi:10.1038/MODPATHOL.2011.4.

38.   Lopatina, T.; Grange, C.; Cavallari, C.; Navarro-Tableros, V.; Lombardo, G.; Rosso, A.; Cedrino, M.; Pomatto, M.A.C.; Koni, M.; Veneziano, F.; et al. Targeting IL-3Rα on Tumor-Derived Endothelial Cells Blunts Metastatic Spread of Triple-Negative Breast Cancer via Extracellular Vesicle Reprogramming. *Oncogenesis* **2020**, *9*, doi:10.1038/S41389-020-00274-Y.

39.   Diéras, V.; Campone, M.; Yardley, D.A.; Romieu, G.; Valero, V.; Isakoff, S.J.; Koeppen, H.; Wilson, T.R.; Xiao, Y.; Shames, D.S.; et al. Randomized, Phase II, Placebo-Controlled Trial of Onartuzumab and/or Bevacizumab in Combination with Weekly

Paclitaxel in Patients with Metastatic Triple-Negative Breast Cancer. *Ann Oncol* **2015**, *26*, 1904–1910, doi:10.1093/ANNONC/MDV263.

40. Curigliano, G.; Pivot, X.; Cortés, J.; Elias, A.; Cesari, R.; Khosravan, R.; Collier, M.; Huang, X.; Cataruozolo, P.E.; Kern, K.A.; et al. Randomized Phase II Study of Sunitinib versus Standard of Care for Patients with Previously Treated Advanced Triple-Negative Breast Cancer. *Breast* **2013**, *22*, 650–656, doi:10.1016/J.BREAST.2013.07.037.

41. Sikov, W.M.; Berry, D.A.; Perou, C.M.; Singh, B.; Cirrincione, C.T.; Tolaney, S.M.; Kuzma, C.S.; Pluard, T.J.; Somlo, G.; Port, E.R.; et al. Impact of the Addition of Carboplatin and/or Bevacizumab to Neoadjuvant Once-per-Week Paclitaxel Followed by Dose-Dense Doxorubicin and Cyclophosphamide on Pathologic Complete Response Rates in Stage II to III Triple-Negative Breast Cancer: CALGB 40603 (Alliance). *J Clin Oncol* **2015**, *33*, 13–21, doi:10.1200/JCO.2014.57.0572.

42. Maniotis, A.J.; Folberg, R.; Hess, A.; Seftor, E.A.; Gardner, L.M.G.; Pe'er, J.; Trent, J.M.; Meltzer, P.S.; Hendrix, M.J.C. Vascular Channel Formation by Human Melanoma Cells in Vivo and in Vitro: Vasculogenic Mimicry. *Am J Pathol* **1999**, *155*, 739–752, doi:10.1016/S0002-9440(10)65173-5.

43. Andonegui-Elguera, M.A.; Alfaro-Mora, Y.; Cáceres-Gutiérrez, R.; Caro-Sánchez, C.H.S.; Herrera, L.A.; Díaz-Chávez, J. An Overview of Vasculogenic Mimicry in Breast Cancer. *Front Oncol* **2020**, *10*, doi:10.3389/FONC.2020.00220.

44. Tang, N.N.; Zhu, H.; Zhang, H.J.; Zhang, W.F.; Jin, H.L.; Wang, L.; Wang, P.; He, G.J.; Hao, B.; Shi, R.H. HIF-1α Induces VE-Cadherin Expression and Modulates Vasculogenic Mimicry in Esophageal Carcinoma Cells. *World J Gastroenterol* **2014**, *20*, 17894–17904, doi:10.3748/WJG.V20.I47.17894.

45. Li, S.; Meng, W.; Guan, Z.; Guo, Y.; Han, X. The Hypoxia-Related Signaling Pathways of Vasculogenic Mimicry in Tumor Treatment. *Biomed Pharmacother* **2016**, *80*, 127–135, doi:10.1016/J.BIOPHA.2016.03.010.

46. Paulis, Y.W.J.; Soetekouw, P.M.M.B.; Verheul, H.M.W.; Tjan-Heijnen, V.C.G.; Griffioen, A.W. Signalling Pathways in Vasculogenic Mimicry. *Biochim Biophys Acta* **2010**, *1806*, 18–28, doi:10.1016/J.BBCAN.2010.01.001.

47. Delgado-Bellido, D.; Serrano-Saenz, S.; Fernández-Cortés, M.; Oliver, F.J. Vasculogenic Mimicry Signaling Revisited: Focus on Non-Vascular VE-Cadherin. *Mol Cancer* **2017**, *16*, doi:10.1186/S12943-017-0631-X.

48. Gu, M.; Zheng, X. Osteopontin and Vasculogenic Mimicry Formation Are Associated with Response to Neoadjuvant Chemotherapy in Advanced Breast Cancer. *Onco Targets Ther* **2017**, *10*, 4121–4127, doi:10.2147/OTT.S129414.

49. Shevde, L.A.; Metge, B.J.; Mitra, A.; Xi, Y.; Ju, J.; King, J.A.; Samant, R.S. Spheroid-Forming Subpopulation of Breast Cancer Cells Demonstrates Vasculogenic Mimicry via Hsa-MiR-299-5p Regulated de Novo Expression of Osteopontin. *J Cell Mol Med* **2010**, *14*, 1693–1706, doi:10.1111/J.1582-4934.2009.00821.X.

50. Salinas-Vera, Y.M.; Marchat, L.A.; García-Vázquez, R.; González de la Rosa, C.H.; Castañeda-Saucedo, E.; Tito, N.N.; Flores, C.P.; Pérez-Plasencia, C.; Cruz-Colin, J.L.; Carlos-Reyes, Á.; et al. Cooperative Multi-Targeting of Signaling Networks by AngiomiR-204 Inhibits Vasculogenic Mimicry in Breast Cancer Cells. *Cancer Lett* **2018**, *432*, 17–27, doi:10.1016/J.CANLET.2018.06.003.

51. Pierce, J.H. Oncogenes, Growth Factors and Hematopoietic Cell Transformation. *Biochim Biophys Acta* **1989**, *989*, 179–208, doi:10.1016/0304-419X(89)90042-5.

52. Metcalf, D. The Molecular Control of Cell Division, Differentiation Commitment and Maturation in Haemopoietic Cells. *Nature* **1989**, *339*, 27–30, doi:10.1038/339027A0.

53. Mangi, M.H.; Newland, A.C. Interleukin-3: Promises and Perspectives. *Hematology* **1998**, *3*, 55–66, doi:10.1080/10245332.1998.11752123.

54. Clark, S.C.; Kamen, R. The Human Hematopoietic Colony-Stimulating Factors. *Science* **1987**, *236*, 1229–1237, doi:10.1126/SCIENCE.3296190.

55. Matsuda, T.; Hirano, T. Association of P72 Tyrosine Kinase with Stat Factors and Its Activation by Interleukin-3, Interleukin-6, and Granulocyte Colony-Stimulating Factor. *Blood* **1994**, *83*, 3457–3461, doi:10.1182/BLOOD.V83.12.3457.3457.

56. Doyle, S.E.; Gasson, J.C. Characterization of the Role of the Human Granulocyte-Macrophage Colony- Stimulating Factor Receptor α Subunit in the Activation of JAK2 and STAT5. *Blood* **1998**, *92*, 867–876, doi:10.1182/BLOOD.V92.3.867.

57. Evans, C.A.; Pierce, A.; Winter, S.A.; Spooncer, E.; Heyworth, C.M.; Whetton, A.D. Activation of Granulocyte-Macrophage Colony-Stimulating Factor and Interleukin-3 Receptor Subunits in a Multipotential Hematopoietic Progenitor Cell Line Leads to Differential Effects on Development. *Blood* **1999**, *94*, 1504–1514, doi:10.1182/BLOOD.V94.5.1504.

58. Bras, A.E.; de Haas, V.; van Stigt, A.; Jongen-Lavrencic, M.; Beverloo, H.B.; te Marvelde, J.G.; Zwaan, C.M.; van Dongen, J.J.M.; Leusen, J.H.W.; van der Velden, V.H.J. CD123 Expression Levels in 846 Acute Leukemia Patients Based on Standardized Immunophenotyping. *Cytometry B Clin Cytom* **2019**, *96*, 134–142, doi:10.1002/CYTO.B.21745.

59. Testa, U.; Pelosi, E.; Castelli, G. CD123 as a Therapeutic Target in the Treatment of Hematological Malignancies. *Cancers (Basel)* **2019**, *11*, doi:10.3390/CANCERS11091358.

60. el Achi, H.; Dupont, E.; Paul, S.; Khoury, J.D. CD123 as a Biomarker in Hematolymphoid Malignancies: Principles of Detection and Targeted Therapies. *Cancers 2020, Vol. 12, Page 3087* **2020**, *12*, 3087, doi:10.3390/CANCERS12113087.

61. Dentelli, P.; Rosso, A.; Olgasi, C.; Camussi, G.; Brizzi, M.F. IL-3 Is a Novel Target to Interfere with Tumor Vasculature. *Oncogene* **2011**, *30*, 4930–4940, doi:10.1038/ONC.2011.204.

62. Lombardo, G.; Gili, M.; Grange, C.; Cavallari, C.; Dentelli, P.; Togliatto, G.; Taverna, D.; Camussi, G.; Brizzi, M.F. IL-3R-Alpha Blockade Inhibits Tumor Endothelial Cell-Derived Extracellular Vesicle (EV)-Mediated Vessel Formation by Targeting the β-Catenin Pathway. *Oncogene* **2018**, *37*, 1175–1191, doi:10.1038/S41388-017-0034-X.

63. Wolf, P. The Nature and Significance of Platelet Products in Human Plasma. *Br J Haematol* **1967**, *13*, 269–288, doi:10.1111/J.1365-2141.1967.TB08741.X.

64. Yáñez-Mó, M.; Siljander, P.R.M.; Andreu, Z.; Zavec, A.B.; Borràs, F.E.; Buzas, E.I.; Buzas, K.; Casal, E.; Cappello, F.; Carvalho, J.; et al. Biological Properties of Extracellular Vesicles and Their Physiological Functions. *J Extracell Vesicles* **2015**, *4*, 1–60, doi:10.3402/JEV.V4.27066.

65. Raposo, G.; Stoorvogel, W. Extracellular Vesicles: Exosomes, Microvesicles, and Friends. *J Cell Biol* **2013**, *200*, 373–383, doi:10.1083/JCB.201211138.

66. Femminò, S.; Penna, C.; Margarita, S.; Comità, S.; Brizzi, M.F.; Pagliaro, P. Extracellular Vesicles and Cardiovascular System: Biomarkers and Cardioprotective Effectors. *Vascul Pharmacol* **2020**, *135*, doi:10.1016/J.VPH.2020.106790.

67. Grange, C.; Papadimitriou, E.; Dimuccio, V.; Pastorino, C.; Molina, J.; O'Kelly, R.; Niedernhofer, L.J.; Robbins, P.D.; Camussi, G.; Bussolati, B. Urinary Extracellular Vesicles Carrying Klotho Improve the Recovery of Renal Function in an Acute Tubular Injury Model. *Mol Ther* **2020**, *28*, 490–502, doi:10.1016/J.YMTHE.2019.11.013.

68. Théry, C.; Witwer, K.W.; Aikawa, E.; Alcaraz, M.J.; Anderson, J.D.; Andriantsitohaina, R.; Antoniou, A.; Arab, T.; Archer, F.; Atkin-Smith, G.K.; et al. Minimal Information for Studies of Extracellular Vesicles 2018 (MISEV2018): A Position Statement of the International Society for Extracellular Vesicles and Update of the MISEV2014 Guidelines. *J Extracell Vesicles* **2018**, *7*, doi:10.1080/20013078.2018.1535750.

69. Gardiner, C.; Vizio, D. di; Sahoo, S.; Théry, C.; Witwer, K.W.; Wauben, M.; Hill, A.F. Techniques Used for the Isolation and Characterization of Extracellular Vesicles: Results of a Worldwide Survey. *J Extracell Vesicles* **2016**, *5*, doi:10.3402/JEV.V5.32945.

70. Tetta, C.; Ghigo, E.; Silengo, L.; Deregibus, M.C.; Camussi, G. Extracellular Vesicles as an Emerging Mechanism of Cell-to-Cell Communication. *Endocrine* **2013**, *44*, 11–19, doi:10.1007/S12020-012-9839-0.

71. Ratajczak, M.Z.; Ratajczak, J. Horizontal Transfer of RNA and Proteins between Cells by Extracellular Microvesicles: 14 Years Later. *Clin Transl Med* **2016**, *5*, doi:10.1186/S40169-016-0087-4.

72. Huang, S.; Dong, M.; Chen, Q. Tumor-Derived Exosomes and Their Role in Breast Cancer Metastasis. *Int J Mol Sci* **2022**, *23*, 13993, doi:10.3390/IJMS232213993.

73. Tang, Q.; Xiao, X.; Li, R.; He, H.; Li, S.; Ma, C. Recent Advances in Detection for Breast-Cancer-Derived Exosomes. *Molecules* **2022**, *27*, doi:10.3390/MOLECULES27196673.

74. Balkwill, F.R.; Capasso, M.; Hagemann, T. The Tumor Microenvironment at a Glance. *J Cell Sci* **2012**, *125*, 5591–5596, doi:10.1242/JCS.116392.

75. Tian, X.; Shen, H.; Li, Z.; Wang, T.; Wang, S. Tumor-Derived Exosomes, Myeloid-Derived Suppressor Cells, and Tumor Microenvironment. *J Hematol Oncol* **2019**, *12*, doi:10.1186/S13045-019-0772-Z.

76. Yang, E.; Wang, X.; Gong, Z.; Yu, M.; Wu, H.; Zhang, D. Exosome-Mediated Metabolic Reprogramming: The Emerging Role in Tumor Microenvironment Remodeling and Its Influence on Cancer Progression. *Signal Transduct Target Ther* **2020**, *5*, doi:10.1038/S41392-020-00359-5.

77. Zhang, L.; Yu, D. Exosomes in Cancer Development, Metastasis, and Immunity. *Biochim Biophys Acta Rev Cancer* **2019**, *1871*, 455–468, doi:10.1016/J.BBCAN.2019.04.004.

78. Antonyak, M.A.; Cerione, R.A. Microvesicles as Mediators of Intercellular Communication in Cancer. *Methods Mol Biol* **2014**, *1165*, 147–173, doi:10.1007/978-1-4939-0856-1_11.

79. Paggetti, J.; Haderk, F.; Seiffert, M.; Janji, B.; Distler, U.; Ammerlaan, W.; Kim, Y.J.; Adam, J.; Lichter, P.; Solary, E.; et al. Exosomes Released by Chronic Lymphocytic Leukemia Cells Induce the Transition of Stromal Cells into Cancer-Associated Fibroblasts. *Blood* **2015**, *126*, 1106–1117, doi:10.1182/BLOOD-2014-12-618025.

80. Hasan, H.; Sohal, I.S.; Soto-Vargas, Z.; Byappanhalli, A.M.; Humphrey, S.E.; Kubo, H.; Kitdumrongthum, S.; Copeland, S.; Tian, F.; Chairoungdua, A.; et al. Extracellular Vesicles Released by Non-Small Cell Lung Cancer Cells Drive Invasion and Permeability in Non-Tumorigenic Lung Epithelial Cells. *Sci Rep* **2022**, *12*, doi:10.1038/S41598-022-04940-6.

81. Fidler, I.J. The Pathogenesis of Cancer Metastasis: The "seed and Soil" Hypothesis Revisited. *Nat Rev Cancer* **2003**, *3*, 453–458, doi:10.1038/NRC1098.

82. Suetsugu, A.; Honma, K.; Saji, S.; Moriwaki, H.; Ochiya, T.; Hoffman, R.M. Imaging Exosome Transfer from Breast Cancer Cells to Stroma at Metastatic Sites in Orthotopic

Nude-Mouse Models. *Adv Drug Deliv Rev* **2013**, *65*, 383–390, doi:10.1016/J.ADDR.2012.08.007.

83. Costa-Silva, B.; Aiello, N.M.; Ocean, A.J.; Singh, S.; Zhang, H.; Thakur, B.K.; Becker, A.; Hoshino, A.; Mark, M.T.; Molina, H.; et al. Pancreatic Cancer Exosomes Initiate Pre-Metastatic Niche Formation in the Liver. *Nat Cell Biol* **2015**, *17*, 816–826, doi:10.1038/NCB3169.

84. Maji, S.; Chaudhary, P.; Akopova, I.; Nguyen, P.M.; Hare, R.J.; Gryczynski, I.; Vishwanatha, J.K. Exosomal Annexin II Promotes Angiogenesis and Breast Cancer Metastasis. *Mol Cancer Res* **2017**, *15*, 93–105, doi:10.1158/1541-7786.MCR-16-0163.

85. Lindoso, R.S.; Collino, F.; Camussi, G. Extracellular Vesicles Derived from Renal Cancer Stem Cells Induce a Pro-Tumorigenic Phenotype in Mesenchymal Stromal Cells. *Oncotarget* **2015**, *6*, 7959–7969, doi:10.18632/ONCOTARGET.3503.

86. Lugano, R.; Ramachandran, M.; Dimberg, A. Tumor Angiogenesis: Causes, Consequences, Challenges and Opportunities. *Cell Mol Life Sci* **2020**, *77*, 1745–1770, doi:10.1007/S00018-019-03351-7.

87. Ferrara, N. VEGF as a Therapeutic Target in Cancer. *Oncology* **2005**, *69*, 11–16, doi:10.1159/000088479.

88. Garcia-Hernandez, A.; Reyes-Uribe, E.; Arce-Salinas, C.; de la Cruz-Lopez, K.G.; Manzo-Merino, J.; Guzman-Ortiz, A.L.; Quezada, H.; Cortes-Reynosa, P.; Breton-Mora, F.; Elizalde-Acosta, I.; et al. Extracellular Vesicles from Blood of Breast Cancer Women Induce Angiogenic Processes in HUVECs. *Tissue Cell* **2022**, *76*, doi:10.1016/J.TICE.2022.101814.

89. Ko, S.Y.; Lee, W.; Kenny, H.A.; Dang, L.H.; Ellis, L.M.; Jonasch, E.; Lengyel, E.; Naora, H. Cancer-Derived Small Extracellular Vesicles Promote Angiogenesis by Heparin-Bound, Bevacizumab-Insensitive VEGF, Independent of Vesicle Uptake., doi:10.1038/s42003-019-0609-x.

90. Seo, S.H.; Hwang, S.-Y.; Hwang, S.; Han, S.; Park, H.; Lee, Y.-S.; Rho, S.B.; Kwon, Y. Hypoxia-Induced ELF3 Promotes Tumor Angiogenesis through IGF1/IGF1R. *EMBO Rep* **2022**, *23*, e52977, doi:10.15252/EMBR.202152977.

91. Vinay, D.S.; Ryan, E.P.; Pawelec, G.; Talib, W.H.; Stagg, J.; Elkord, E.; Lichtor, T.; Decker, W.K.; Whelan, R.L.; Kumara, H.M.C.S.; et al. Immune Evasion in Cancer: Mechanistic Basis and Therapeutic Strategies. *Semin Cancer Biol* **2015**, *35 Suppl*, S185–S198, doi:10.1016/J.SEMCANCER.2015.03.004.

92. Shen, T.; Huang, Z.; Shi, C.; Pu, X.; Xu, X.; Wu, Z.; Ding, G.; Cao, L. Pancreatic Cancer-Derived Exosomes Induce Apoptosis of T Lymphocytes through the P38 MAPK-

Mediated Endoplasmic Reticulum Stress. *The FASEB Journal* **2020**, *34*, 8442–8458, doi:10.1096/FJ.201902186R.

93. Szajnik, M.; Czystowska, M.; Szczepanski, M.J.; Mandapathil, M.; Whiteside, T.L. Tumor-Derived Microvesicles Induce, Expand and up-Regulate Biological Activities of Human Regulatory T Cells (Treg). *PLoS One* **2010**, *5*, doi:10.1371/JOURNAL.PONE.0011469.

94. Blank, C.U.; Haining, W.N.; Held, W.; Hogan, P.G.; Kallies, A.; Lugli, E.; Lynn, R.C.; Philip, M.; Rao, A.; Restifo, N.P.; et al. Defining "T Cell Exhaustion." *Nat Rev Immunol* **2019**, *19*, 665–674, doi:10.1038/S41577-019-0221-9.

95. Wang, W.; Chen, D.; Zhao, Y.; Zhao, T.; Wen, J.; Mao, Y.; Chen, C.; Sang, Y.; Zhang, Y.; Chen, Y. Characterization of LAG-3, CTLA-4, and CD8+ TIL Density and Their Joint Influence on the Prognosis of Patients with Esophageal Squamous Cell Carcinoma. *Ann Transl Med* **2019**, *7*, 776–776, doi:10.21037/ATM.2019.11.38.

96. Zhu, X.; Hu, H.; Xiao, Y.; Li, Q.; Zhong, Z.; Yang, J.; Zou, P.; Cao, Y.; Meng, F.; Li, W.; et al. Tumor-Derived Extracellular Vesicles Induce Invalid Cytokine Release and Exhaustion of CD19 CAR-T Cells. *Cancer Lett* **2022**, *536*, doi:10.1016/J.CANLET.2022.215668.

97. Qing, Y.; Li, Q.; Ren, T.; Xia, W.; Peng, Y.; Liu, G.L.; Luo, H.; Yang, Y.X.; Dai, X.Y.; Zhou, S.F.; et al. Upregulation of PD-L1 and APE1 Is Associated with Tumorigenesis and Poor Prognosis of Gastric Cancer. *Drug Des Devel Ther* **2015**, *9*, 901, doi:10.2147/DDDT.S75152.

98. Ricklefs, F.L.; Alayo, Q.; Krenzlin, H.; Mahmoud, A.B.; Speranza, M.C.; Nakashima, H.; Hayes, J.L.; Lee, K.; Balaj, L.; Passaro, C.; et al. Immune Evasion Mediated by PD-L1 on Glioblastoma-Derived Extracellular Vesicles. *Sci Adv* **2018**, *4*, doi:10.1126/SCIADV.AAR2766.

99. Fleming, V.; Hu, X.; Eline Weller, C.; Weber, R.; Groth, C.; Riester, Z.; H€ User, L.; Sun, Q.; Nagibin, V.; Kirschning, C.; et al. Tumor Biology and Immunology Melanoma Extracellular Vesicles Generate Immunosuppressive Myeloid Cells by Upregulating PD-L1 via TLR4 Signaling., doi:10.1158/0008-5472.CAN-19-0053.

100. Guo, X.; Qiu, W.; Liu, Q.; Qian, M.; Wang, S.; Zhang, Z.; Gao, X.; Chen, Z.; Xue, H.; Li, G. Immunosuppressive Effects of Hypoxia-Induced Glioma Exosomes through Myeloid-Derived Suppressor Cells via the MiR-10a/Rora and MiR-21/Pten Pathways. *Oncogene 2018 37:31* **2018**, *37*, 4239–4259, doi:10.1038/s41388-018-0261-9.